ADDIS ABABA UNIVERSITY SCHOOL OF GRADUATE STUDIES
FACULTY OF TECHNOLOGY DEPARTMENT OF CIVIL ENGINEERING

Comparison of Two Model Approaches to Investigate Hydrological Processes in Five Selected Catchments in the Upper Blue Nile River Basin, Ethiopia.

MSc Thesis by

Demeke Amena

May, 2011

Department of Civil Engineering

Comparison of Two Model Approaches to Investigate Hydrological Processes in Five Selected Catchments in the Upper Blue Nile River Basin, Ethiopia.

A thesis submitted to School of Graduate Studies, Addis Ababa University in partial fulfillment of the requirements for the Degree of Masters of Science in Civil Engineering.

Addis Ababa University 2011
Author: Demeke Amena
Supervisor: Dr.Ing. Yonas Michael
Co-Supervisor: Mr. Sirak Tekleab

Abstract

The successful application of hydrologic models depends not only on the model structure, the different time and space scale associated, but also on the accuracy of the simulated discharge. The key issue for operational users of hydrologic models is whether physically-based distributed models perform sufficiently better than conceptual models to justify the increased time and effort required for their application. The main objective of the research was comparison of two modelling approaches using on one hand quasi-semi-distributed conceptual model HBV–Light and on the other hand spatially distributed hydrologic model ArcSWAT. These models were applied to five test catchments representing wide variability in geographic location, climatic condition, areal extent and physiographical characteristics located in the Upper Blue Nile River Basin.

The automatic calibration methodology, which is used in this study, applied a hierarchy of three techniques, namely screening, parameterization, and parameter sensitivity analysis, at the parameter identification stage of model calibration. Operating in continuous river-flow simulation mode, to demonstrate their effectiveness, a split-sample test was applied to the test catchments using a number of performance evaluation criteria.

The monthly Auto-calibration and Validation results show that with increasingly secured efficiency the two models can equivalently capture monthly and seasonal flow patterns. This finding justifies that there is no significant benefit in applying the spatially-distributed model and that the simpler conceptual models would provide acceptably better simulations for monthly and seasonal flows. From calibration and validation results on daily time step, the performance of the SWAT is clearly not as good as the HBV model. In the case of SWAT daily discharge generally, however, showed less accurate simulation with some major discrepancies, which is a common attribute shared by many other studies, and r^2 of only less than 0.6 and Nash-Sutcliffe efficiency N_{SE} of only less than 0.5 automatically were observed for all test catchments. This study confirms that simpler models for continuous river-flow simulation can surpass their complex counterparts in performance. There is a strong justification, therefore, for the claim that increasing the model complexity, thereby increasing the number of parameters, does not necessarily enhance the model performance. It is suggested that, in practical hydrology, the simpler models, “based largely on exercises in pattern recognition and curve fitting, through analysis of the available data” (O’Connor, 1998), can still play a significant role as effective simulation tools, and that performance enhancement is not guaranteed by the adoption of complex model structures.

Acknowledgments

It is deep-rooted in the Christian traditions and conducts that the "one *who does not express thanks to people, cannot be grateful to the Lord God"*. Therefore, after praising and thanking the great God, Glorified and Exalted is He, I would like to use this little space to express my gratitude to the people without their support, this work would have not been realized.

First and foremost I would like to record my heartiest thanks towards Dr.Ing. Yonas Michael, my research senior supervisor, for his continuous technical and encouragement throughout my MSc. Program. I appreciate the time and effort that he has devoted to me in the process of the research work. His sincere help, insightful assistance and guidance were extremely important in order to bring this work to its completion.

I would also like to extend my thanks to Mr. Sirak Tekleab, my research co-supervisor, for his advices, and critical reading and review of my work. He has been teaching me, directly and indirectly, that success is fruit provided by one tree; working hard. I would like also to thank the Blue Nile hydro-solidarity research project, which has been funded by WOTRO, The Netherlands, for its financial support for the execution of this research.

I would also like to acknowledge Dr.Ing. Yilma Seleshi, head of Civil Engineering Department at AAU, Ethiopia, for his support. Some of the ideas of this research are based on concepts I have learnt in his "Applied Hydrology" course. Special thanks are also expressed to staff members of Department of Civil Engineering at AAU, Ethiopia, Dr.Ing. Dereje Hailu, Dr. Ing. Semu Ayalew and Dr.Ing. Habtamu, for their comments and suggestions for the improvement of the research.

This milestone could not have been possible without the love, support, and sense of humour of my mother, brothers and friends. Thanks guys, you all mean so much to me.

Table of Contents

Acronyms

ArcSWAT – The ArcMap Integrated SWAT Hydrological Model
CN – Moisture condition Curve Number
DEM – Digital Elevation Model
DEW02 – Dew Point Temperature Calculator
ET- Evapotranspiration
FAO – Food and Agricultural Organization of the United Nations
GIS – Geographic Information System
HBV-Hydraologiska Byrans Vattenbalansavde
HRU – Hydrologic Response Unit
ITCZ- Intertropical Convergence Zone
+MSL – above mean sea level
MoWR – Ministry of Water Resources, Ethiopia
NMA – National Meteorological Agency, Ethiopia
N_{SE}- Nash Sutcliff Efficiency
PET – Potential Evapotranspiration
ROTO – Routing Outputs to Outlet
SCS – Soil Conservation System
SDSM-Statistical DownScaling Model
SRTM-Shuttle Radar Topographic Mission
SWAT – The Soil and Water Assessment Tool
UNESCO-United Nation Educational Scientific and Cultural Organization
UTM-Universal Transverse Mercater
WGEN – Weather Generator

List of Figures

List of Tables

1. Introduction

1.1. Water Resources Issues in the Blue Nile River

Water resource management concerns have passed through different phases that led to the current state of dealing with equally important and exclusively priority water demand and environmental aspects. The increasing population growth, economic development and climate change have been proved to be causes of the rising water demand, necessity of improving flood protection systems and water scarcity. Being one of the rivers which started to be developed in the ancient period the Nile River is also subject to economic and environmental challenges emanating from the need to balance availability of water with the demand for water (Conway and Hulme, 1996). Under the challenge program for Water and Food, the improved water and land management in the Ethiopian highlands has lots of positive and negative impacts on downstream stakeholders dependent on the Blue Nile.

Figure 1.1*: Map of the Nile Basin (source: NBI)*

The Nile Basin is shared by ten riparian countries: Burundi, Egypt, Eritrea, Ethiopia, Kenya, Rwanda, Sudan, Tanzania, Uganda, and the Democratic Republic of the Congo. Due to increased hydropower, food and agricultural need generated by the rapidly growing population in the riparian states, water demand in the basin becomes conflicting issue. In order to "achieve sustainable socio-economic development through the equitable utilization of, and benefit from, the common Nile Basin water resources", the governments of Nile River riparian countries established what is called NBI aimed at meeting the shared vision.

The Blue Nile is located between $160^0$2' N and $70^0$40' N latitude, and $320^0$30' E and $390^0$49' E longitude and has an estimated area of 311,437 sq. km. From its source Gish Abbay in West Gojam, Abay flows northward as the Gilgel Abbay into Lake Tana. The Blue Nile River (also called Abbay River in Ethiopia) exits from the south east of Lake Tana and flows south and then westwards cutting a deep gorge towards the western part of Ethiopia. Among the eight major sub-basins of the Nile Basin, the Blue Nile contributes more than 80% flow of the Nile during the wet season (Conway and Hulme, 1993; Mishra et al., 2003; Rozanski et al., 2000) and 64 % of the water that reaches Aswan in Egypt (El-Khodari, 2003). From Lake Tana, the river stretches over a length of around 900 km to the Sudan border and 1700 km to Khartoum. Despite its high contribution to the Nile River system, the Blue Nile has suffered from limited hydrological and climatic data availability, which hampers an in-depth study of the hydrology of the basin.

Through the emerging cooperation of Nile Basin riparian countries, various development projects are planned in the Blue Nile Basin. Implementation of those projects needs understanding the catchment hydrology very well. Moreover, absence of sufficient data and published literature together with the size and complexity of the sub-basins (Conway, 2000; Kebede et al., 2006) demands putting a lot of effort to come across appropriate methodologies and tools to make optimal use of water resource development alternatives.

1.2. Background

Along the channel system of a stream, it is common practice to observe concentrated population and their economics; and nowadays, damages and losses of lives are increasing due to severe floods. This shows that the problem of flood requires more attention in both flood forecast and flood protection in short and long term. To be able to deal with these water problems, it is

common to make use of hydrological models. The successful application of such models depends not only on the model structure, the different time and space scale associated, but also on the accuracy of the observed and simulated run-off as the main output. In recent decades, the advent of increasingly efficient computing technology has provided hydrologists with exciting new tools for the mathematical modeling of hydrological systems including, but extending far beyond, the more traditional river-flow forecasting applications.

Elaborate physically-based distributed modeling, and elegant mathematical techniques using Artificial Neural Networks, Fuzzy systems Wavelets, etc. are being used, all with high levels of complexity, but not necessarily with increased levels of efficiency attainment, particularly in the context of flow forecasting. Most such exercises are certainly significant from a research point of view, as they attempt to throw more light on the physical processes involved, but data demands, lack of parsimony in model parameters, and structural complexity can still be a major deterrent when it comes to applying these models in real-life problem solving. In the discharge forecasting context, even simple black-box type system-theoretic models, or physically-inspired lumped conceptual models, can produce better and more reliable discharge forecasting results than complex distributed models (Misgana, 2004).

But, in many developing countries such as Ethiopia, and specifically in the Blue Nile basin, the stream flow observation network is relatively sparse. Up to now, this situation is not improved and the main reason is the lack of funding in developing countries that have more immediate economic issues. However, the economic and social development of each country to some extent depends on the availability of water resources. As a way out in the absence of stream gauging stations, models can be an alternative to estimate the flow.

Catchment modeling can be used to assess the water resource potential and needs choosing the appropriate modeling approach. Uhlenbrook et al. (2004) indicated that applicability of lumped, physically based and conceptual model approaches are restrained by various factors. Use of lumped type modeling approach is mired in its incapability to extrapolate output for future change in model variables. On the one hand, the need for vast data and the sub-grid variability of model parameters make the use of physically based distributed modeling approach difficult for basins of larger sizes than experimental headwaters. Although the availability of input data and their simplicity make conceptual rainfall-runoff models handier than the other two approaches,

indistinct relation between the model parameters and the catchment properties necessitate checking the performance of models. Spatial and temporal variability and complexity of hydrological processes and limited availability of spatially and temporally distributed hydrologic, climatologic, geologic, and land use land cover data challenge the ability to design and forecast.

It is essential that a model used in water-resources planning and management be sufficiently accurate for its intended purpose. Because a model is a simplified depiction of the natural system, its accuracy is subject to question until proven. The acceptability of a model can only be determined by a confrontation with observation. Therefore, the existence of a model does not obviate the need for data from the watercourse, but in fact imposes additional needs and requirements on the data base.

Various research works have been conducted in the Upper Blue Nile catchments to understand hydrologic functioning of the catchment using a conceptual HBV and a Conceptual physically based semi-distributed model SWAT (e.g. Misgana, 2004; Ashenafi, 2007; Rahel, 2007; Irena, 2007; Abdo , 2008; Abeyou, 2008; Perera, 2009; Setegn et al., 2008; Mecca, 2009; Yihun, 2009). Nevertheless; the optimized parameters, which represents the hydrologic system varies from one study to another study in both models. Moreover; lack of detail model parameter identifiability and uncertainty assessment in model parameters and model structure leads to multiple models, which ultimately gives a good hydrograph fit with less understanding of the realistic representation of the hydrologic system.

1.3. Statement of the Problem

In the past few decades several project studies and research activities have been conducted on Upper Blue Nile Basin by different international consultants and academia. With all these previous studies carried out the performance of the models question still persists while the need for a better description of hydro-system raises on the other hand. The choice of a hydrological model depends on the purpose of the applications. Nowadays, there is a lot of discussion on the pro and con's of using lumped or distributed models. Beven (2001) pointed out that if the sole objective is to simulate the rainfall- runoff processes and to predict discharges at the outlet of the catchment, then simpler models (lumped and semi-distributed) are adequate. On the other hand, Refsgaard et al. (1996) argue that there are many modelling objectives

such as prediction of effects of land use change, groundwater abstraction, simulation of water quality, and soil erosion for which distributed models are the only solution. For finding mitigation measures to this and other related questions, the conceptual (HBV-Light) and spatially distributed (ArcSWAT) models are chosen to simulate the discharges at the outlet of five selected catchments in the Upper Blue Nile Basin in order to come in to general consensus which model performs better in this Basin. Therefore, this thesis work bases at answering the core question that asks "which rainfall-runoff model more adequately estimate runoff generated in these catchments, within acceptable accuracy.

1.4. Objectives and Research Questions

1.4.1. Objectives

The main objective of this research work is to compare two modelling approaches using on one hand a conceptual HBV model and on the other hand a conceptual physically based semi-distributed SWAT model to investigate the hydrological processes of five selected catchments in the Upper Blue Nile River Basin.

Specific objectives:

- Calibration and validation of the two models for the selected catchments, and identification of parameters that greatly affect runoff estimation.
- To gain an insight on the benefit associated with increasing catchment data using application of hydrological models.

1.4.2. Research Questions

Based on the above objectives, the following research questions are formulated:

- Which hydrological model (HBV or SWAT) outperforms in simulating the discharge at the outlet of a catchment when various catchment sizes are considered?
- Is the performance of models in these catchments guaranteed by increasing the required input data or model complexity?

1.5. Delimitation

ArcSWAT documentation (Winchell et al., 2007) recommends a baseline period of at least 20 years should be used to simulate runoff using the SWAT model so as to get better output from it. However, due to limitation on to data availability this study considered the period from 1990 to 2005, which ought to be from 1986 to 2005.

Operational validation according to Klemes (1986) should include four levels of testing: (1) split-sample test, (2) proxy-basin test, (3) differential split-simple test, and (4) proxy-basin differential split sample test in order of increasing complexity. However, this study limited to the first split-sample test due to insufficient data availability and because of numbers of test catchments were many, which requires a prolonged research time.

1.6. Structure of the Thesis

This thesis contains seven chapters organized as follows:

Chapter one gives a general introduction to the study with emphasis on a general over view of water resources issues of the Nile River Basin, background, statement of the problem, research question, objectives and delimitation of the study. Chapter two gives a brief description of the study area and data availability. Literature review part, involving hydrologic model classification and previous works in the study area, is compiled and presented in Chapter three. Chapter four discuses the methodology adopted including hydrometreological and hydrological data analysis. Chapter five deals with setting-up of the test catchments for both HBV and SWAT hydrologic model environments. Comparative performance evaluation of the models and discussion of the results obtained were compiled and presented in chapter six. Chapter seven ends with conclusion and recommendations of this study.

2. Study Area and Data Availability

2.1. Study Area

2.2.1. Geographic Location

The Ethiopia part of Blue Nile also called Abay Basin in Ethiopia is located in the northwestern region of Ethiopia between 7^0 40' N and 12^0 51' N latitude, and 34^0 25' E and 39^0 49' E longitude and covers an area of approximately 199,812 km^2. It shares a boundary with the Tekeze basin to the north, the Awash basin to the east and south east, the Omo-Gibe basin to the south, and the Baro-Akobo basin to the south west (Aster &et. al.,2009) . The Upper Blue Nile River exits from the south east of Lake Tana, which is the country's largest freshwater lake; and flows south and then westwards cutting a deep gorge towards the western part of Ethiopia.

Five test catchments such as Gilgel-Abay, Chemoga, Muger, Guder and Didessa, which represent wide variability in geographic location, climatic conditions, areal extent and various physiographical characteristics in the Upper Blue Nile River Basin have been selected. The locations of these catchments are shown in Table 2.1.

Table 2.1*: Facts and figures of the five study areas.*

Study Area	Sub-basin of	Latitude (North)	Longitude (East)	Total Sub-basin Area(sq. km)	Study Catchment Area(sq. km)
Gilgel Abay	Tana	10º56' to 11º51'	36º44' to 37º23'	15,054	1664
Chemoga	South Gojam	10º15' to 10º38'	37º45' to 37º54'	16,762	364
Muger	Muger	10º56' to 11º51'	38º34' to 38º53'	8,188	489
Guder	Guder	8º41.5' to 8º58'	37º30' to 37º39'	7,011	524
Didessa	Didessa	7º42' to 9º10'	36º4' to 37º2'	19,630	9981

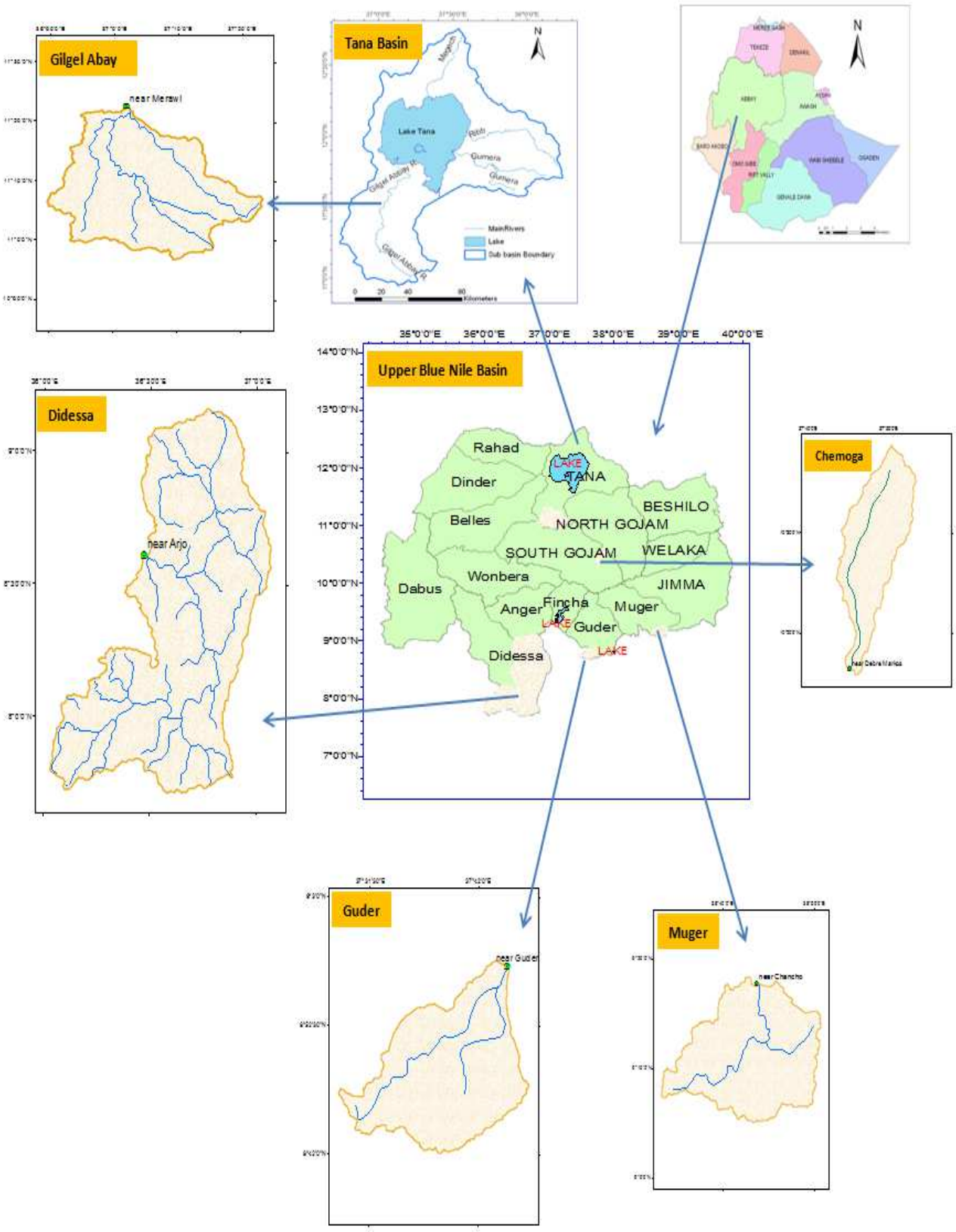

Figure 2.1*: Upper Blue Nile (Abay) Basin, its Sub-basins and locations of the five study catchments.*

2.1.2. Topography

The topography of the Abay basin signifies two distinct features; the highlands, ragged mountainous areas in the center and eastern part of the basin and the lowlands in the western part of the basin. The altitude in the basin ranges from 498m +MSL in the lowlands up to 4261m +MSL in the highlands. The Ethiopian highlands extend from 1500 m+MSL up to as high as 4260 m +MSL, with a slope of greater than 25 percent in the eastern part. Whereas the Ethiopian lowlands flatten 1000m+MSL to 500m +MSL with a slope of less than 7 percent, in Dinder and Rahad sub basins. The map in Figure 2.2 shows the elevation and the slope of the basin.

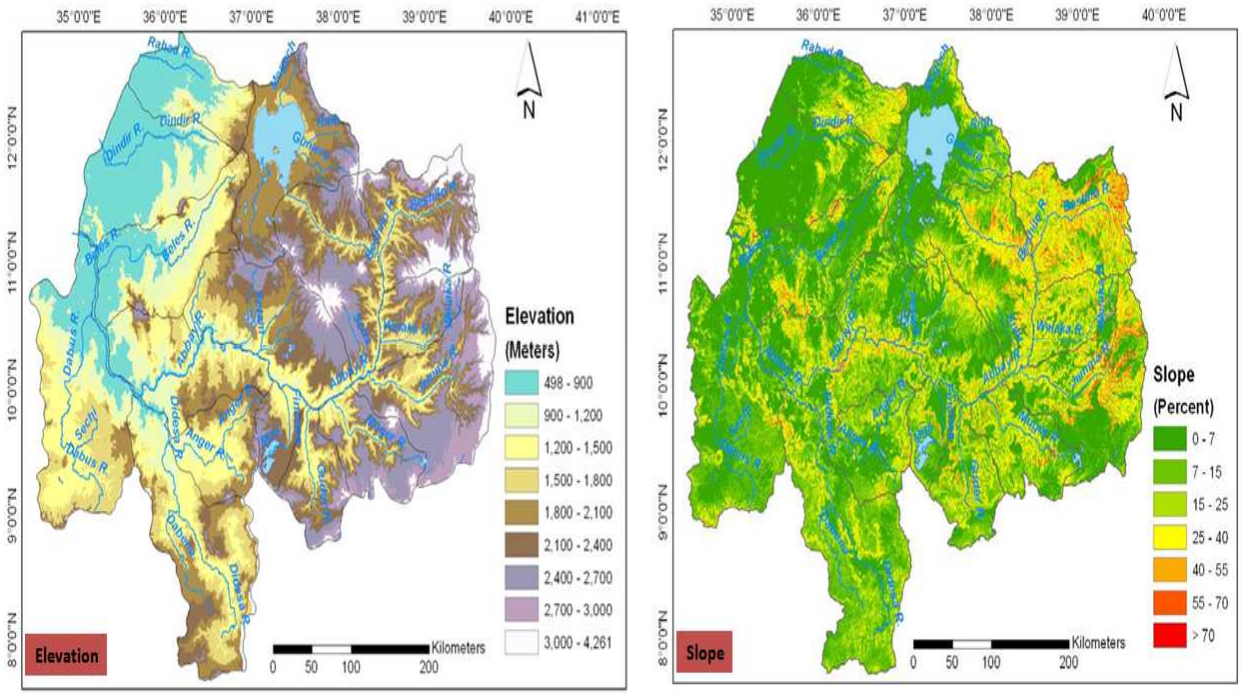

Figure 2.2*: Topography of the Upper Blue Nile River Basin (Source:Atlas of the Blue Nile Basin; Aster &et. al.,2009)*

Gilgel Abay catchment is located south of Lake Tana Sub-basin. Rugged mountainous topography characterizes the southern part, along its periphery in the west and southeast of the catchment whiles the remaining portion of the catchment is typically low laying plateau. The elevation ranges from 1787 m to 3524 m +MSL. From the slope map, around 70% of the catchment area falls in the slope range from 0-8% and 25% of the area falls in the slope range of 8-30%. The remaining 5% of the area has slope greater than 30%.

Topography of Chemoga catchment is dominated by highlands of high altitude, greater than 2200 m +MSL up to 3930m +MSL. The excessive slope area of the watershed lies in the north and decrease southwestwards.

The altitude in Muger sub-basin ranges between 953m +MSL and 3550m +MSL. The highlands in the eastern and southern part of the sub basin are higher in altitude, greater than 2600 meters up to 3550 meters. The lowlands along the Muger River have lower altitude less than 1700m+MSL. Generally, this catchment is characterized by slope of varying range.

Guder sub-basin has an elevation range of approximately between 953m+MSL and 3301m+MSL. The highlands in the southern part of the sub-basin are higher in altitude, greater than 2400 meters up to 3300 meters. The lowlands along the river have lower altitude less than 1800m+MSL.

The altitude in Didessa sub-basin ranges approximately between 630m+MSL and 3130m+MSL. The highlands in the southern part of the sub-basin are higher in altitude, greater than 2100m+MSL up to 3127 m+MSL. The lowlands have lower altitude less than 1100m+MSL in the northern parts of the sub-basin.

2.1.3. Climate

The climate of Ethiopia is mainly controlled by seasonal migration of Intertropical Convergence Zone (ITCZ) and its associated atmospheric circulation, but the topography has also an effect on the local climate. The traditional climate classification of the country is based on altitude and temperature shows the presence of five climatic zones namely: Wurch (cold climate at more than 3000 m altitude), Dega (temperate like climate-highland with 2500-3000 m altitude), Woina Dega (warm-1500-2500 m altitude), Kola (hot and arid type, less than 1500 m in altitude), and Berha (hot and hyper-arid type) climate (NMA, 2001).

In the Upper Blue Nile River Basin, rainfall ranges between 787 mm and 2200 mm per year; The Ethiopian highlands having highest rainfall ranging from 1500 to 2200 mm, whereas lowlands have rainfall less than 1500 mm. The lowest rainfall recorded less than 1000 mm per annum in the Beshelo, Welaka, Jemma, Muger, Guder, and parts of Dinder and Rahad. There is high spatial and temporal variation of rainfall in the study area (Aster &et. al.,2009).

The highest temperature observed in the north western part of the Abay basin with the maximum temperature being 28°C - 38°C and minimum temperature 15 °C – 20 °C. Lower temperature observed in the highlands of Ethiopia in the central and eastern part of the basin with maximum and minimum temperature ranges from 12 °C – 20 °C and -1°C to 8°C respectively (Aster &et. al.,2009).

Potential Evatpotranspiration (PET) in the basin ranges between 1056 mm and 2232 mm per year. High PET is observed between 1800 mm and 2232 mm per year in North Western parts of the basin, in Dinder, Rahad, and parts of Beles and Didessa sub-basins. The Eastern and southern parts having lower PET ranging between 1200 and 1800 mm per year and the lowest PET below 1200 mm per year observed in the parts of the highlands. This is highly correlated with the temperature.

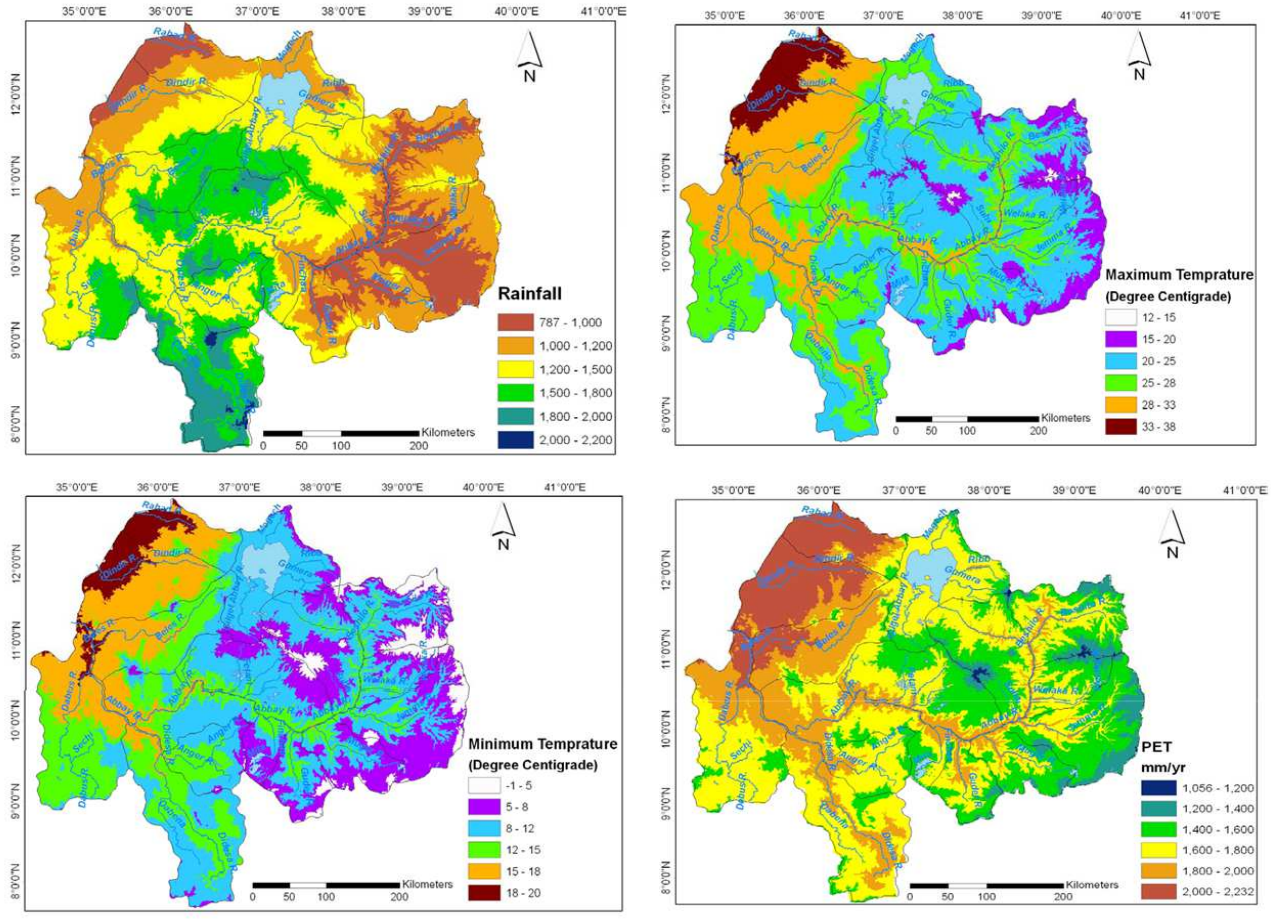

Figure 2.3*: Rainfall Distribution, Maximum Temperature, Minimum Temperature and Potential Evapotranspiration in the Upper Blue Nile River Basin (Source: Atlas of the Blue Nile Basin; Aster Denekew & et. al., 2009)*

Based on the monthly rainfall distribution (fig. 2.1) of Gilgel Abay catchment, July and August are the wettest months of the year which gets monthly rainfall amounts larger than 300mm. The year can be divided into two seasons: a rainy season mainly centered on the months of June to September, and a dry season from October to March. Annual Rainfall distribution ranges from 964 mm up to 2000 mm in this basin. The maximum temperature recorded at Bahirdar station varies between 24°C and 30°C and the minimum temperature varies between 9°C and 15°C.

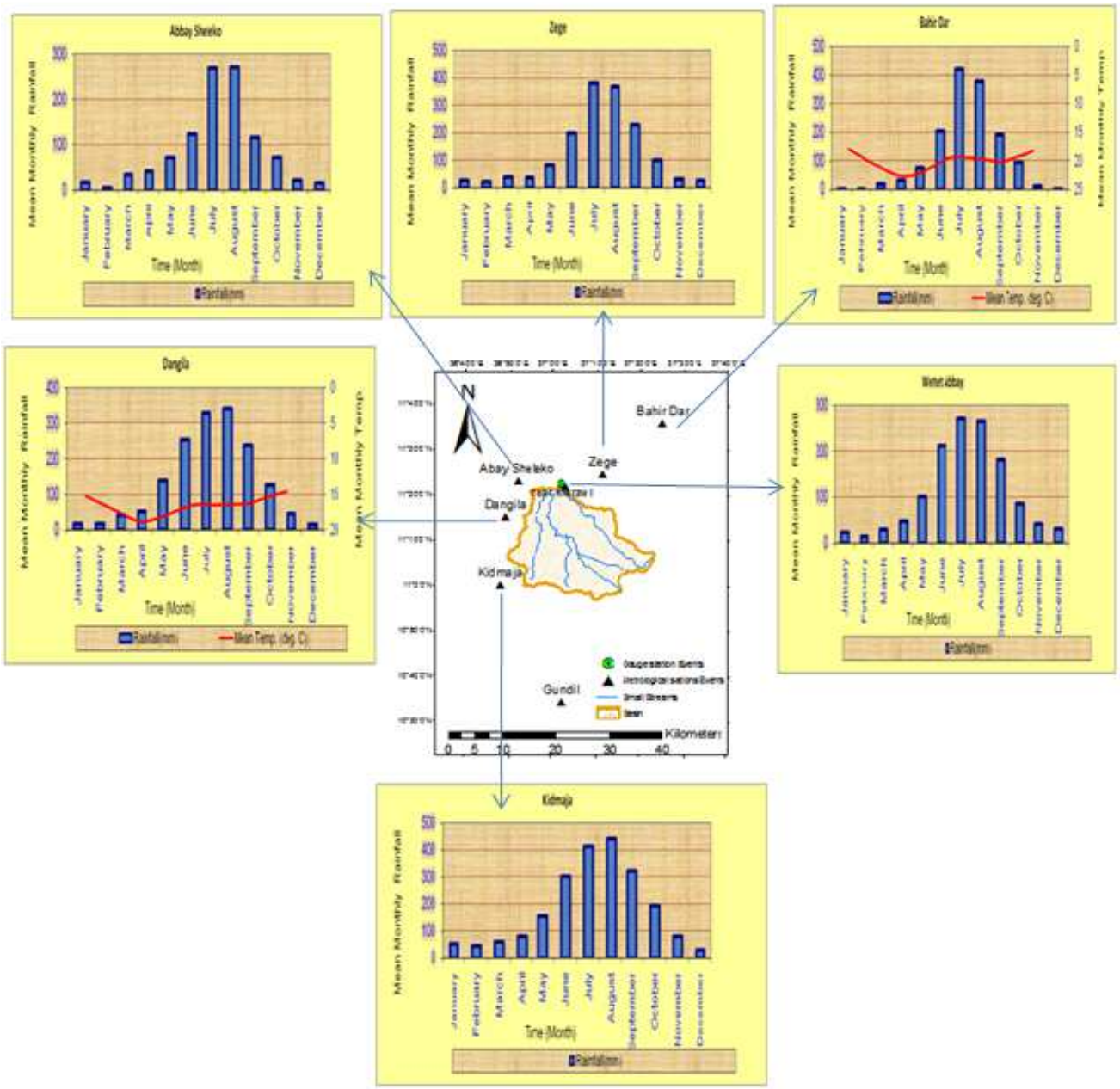

Figure 2.4: ***Mean monthly rainfall and Temperature distributions (1990-2005) at various stations for Gilgel Abay Catchment.***

In Chemoga Catchment the hydrologic year can be divided into two seasons: a rainy season mainly centered on the months of June to September, and a dry season from October to March. The maximum temperature recorded at Debre Markos station varies between 18.84°C and 25.31°C and the minimum temperature varies between 8.6°C and 11.93°C.

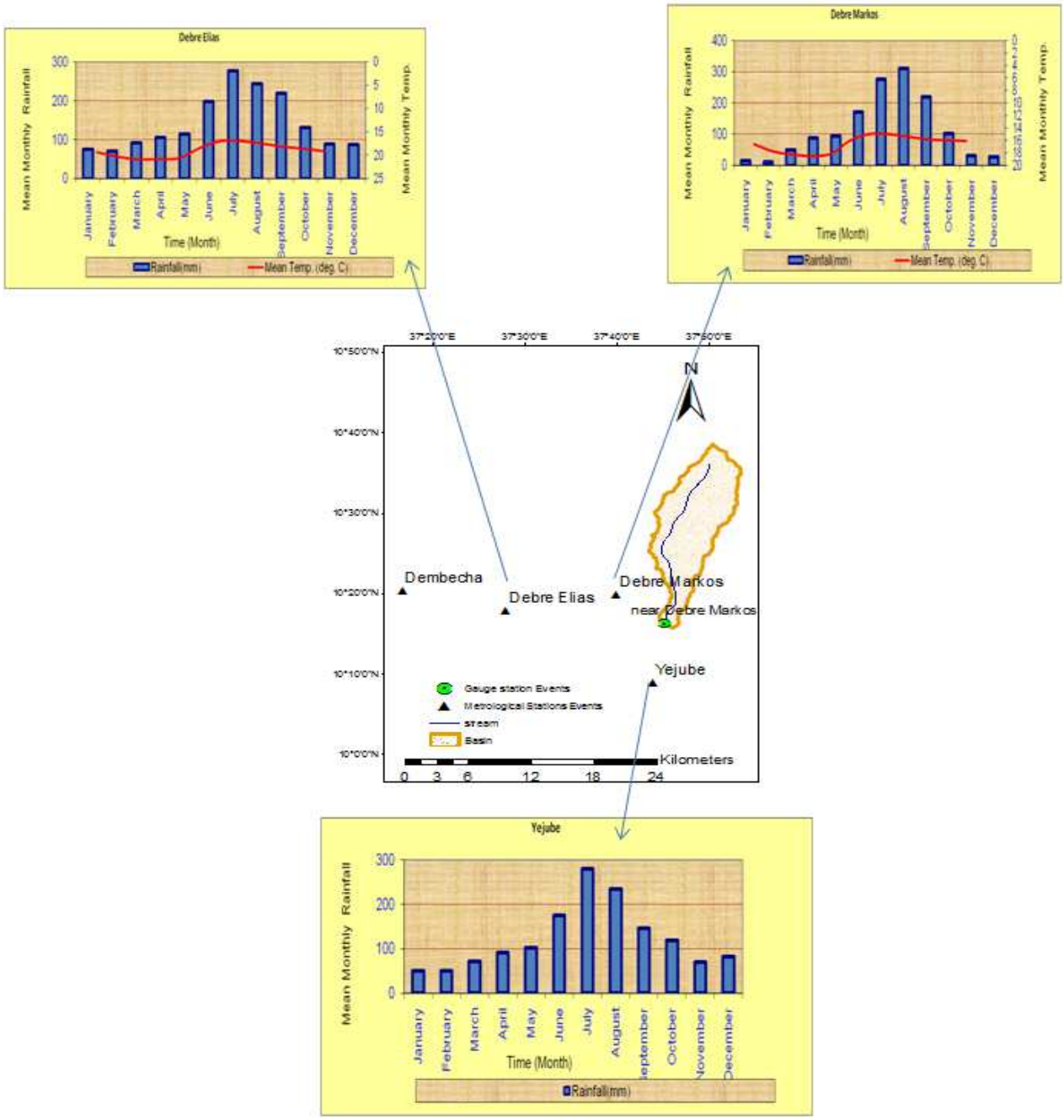

Figure 2.5: ***Long-term average meteorological observations (1992-2005) at various stations for Chemog catchment.***

The Muger sub-basin has an annual rainfall ranging between 833 mm and 1326 mm. July and August are the wettest months of the year which gets monthly rainfall amounts larger than 250mm. The annual maximum and minimum temperature in the sub-basin varies between 16^{0}C - 31.5^{0}C and 3^{0}C -16.5^{0}C respectively.

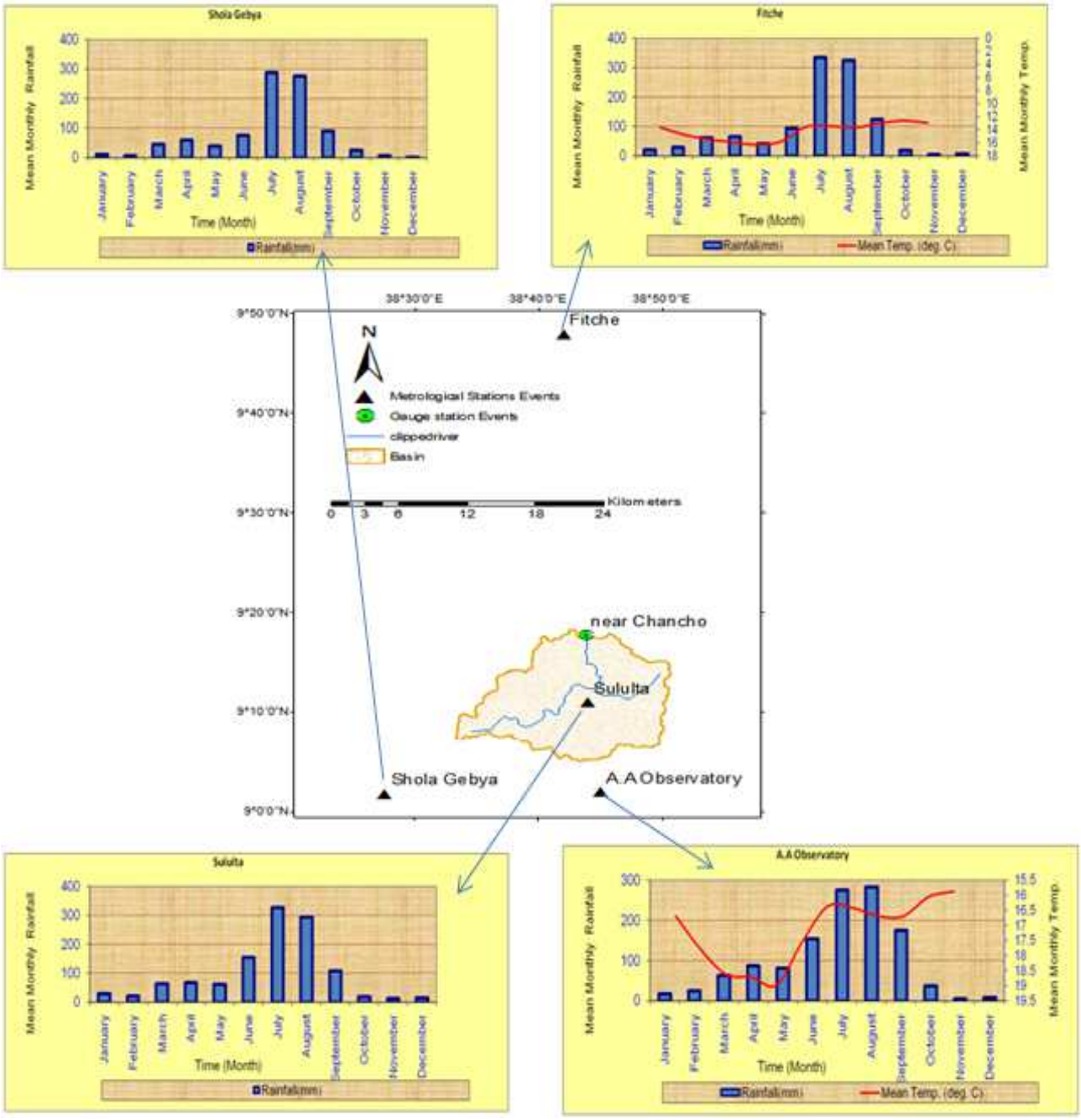

Figure 2.6: ***Long-term average meteorological observations (1992-2005) at various stations for Muger catcment.***

Guder subbasin has an annual rainfall ranging between 901 mm and 1650 mm. June, July and August are the wettest months of the year which gets monthly rainfall amounts larger than 200mm. The annual maximum and minimum temperature in the sub-basin varies between 18^{0}C - 31.5^{0}C and 5^{0}C - 16.5^{0}C respectively. Temperature is higher along the river with a maximum of 28^{0}C - 31.5^{0}C and minimum of 13^{0}C -16.5^{0}C

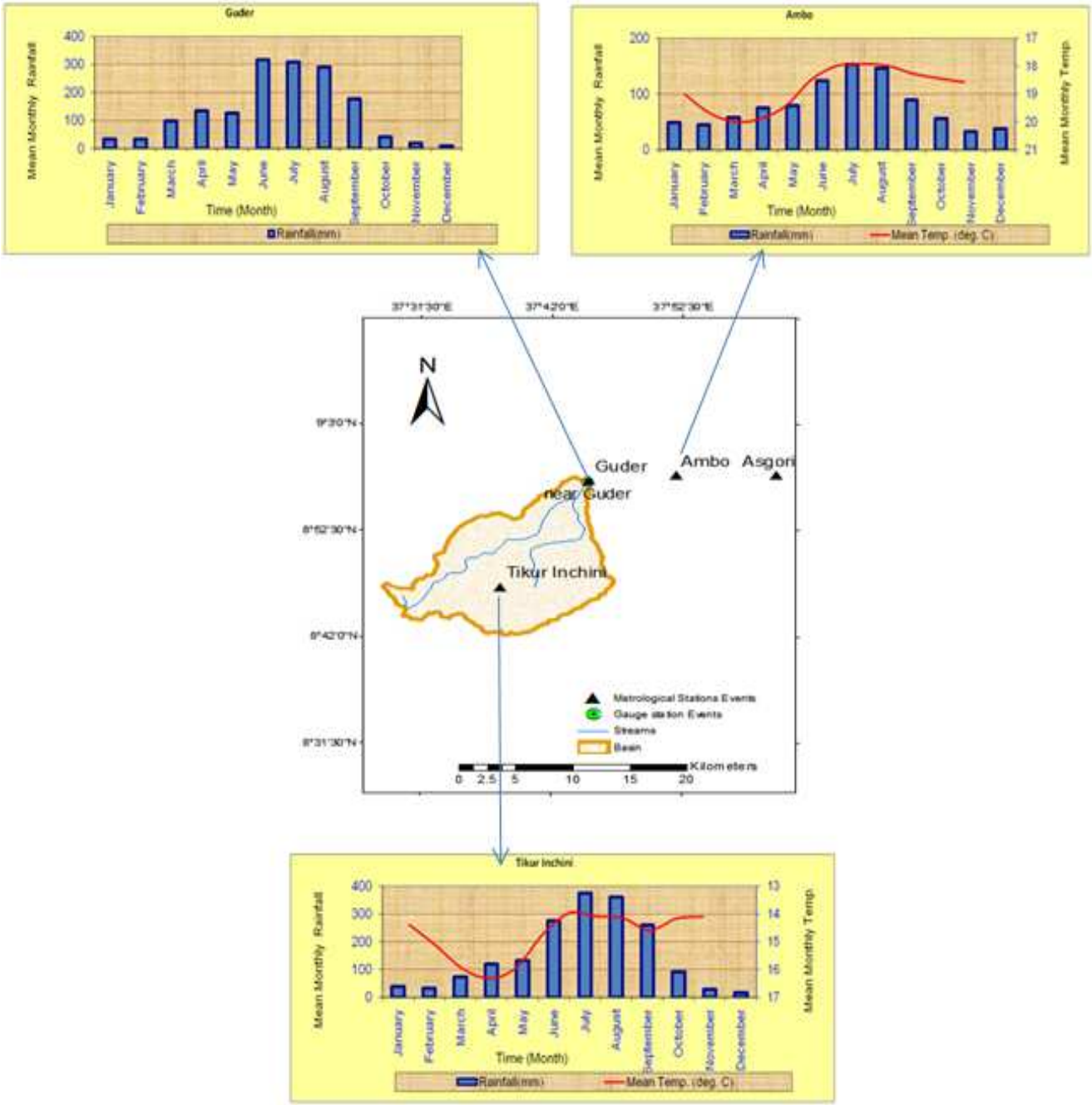

Figure 2.7: ***Average monthly meteorological observations (1990-2005) at various stations for Guder catcment.***

Didessa sub-basin has an annual rainfall ranging between 1200 mm and 2200 mm. The year can be divided into two seasons: a rainy season mainly centered on the months of March to October, and a dry season from November to April. The annual maximum and minimum temperature in this basin varies between 20^{o}C - 33^{o}C and 6.5^{o}C - 19^{o}C respectively.

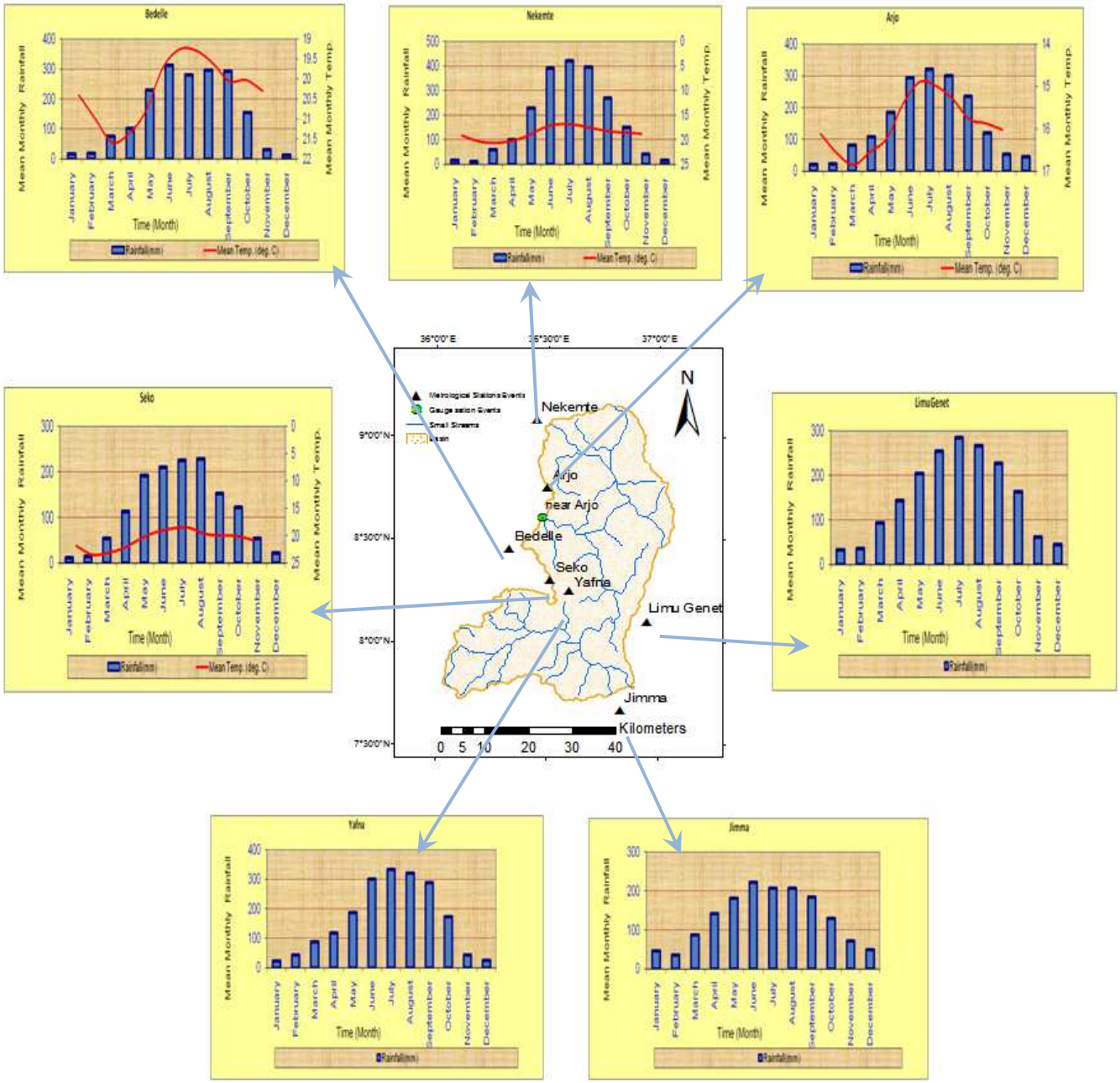

Figure 2.8: ***Mean monthly rainfall and Temperature distributions (1990-2005) to various stations for Didessa Catchment.***

2.1.4. Drainage Network

From its source Gish Abbay in West Gojam, Abay flows northward as the Gilgel Abay into Lake Tana. The Blue Nile River (also called Abay River in Ethiopia) exits from the south east of Lake Tana and flows south and then westwards cutting a deep gorge towards the western part of Ethiopia. A number of tributaries joined this River in Ethiopia: Beshilo, Derame, Jema, Muger, Finchaa, Didessa and Dabus from the east and south; and the Suha, Chemoga, Keshem, Dera and Beles from the north. The Dinder and Rahad rise to the west of Lake Tana and flow westwards across the border joining the Blue Nile below Sennar. The Upper Blue Nile Basin is subdivided into 16 sub-basins based on the major rivers in the basin, the Abbay River and its tributaries (Figure 2.1).

The Gilgel Abbay catchment is the largest of the four main sub-basins of Lake Tana Basin. It drains the southern part of Lake Tana basin to perennially feed Gilgel Abay River which empties itself in Lake Tana, and covers an area of 3156 km^2. On its way downstream, the river receives inflow from several rivers and streams: such as Koga, Kilti, Bered, Areb till it reaches to the outlet at Lake Tana. The total drainage area of the river is around 4100 km^2 and the longest flow path of river from source to the outlet of the catchment is around 163.2 km (Abeyou, 2008).

The Muger River is a north-flowing tributary of the Abay River in central Ethiopia, which is notable for its deep gorge. Its confluence with the Abay is at 9°54′N 37°56′E9.9°N 37.933°E9.9; 37.933 Coordinates: Tributaries of the Muger include the Labbu. The Muger has a drainage area of about 8,188 square kilometers.

The Guder is a river of central Ethiopia, and it is a tributary of the Upper Blue Nile on the left side; tributaries of the Guder include the Dabissa and the Taranta. The Guder has a drainage area about 7,011 square kilometers in size.

The Didessa River is a river in western Ethiopia. A tributary of the Abay River, it rises in the mountains of Gomma, flowing in a northwestern direction to its confluence where the course of the Abay has curved to its southernmost point before turning northwards at about 9°57′N 35°41′E9.95°N 35.683°E Coordinates: The Didessa's drainage area is about 19,630 km^2, covering portions of the Benishangul-Gumuz Region and the Mirab Welega Zone of the Oromia Region.

Tributaries on the right bank include the Enareya, Aet, Wama, and the Angar rivers; on the left side the most important tributary is the Dobana River.

2.1.5. Geology, Soil and Land Cover

The geology of the whole Abay basin signifies different formations such as Basalt, Alluvium, Lacustrine deposit, sand stone, granite and marbles. The dominant rock is Basalt (Tarmaber basalt, followed by Ashange basalt, and Amba Aiba basalt). The major dominant soil types in the basin are Alisols and Leptisols, followed by Nitosols, Vertisols, Cambrisols, Fluvisols and Luvisols. The land cover for the Abay basin is mainly characterized by dominantly cultivated, in the eastern part, and grass land, wood lands, and forest to the western part according to the Ethiopian Ministry of Water Resources land cover classification.

The geology of the Gilgel Abay catchment is dominated by quaternary volcanic rocks overlay the older Tertiary volcanic. The Quaternary volcanic sequence comprises blocky and fractured vesicular basalt, some basaltic breccias and tuffs perhaps as much as 200-300 m thick (SMEC, 2007). Major soil types identified in the watershed are Luvisols, Vertisols, Nitisols, Alisols and Regosols. The most dominant soil type is Haplic Luvisols. The main land covers in the Gilgel Abay catchment are grassland, marshland, cultivated land, forest and grassland with frequent patches of shrubs, woods and trees.

The geology of Muger sub-basin is mainly dominated by Basalt and Sandstone. There are alluvium deposits in southern and eastern parts of the basin. Dominant soil types identified in the gauged watershed are Leptosols, Luvisols, Vertisols, and Cambisols. The most dominant soil types are Leptosols and Luvisols respectively. The land use in Muger basin is dominated by Agro-pastoral and Agriculture while Pastoral land is also observed in some parts of the sub basin.

The geology of Guder catchment is mainly dominated by Adigrat Sand Stone and Basalt. A scattered deposit of Alluvium is also available in the basin. The dominant soil types in the gauged part of the catchment are Leptosols, Vertisols, Luvisols, Nitisols and Alisols. The land use in Guder sub basin is dominated by Agro-pastoral and Agriculture. Pastoral lands are also observed in some parts of the sub-basin.

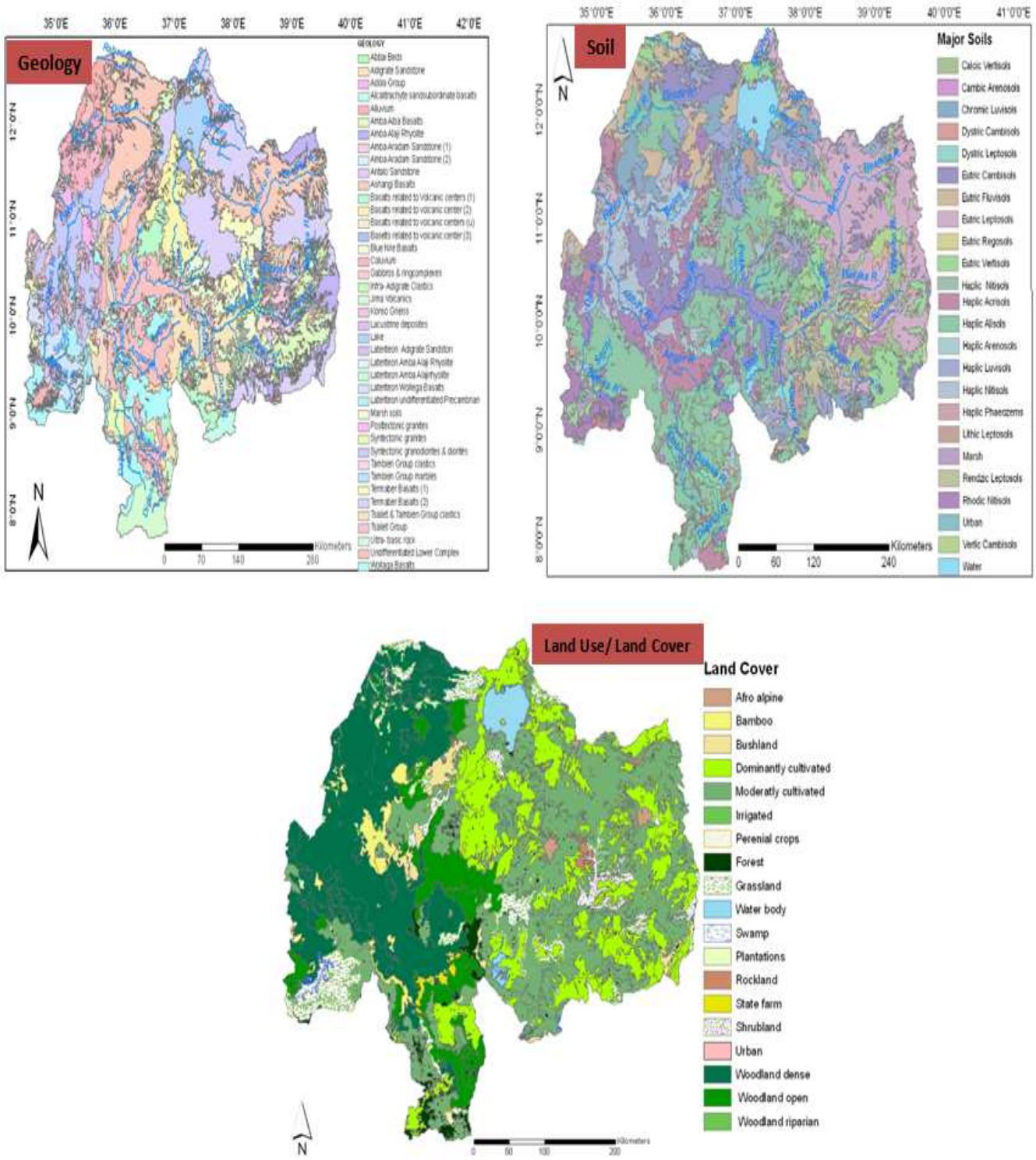

Figure 2.9: ***Geology, Soil, and Land Use and Covers maps of Upper Blue Nile River Basin. (Source: Ministry of Water Resources of Ethiopia).***

The geology of Didessa sub-basin is mainly dominated by Basalt and volcanics. There are also granite, colluvium and alluvium deposits. The dominant soils in the basin are Alisols, and

Acrisols, with the occurence of Vertisols and Nitosols. The Didessa sub basin is dominated by woodlands. The central and southern parts of the sub basin are cultivated.

2.2. Data Availability

2.2.1. Metrological Data

Meteorological data was required for two purposes in this research. First the data was used as input to the two models in hydrological model development; second the data was used for performance evaluation (verification) of the models outputs. Based on these objectives, meteorological data was collected from the Ethiopian National Meteorological Agency in Addis Ababa. Since there are few meteorological stations which have relatively long period of record inside the selected catchments, data was also collected from the stations surrounding the catchments as shown in Figure 2.4 through Figure 2.8.

The number of meteorological variables collected varies from station to station depending on the class of the stations that are grouped into three. The first groups of stations, which are called Class-1, contain only rainfall data, Class-2 stations include maximum and minimum temperature in addition to rainfall data; and that of Class-3 stations contains variables like humidity, sunshine hours, and wind speed in addition to rainfall, maximum temperature and minimum temperature.

Table 2.2*: List of station, location and metrological variables.*

Catchment	No	Station Name	Latitude (Degrees)	Longitude (Degrees)	Rain fall	Max. Temp	Min. Temp	Relative Humidity	Wind Speed	Sun shine Hours
GilgelAbbay	1	Dangila	11.12	36.42	✓	✓	✓	✓	✓	✓
	2	Bahir Dar	11.60	37.42	✓	✓	✓	✓	✓	✓
	3	Zege	11.41	37.19	✓	✓	✓			
	4	Wetet Abay	11.37	37.05	✓					
	5	Abay Sheleko	11.38	36.87	✓	✓	✓			
	6	Kidmaja	11.00	36.48	✓	✓	✓			
	7	Merawi	11.25	33.09	✓					
	8	Gundil	10.57	37.04	✓	✓	✓			
Chemoga	9	Debre Markos	10.33	37.6	✓	✓	✓	✓	✓	✓
	10	Debre Elias	10.30	37.47	✓	✓	✓			
	11	Yejube	10.15	37.733	✓					
	12	Rob Gebya			✓					

	13	Dembecha	10.34	37.28	✓	✓	✓			
Muger	14	A.A Observatory	9.03	38.75	✓	✓	✓	✓	✓	✓
	15	Fitche	9.08	38.70	✓	✓	✓	✓	✓	✓
	16	Sululta	9.183	38.733	✓					
	17	Shola Gebya			✓					
Guder	18	Ambo	8.97	37.87	✓	✓	✓	✓	✓	✓
	19	Guder	8.57	39.47	✓	✓	✓			
	20	Tikur Inchini	8.78	37.63	✓	✓	✓			
	21	Asgori	8.97	38.00	✓	✓	✓			
Didessa	22	Arjo	8.75	36.50	✓	✓	✓	✓	✓	✓
	23	Nekente	9.08	36.45	✓	✓	✓	✓	✓	✓
	24	Seko	8.30	36.52	✓	✓	✓			
	25	Bedelle	8.45	36.33	✓	✓	✓	✓	✓	✓
	26	Yafna	8.250	36.00	✓					
	27	Jimma	7.667	36.833	✓	✓	✓	✓	✓	✓
	28	Limu Genet	8.10	36.950	✓					
	29	Gimbi	9.167	35.783	✓	✓	✓	✓	✓	✓

2.2.2. Hydrological Data

The stream flows of the respective rivers were required for calibrating and validating the models. The gauging stations for each catchment which have relatively long continuous periods of record were selected; and therefore, daily stream flow data for these stations were collected from Hydrology Department of Ethiopian Ministry of Water Resources as shown in table below.

Table 2.3*: Steam flow gauging stations*

River	Gauge Station	Location		Period of Record collected
		Latitude (degrees)	Longitude (degrees)	
Gilgel Abbay	Near Merawi	11.37	37.03	1990 to 2005
Chemoga	Near Debre Markos	10.3	37.73	1990 to 2002
Muger	Near Chancho	9.30	38.73	1992 to 2005
Guder	Near Guder	8.95	37.75	1990 to 2005
Didessa	Near Arjo	8.68	36.42	1990 to 2004

3. Literature Review

This chapter describes the literature review related to the objectives of this study. First of all, a description of hydrologic rainfall-runoff modelling and evaluation of models performance is given to demonstrate how a model performs adequately for the intended application. Next, some previous research works done in the study area are reviewed.

3.1. Hydrologic Rainfall-Runoff Modelling

Understanding the rainfall-runoff relation has been a subject of hydrological research for a long time see (E.g. Misgana, 2004; Ashenafi, 2007; Rahel, 2007; Lijalem, 2007; Irena, 2007; Abdo , 2008; Abeyou, 2008; Perera, 2009; Setegn et al., 2008; Mecca, 2009; Yihun, 2009). These studies concluded that runoff occurs due to a complex interaction between surface, unsaturated, and saturated flow.

Up to now, there are large ranges of hydrological models that have been developed, which are classified in different ways. Based on the way they give spatial representation of the study region models are classified as lumped and distributed. Lumped type models represent a catchment as a point and require only one representative value of each model input for the whole catchment. Alternatively, distributed models allow dividing the catchment in to two or more sub-catchments and require one representative value of each model input variable per sub-catchment. Further classification of hydrological models as physically-based or conceptual is on the basis of the level of complexity and physical completeness in the formulation of structure (Bergstrom and Graham, 1998). Physically-based models simulate flows and storage by using equations derived from the conservation laws of physics, whereas conceptual models use reasonable a priori relationship to simulate flows and storages (Dingman, 2002). Physically-based hydrological models are theoretically better process-based than conceptual models but require extensive data and need less tuning of parameters. Nonetheless, with their less data demanding character the principle on which conceptual rainfall-runoff models based is sufficient to produce reasonably accurate output. Especially in condition where there is scarce of data in the study area, which is a common situation in many developing countries (Ashenafi, 2007), conceptual models are essential tools. However, Bergstrom and Graham (1998) discussed that, nowadays both physically-based and conceptual models are applied by dividing large catchments into sub-catchments (fig. 3.3)

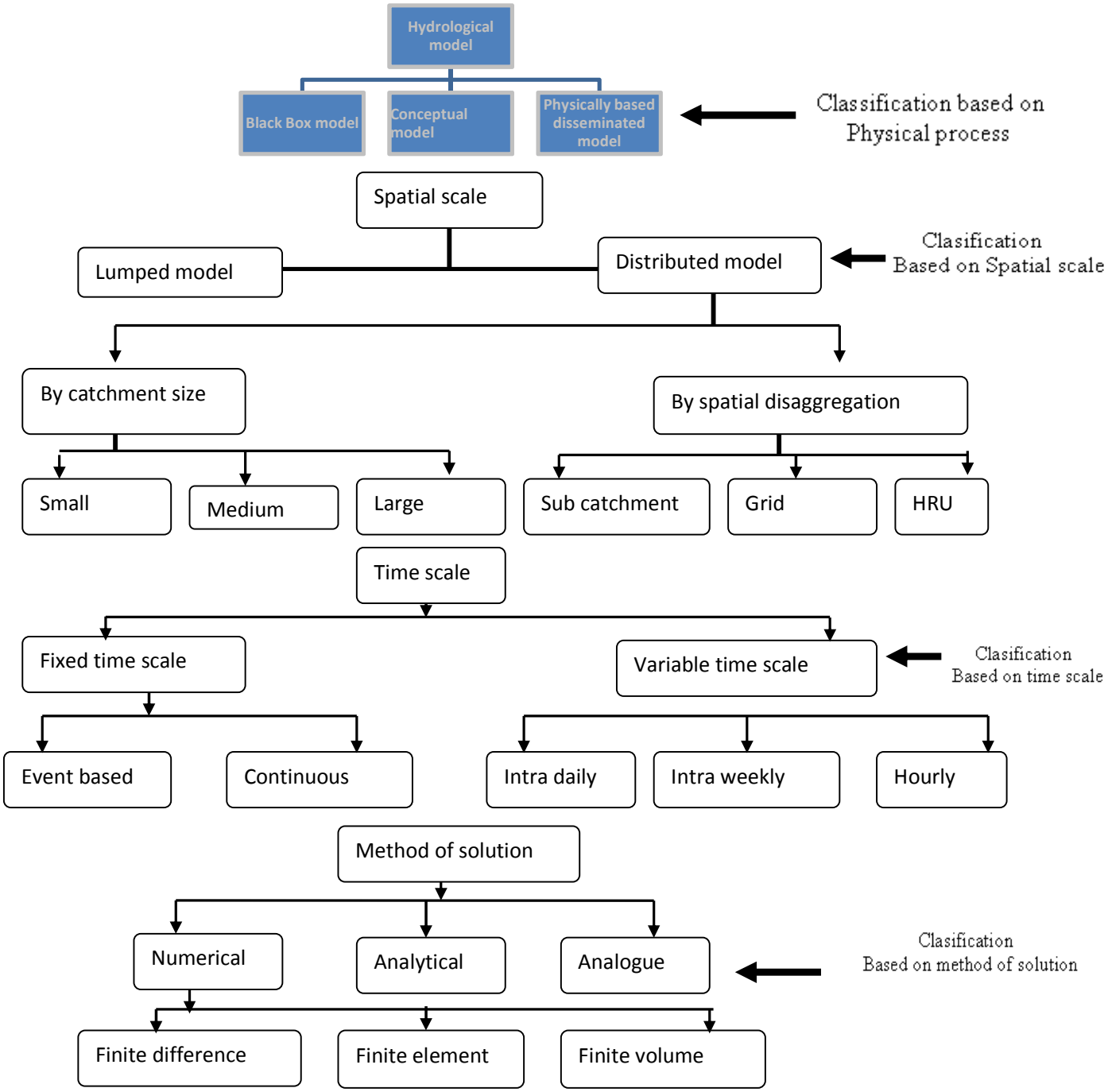

Figure 3.1: ***Simplified flow chart of hydrological model classification (Source: Sirak, 2008)***

3.2. Evaluation of Model Performance

3.2.1. Concept of Operational Validation

The issues of model validation can be confusing for model developers and model users. Firstly, the terms verification and validation have been used interchangeably by some researchers but also have been distinctly defined by others. Rykiel(1996) defines model verification as a demonstration that the computer model is a correct implementation of the logical model. Validation has been defined as a demonstration that a model performs adequately for the intended application. As there is no set of standard in the hydrological modelling definition of these terms, I used the terms interchangeably to refer to the models' ability to simulate an independent data set other than from which it was calibrated although the usage may differ from that promoted by some hydrologic modellers.

Secondly, it is important to distinguish between operational validation, used in this study, and conceptual validity, which concerns a model's theoretical basis. An operationally validated model may work well for a specific use but may not be conceptually valid, i.e. a correct representation of the real system (Rykiel, 1996). For example, many simulation models are developed to meet practical management needs. These models are usually validated by comparing simulated to observed values to determine model performance. The ambiguity arises when inferences about the model's ability to reproduce reality are made from the validation results. A model's output may agree with observed data, but this correspondence does not guarantee that its internal structure is able to reproduce the actual processes operating in the real system. Any inferences made regarding the scientific basis of the model would be scientific hypothesis testing and not model validation.

Operational validation means that a model is acceptable for its intended purpose since it meets specified performance requirements (Rykiel, 1996). Validation does not require that the model applies to more than one condition unless that situation is part of the validation requirement. Good predictions do not have to be obtained only from a model that is entirely mechanistically correct and, conversely, invalidation does not imply that the scientific content of a model is wrong.

The models used in this study were operationally validated by simulating entire observed hydrographs of rainfall-runoff events for the purpose of model comparison. In this study, Klemes' (1986) split-sample test evaluation scheme, introduced in the following section, and graphical and numerical criteria were used for the operational validation of the models.

3.2.2. Klemes' Hierarchical Approach to Operational Testing

Klemes (1986) proposed a hierarchical method for the comparison of different types of hydrological models. The system is hierarchical since the modelling tasks are ordered according to their increasing complexity and demands on model capability.

Klemes' system includes tests for geographic and climatic transposability. Transposability refers to a model's ability to perform satisfactorily when applied to other catchments or climatic conditions for which it was not calibrated. Model transposability has long been recognized as the major aim and the most difficult aspect of hydrological simulation models (Klemes, 1986). In many countries, especially in the developing world, basic data for water assessment are sparse or in some cases almost non-existent. This lack of available data is one reason why it is important to develop realistic models that can be applied to ungauged catchments where a historical record of streamflow is not available. Despite this fact, relatively little effort has been expended on the testing of the transposability of existing model types in comparison to the number of published papers on hydrologic modelling.

The procedure recommended by Klemes consists of four levels of testing and aims to test (1) not only a model's ability to simulate current conditions in a given catchment (split-sample test), but also (2) its geographic transposability to other catchments within the same region (proxy-basin test). The proxy-basin test for transposability is crucial when dealing with the problem of rainfall-runoff modelling on ungauged basins. A model's transposability within a catchment (3) is also tested in how well it would reflect changes in climatic inputs or land use (differential split-simple test). The differential split-sample test can also be used to evaluate a model's ability to predict unusually large or rare events that may not be represented in the record runoff data. The highest level of testing involves evaluating model performance when testing for (4) geographic and climatic transposability simultaneously (proxy-basin differential split sample test). Such universal transposability is the ultimate goal of hydrological modelling, a goal that may not be attained in decades to come (Klemes, 1986). However, models with this capability

are in high demand and hydrologists are being encouraged to develop them despite the fact that so far even the much easier problem of simple geographical transposability within a region has not yet been satisfactorily resolved (e.g., Chiew and McMahon, 1994; Karnieli et. al., 1994). It is important to implement a standard testing framework such as Klemes proposed so as to raise the level of operational credibility given to simulation models, to discourage exaggerated claims of model performance and to encourage research leading to better models

3.3. Previous Works in the Study Area

Various study works have been conducted in Upper Blue Nile Basin to investigate hydrological processes with computer assisted models, and some of which previously conducted in the basin are tabulated in Table 3.1.

Table 3.1*: Previously done researches on application of Hydrological Model in Rainfall-runoff processes.*

Investigator	Research Topic	Implemented Model	Investigated Catchment
Ashenafi Seifu, (2007)	Catchment Modeling and Preliminary Application of Isotopes for Model Validation in Upper Blue Nile Basin, Lake Tana, Ethiopia	HBV-light	-Gilgel-Abbay
Abeyou ,(2008)	Hydrological Water balance of Lake Tana Upper Blue Nile Basin, Ethiopia	HBV-96	-Lake Tana -Gilgel-Abbay -Rib -Koga -Gumera
Irena, (2007)	Rainfall estimation by Remote Sensing for conceptual rainfall-runoff modeling in the Upper Blue Nile basin	HBV-96 SAC-SMA	Gumero within in Jemma
Sirak Tekleab, (2008)	Watershed Modelling of Lake Tana Basin Using SWAT	AVSWAT	-Lake Tana -Gumera -Rib -Megech -Gilgel-Abbay
Abdo, (2008)	Assessment of Climate Change Impacts on the Hydrology of Gilgel Abbay Catchment in Lake Tana Basin, Ethiopia	HBV-96	Gilgel-Abbay
Mecca Selman, (2008)	Water Balance Modelling for Reservoir Planning in Ribb Catchment, Ethiopia	HBV-96	Rib

Rainfall Estimation by Remote Sensing for Conceptual Rainfall-Runoff modelling in the Upper Blue Nile River Basin (Irena, 2007). The objectives of this study are: estimation of rainfall from satellite imagery and assessing the performance of conceptual rainfall-runoff model using ground truth and satellite data as input. This work didn't take into account the issues associated with calibrating satellite data, but with the direct use of available rainfall data as input to hydrological models. Secondly, two conceptual models SAC-SMA and HBV-96 are chosen to test their performance by applying two different input data in Gumero sub-catchment. Based on ground truth input data, both models are calibrated by adjusting the parameters manually. Considering both quantitatively and qualitatively judgment, the performance of the model was not as satisfactory as expected. The satellite data are applied to the models to see how they perform, and the models responded to the network and satellite data, although some deviations are observed. These deviations are related to the results established from RS, which have direct impact to the hydrological model. Thus, further study in rainfall estimation from satellite should be carried out.

Catchment Modeling and Preliminary Application of Isotopes for Model Validation in Upper Blue Nile Basin, Lake Tana, Ethiopia (Ashenafi Seifu, 2007): In this study the catchment modeling was conducted with the object of understanding hydrologic functioning and runoff generation mechanisms of Gilgel Abay catchment and correlating response pattern of Gilgel-Abay catchment with the inter-annual water level variation of Lake Tana by using stable isotopes, catchment modeling was carried out by using the HBV model. The catchment was divided in to two gauged (Upper Gilgel Abay Sub-catchment (UGASC) and Koga Sub-catchment (KSC)) and one ungauged sub-catchments. Manual calibration of the daily time step models for all the three catchment representations (CRs) (lumped, lumped with multiple vegetation zones and semi-distributed) showed good ($R_{eff} > 0.75$) and satisfactory ($R_{eff} > 0.6$) efficiencies in UGASC and KSC, respectively. But the fifteen days time step models demonstrated good model performance in both sub-catchments. Model parameter transferability test conducted on the daily time step models showed poor performance in both sub-catchments; whereas the fifteen days time step model showed high R_{eff} values. However, on the basis of subjective evaluation transferability of the model parameters was not favored. As a result of running 1000000 Monte Carlo simulations (per CR), the dissimilar hydrologic behaviors of UGASC and KSC explained the unfeasibility of transferring model parameter set values between the two sub-catchments.

Hydrological Balance of Lake Tana Upper Blue Nile Basin, Ethiopia (Abeyou, 2008): Daily flows from ungauged catchments are estimated by transferring model parameters from gauged catchments using a regionalization procedure, a spatial proximity procedure and catchment area ratio's methods. In regionalization gauged catchment model parameters of the conceptual rainfall-runoff model HBV are transferred to ungauged catchments based on catchment characteristics to allow for runoff simulation. In proximity procedure model parameters of gauged catchments are transferred to neighboring ungaugeg catchment. In area ratio model parameter set of gauged catchments are transferred to ungauged catchments of comparable area.

Assessment of Climate Change Impacts on the Hydrology of Gilgel Abay Catcment in the Lake Tana Basin, Ethiopia (Abdo, 2008): This report presents the results of a study on downscaling large scale atmospheric variables simulated with General Circulation Models (GCMs, which are considered as the most advance tools for estimating future climate change scenarios operate on a coarse scale) to meteorological variables at local scale in order to investigate the hydrological impact of possible future climate change in Gilgel Abbay catchment. Statistical Down Scaling Model (SDSM) was employed to convert the GCM output into daily meteorological variables appropriate for hydrological impact studies. The meteorological variables (minimum temperature, maximum temperature and precipitation) downscaled from SDSM were used as input to the HBV hydrological model which was calibrated (R^2=0.86) and validated (R^2=0.76) with historical data to investigate the possible impact of climate change in the catchment. The results obtained from this investigation indicate that there is significant variation in the seasonal and monthly flow. In the main rainy season (June-September) the runoff will be reduced by 12% in the 2080s. The result from synthetic (incremental) scenario also indicates that the catchment is sensitive to climate change. As much as 33% of the seasonal and annual runoff will be reduced if an increment of 2^{o}C in temperature and reduction of 20% rainfall occur simultaneously in the catchment.

Water Balance Modelling for Reservoir Planning in Ribb Catchment, Ethiopia (Mecca Selman, 2008): For the case of runoff assessment per land cover unit, the catchment area has been classified into five land cover units (bareland, crops, forest, grassland and water) using Landsat images. Catchment extraction was established from ASTER image elevation data and the catchment is divided in to three subbasins. The HBV-96 model was applied to simulate the runoff from Ribb

River using daily hydrometeorological data. The Nash-Sutcliff efficiency between observed and simulated of calibration and validation of the model shows that $R^2 = 0.8$ for calibration and $R^2 = 0.81$ for validation.

Watershed Modelling of Lake Tana Basin Using SWAT (Sirak Tekleab, 2008): In this study work due emphasis have been given for the estimation of runoff contribution from gauged and ungauged catchments to Lake Tana using semi distributed model known as SWAT. The model was calibrated and validated over the gauged upper reaches of major catchments of Gilgel Abay, Koga, Gumera, Rib and Megech. The model was calibrated for the period from 1996-2001 and validated for the period from 2002-2004. The performance of the model was evaluated on the basis of performance rating criteria, coefficient of determination, Nash & Sutcliff efficiency, and percent deviation. The overall performance of the model appears satisfactory. The R^2 for all catchments vary between 0.69 to 0.89 during calibration and 0.81 to 0.86 during validation. The hydrograph fit between the estimated and observed is also adequately represented except the underestimated, which stands out for Gilgel Abay, Gumera and Megech catchments for the year 2003. The year 2003 has been underestimated due to many missed rainfall data of the surrounding stations. The Curve Number (CN) has been found the most sensitive parameters in all the catchments indicating the importance of this parameter during modeling and fine tuning. However, the level of sensitivity of this parameter differs from catchment to catchment. The calibrated parameters were transferred to un-gauged catchments to estimate the ungauged flow contribution based on similarity of the hydrologic response unit (HRUs).

4. Methodology

4.1. Hydrometeorological and Hydrological Data Analysis

Hydrological modelling to a large extent depends on hydrometeorological (precipitation, temperature and potential evapotranspiration) and hydrological (river discharge and lake water level) data. Reliability of the collected raw hydrometeorological and hydrological data significantly affects quality of the model input data and, consequently, the model simulation (Ashenafi, 2007). This portion sequentially presents, rough data screening of raw hydrometeorological and hydrological data, completion of identified missing data, and analysis done to check consistency and homogeneity of the data sets.

4.1.1. Data Screening

4.1.1.1. Rainfall data

Rough rainfall data screening of all meteorological stations in the study area was first done by visual inspection of daily rainfall data. Because of long breaks in rainfall records of some stations and absence of lengthy overlapping period of record this inspection was done in the records of the hydrologic years from 1990 to 2005. Visual assessment of the tabulated daily rainfall data records for existence of misplaced decimal points and non-numeric figures were conducted. To detect consistency of daily observations, the meteorological stations were grouped in to five regions based on their respective catchment (see Appendix C).

Beside the visual and graphical data comparison, assessment of spatial homogeneity of the daily rainfall data indicated good correlation between records of all meteorological stations with the exception of Merawi. Despite the noticeable rainfall amount variation pattern in the areas, computation of correlation coefficient on the daily records between January 1990 and December 2005 showed values between 0.2 and 0.6. This is not bad for a daily rainfall data series.

4.1.1.2. River Discharge

The initial step taken during the river discharge data screening as suggested by Gordon et al. (1992) was quick visual scan of the data time series to detect gross errors such as erroneous peak flow, missed recordings, and flows of constant rate. It helped to detect years with magnitude change in the data, long periods of missing records, and short-term missing data.

4.1.2. Missing Data Completion

Missing data is a common problem in hydrology. To perform hydrological analysis and simulation using data of long time series, filling in missing data is very important. The missing data can be completed by using meteorological and/ or hydrological stations located in the nearby, provided that the stations are located in a hydrologically homogenous region. Joint application of the regression analysis and simple ratio techniques made possible completing short and long period breaks in data series for given meteorological and stream flow gauging stations.

4.2. Hydrological Model Selections

Many investigations were done in the past two decades on the application of hydrological model for simulation of runoff on variety of water resource issues. These investigations can range from the evaluation of annual and seasonal streamflow variation using simple water-balance models to the evaluation of variations in surface and groundwater quantity, quality and timing using complex distributed-parameter model that simulate a wide range of water, energy and biochemical processes. The choices of a model for a particular case study depend on many factors, the purpose of the study and model availability being the dominant ones (Irena, 2007).

For detailed assessment of surface flow, conceptual models were applied in many parts of the world. One of the more frequently used conceptual model for discharge estimation is the HBV model. Even if HBV is a simple model, its application under various physiographic and climatological conditions has proved its strength and generality of its structure (Lindstrom, 1997). HBV was applied in the Baltic Sea basin (Bergstrom & et al., 1998), its performance was analyzed in four large river basins located in different climatic zones in Africa, Europe and South America (Liden and Harlin, 2000) and according to Bergstrom and Graham (1998) it has been applied to several hundred catchments in more than 40 countries world-wide. In conclusion, the HBV model is selected for this study because of the following reason:

1. the input data requirement is moderate;
2. the model simulate the major hydrological process in the catchments;
3. the model was tested for the runoff simulation on hydrological study in different parts of the world and
4. the availability of the model

Many comprehensive spatially distributed hydrologic models have been developed in the past decade due to advances in hydrologic sciences, Geographical Information System (GIS), and remote sensing. Among the many hydrologic models developed in the past decade, the Soil and Water Assessment Tool (SWAT), developed by Arnold et al. (1993), has been used extensively by researchers. SWAT has been integrated with GRASS GIS (Srinivasan and Arnold 1994; Srinivasan et al. 1998) and with ArcView GIS (Di Luzio et al. 2002), and the hydrologic components of the model have been validated for numerous watersheds under varying hydrologic conditions (Arnold and Allen 1996; Arnold et al. 1998; Misgana,2004; Lijalem, 2006; Rahel 2007; Sirak, 2008; Yihun, 2009. In order to optimally calibrate the model parameters, especially for large-scale modeling, an auto-calibration routine has been added to SWAT (Eckhardt and Arnold, 2001; Van Griensven and et al., 2002). SWAT has been used by many investigators since it

(1) Uses readily available inputs for weather, soil, land, and topography,
(2) Allows considerable spatial detail for basin scale modeling, and
(3) It is capable of simulating crop growth and land management scenarios.

A conceptual HBV model and a physically based semi-distributed SWAT model were used in this study. For completeness, brief descriptions of these models are provided in this section.

4.3. HBV-Light Model

The HBV model is a conceptual hydrological model for continuous simulation of runoff. It was originally developed at the Swedish Meteorological and Hydrological Institute (SMHI) in the early 70´s to assist hydropower operations (Bergström and Graham, 1998) by providing hydrological forecasts. The model was named after the abbreviation of Hydrologiska Byråns Vattenbalans-avdelning (Hydrological Bureau Waterbalance-section).

4.3.1. HBV Model Structure

The HBV model is a conceptual model of catchment hydrology which simulates daily discharge using as input variables: daily rainfall and temperature and monthly estimates of potential evaporation. The model consists of subroutines for snow accumulation and melt, soil moisture accounting procedure where groundwater recharge and actual evapotranspiration are coupled,

routines for response and transformation function for runoff generation and finally, a simple routing procedure. Further descriptions of the model can be found elsewhere (Bergstrom, 1992, 1995; Harlin & Kung, 1992; Seibert, 1997). The version of the model used in this study, "HBV light 1.2" (Seibert, 1997), corresponds to the version HBV-96 described by Bergstrom (1992).

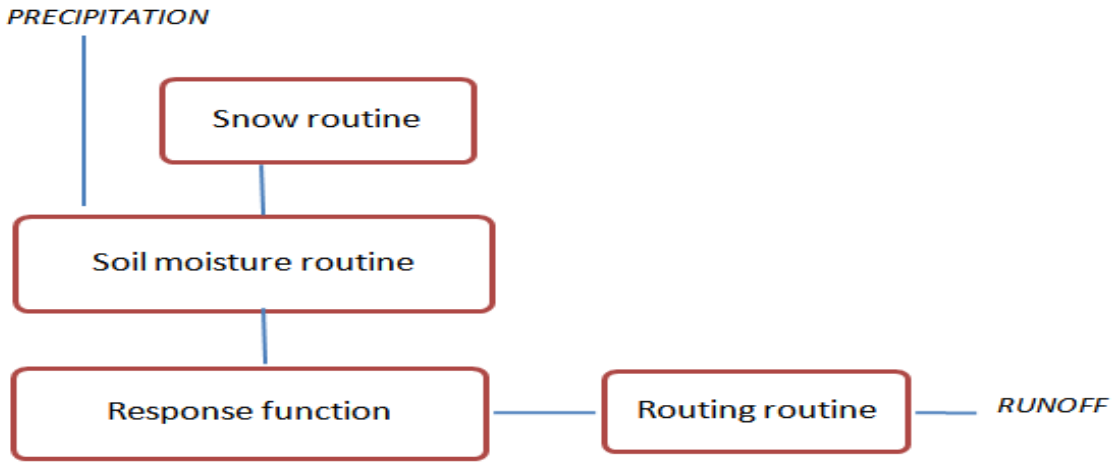

Figure 4.1: ***Routes in the HBV model.***

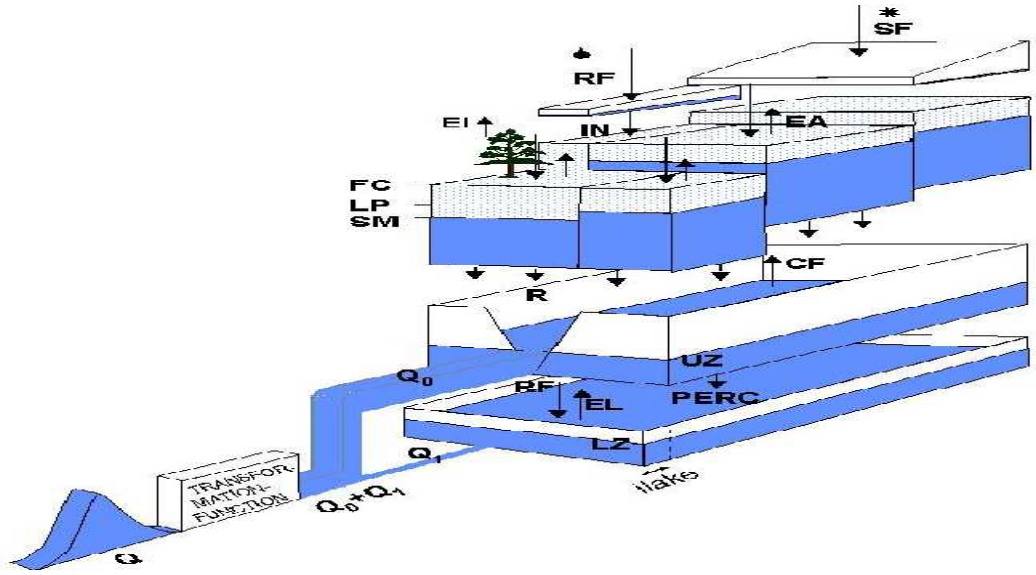

Figure 4.2: ***Schematic presentation of the HBV model (IHMS, 2006).***

Where

SF: Snow fall, RF: Rainfall, EI: Evapotranspiration, IN: Infiltration, EA: Actual evaporation, FC: Maximum soil moisture storage, SM: Compound soil moisture routine, CF: Capillary rise, R: Seepage, UZ: Upper zone reservoir, Qo: Direct runoff from upper reservoir, EL: lake evaporation, PERC: percolation capacity, LZ: Lower zone reservoir and Q1: Base flow lower reservoir. Note all units are in mm.

As shown in the figure 4.3, overland flow is not incorporated which is mostly a case in Europe not in Ethiopia opposed to the actual process. However, in this study, performance comparisons were made based on operational validity not that of conceptual validity, model's theoretical basis.

4.3.1.1. Soil Moisture Routine

The soil moisture accounting routine is the main part controlling runoff formation. This routine is based on the three parameters:

- FC = maximum soil moisture storage (mm),
- LP = soil moisture value above which ET_{act} reaches ET_{pot} (mm) and that of
- BETA= parameter that determines the relative contribution to runoff from rain or snowmelt (-)

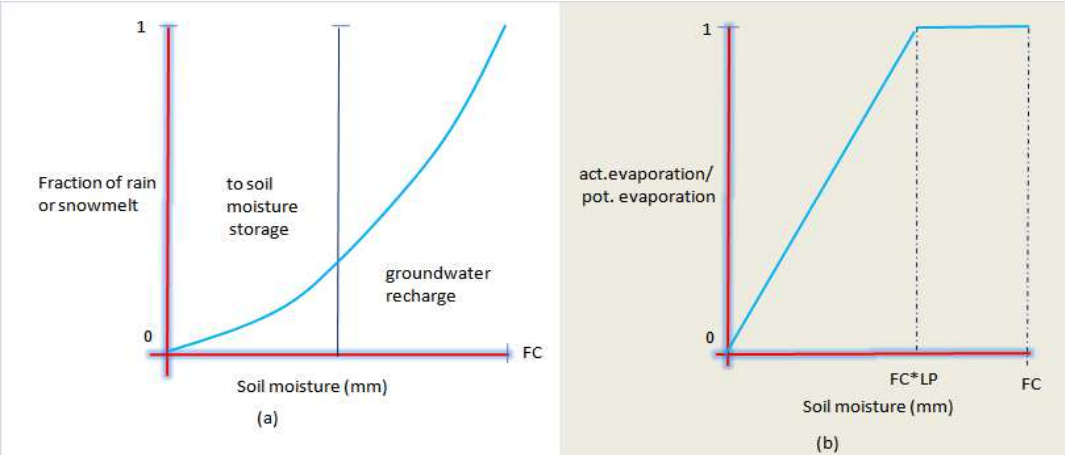

$$\frac{recharge}{p} = \left(\frac{S_{sm}}{FC}\right)^{BETA} \text{----------(4.1)}$$

Figure 4.3: ***(a) Contributions from rainfall or snowmelt to the soil moisture storage and to the upper groundwater zone; (b) Actual evaporation as affected by soil moisture content in relation to threshold level for E_A=E_P (source: Seibert, 2005).***

Where: S_{sm} is computed soil moisture storage; and note that FC is a model parameter and not necessarily equal to measured values of 'field capacity'.

4.3.1.2. Response Routine

The model of a single linear reservoir is a simple description of a catchment where the runoff Q(t) at time t is supposed to be proportional to the water storage S(t).

Figure 4.4: ***A realization of a single linear reservoir is a box with a porous outlet, thus obtaining Equation (4.1) from Darcy's law.***
Where S = storage (mm), Q = outflow (mm day-1), t = time (day) and k = storage (or recession) coefficient (day^{-1})

$$Q(t) = k \cdot S(t) \quad \text{---------- (4.2)}$$

The water balance equation of a catchment $P(t) = E(t) + Q(t)\frac{dS(t)}{dt}$ and ignoring precipitation and evapotranspiration together with equation 4.1 the differential equitation gives solution function

$$Q(t) = Q(t_o).\, e^{(t_o - t)k} \quad \text{---------- (4.3)}$$

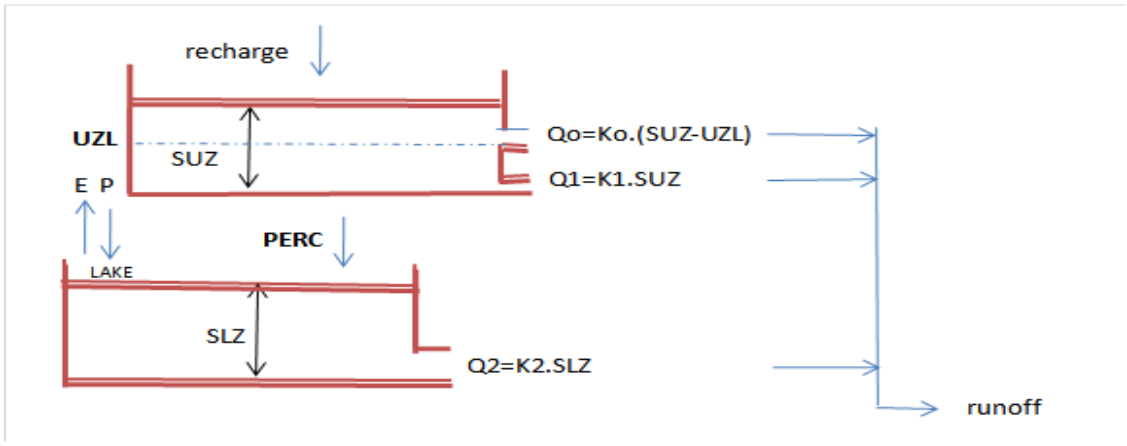

Figure 4.5: ***Response function and Response routine of the HBV model***

Where; recharge = input from soil routine ($mm\ day^{-1}$)
SUZ = storage in upper zone (mm) and has no upper limit.
SLZ = storage in lower zone (mm)
UZL = threshold parameter (mm)
PERC = max. Percolation to lower zone ($mm\ day^{-1}$)
K_i = Recession coefficient (day^{-1})
Q_i = runoff component ($mm\ day^{-1}$)

Note that SUZ has no upper limit, Q_2 can never exceed PERC, and SLZ can never exceed PERC/K2

If lnQ is plotted against time during a dry period, the slopes of the hydrograph at different runoff values provide good first estimates of the response-function parameter.

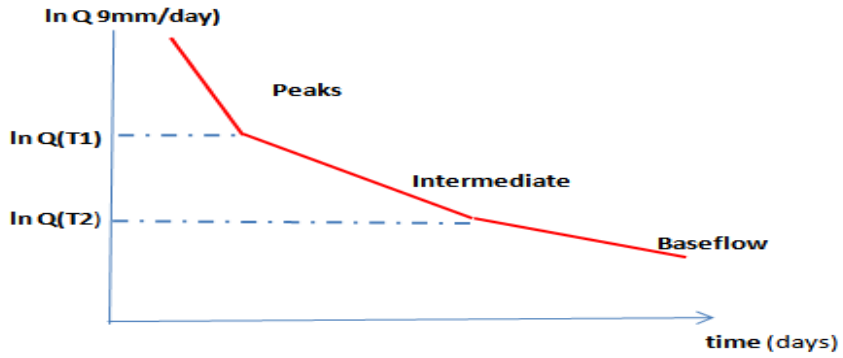

Figure 4.6: ***Schematic shape of recession in relation to the different parameter***
Slope of the recession: -Peaks: K0 + K1 + K2 with thresholds Q(T1) ≤ PERC+K1UZL and Q(T2) ≤ PERC

-Intermediate: K1 + K2

-Baseflow: K2

4.3.1.3. Routing Routine and Transformation Function

The generated runoff of one time step is distributed on the following days using one free parameter, MAXBAS, which determines the base in an equilateral triangular weighting function.

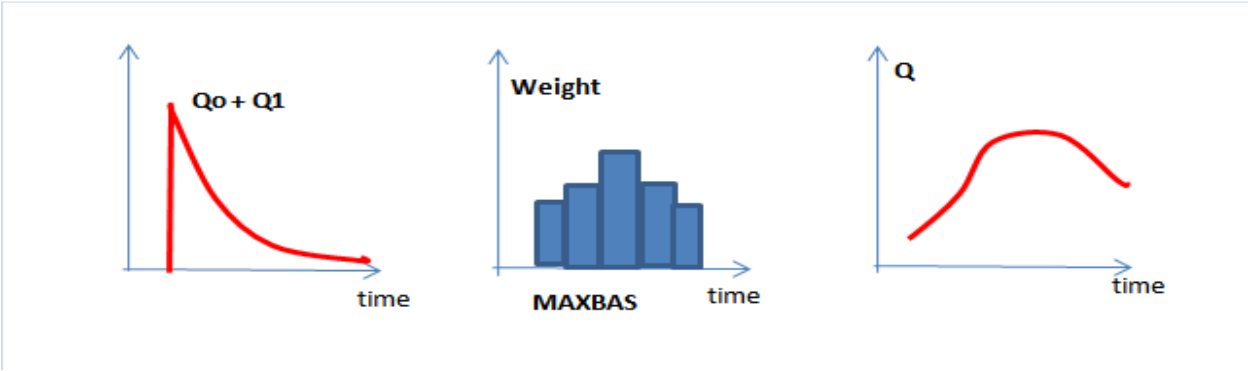

Figure 4.7: ***The transformation function (IHMS, 2006)***

4.3.2. HBV Model Inputs

Daily values of areal rainfall and areal temperature and mean daily or monthly estimates of potential evapotranspiration are main input data of the model. Besides, in the absence of daily

potential evapotranspiration data, long-term daily mean temperature data was put as an input data to correct the long-term mean evaporation (Seibert, 2002).

Table 4.1*: Input-output relationships*

Submodel	Input data	Output data
Snow routine	Precipitation, Temperature	Snow pack, snow-melt
Soil routine	PET, Precipitation, snowmelt	AET, 'soil moisture', groundwater recharge
Response function	Groundwater recharge, (PET)	Runoff, 'Groundwater level'
Routing routine	Runoff	Simulated runoff

Precipitation

The areal average precipitation Parea is calculated as weighted mean of precipitation stations in and around the catchment.

$$Parea = \Sigma Ci\ Pi \text{ ---------- (4.4)}$$

The weight Ci of station i can be determined...

... Subjectively

... by Thiessen polygons

... by the isohyetal or the hypsometric method

The catchment can be divided into different elevation zones. For each zone the precipitation will be corrected according to its increase with elevation above sea level (usually 10-20% per 100 m, parameter PCALT).

$$P(h) = P_A \left[1 + \frac{PCALT(h-h_o)}{10000}\right] \text{---------- (4.5)}$$

Where, P_A= areal rainfall [mm/day], P_i=point rainfall measurement at station i [mm/day], P (h)=areal rainfall at the center of elevation zone [mm/day], h=height of elevation zone amsl [m], ho-height of rainfall observation amsl [m], PCALT-rate of rainfall increase over 100 m.

Temperature

Temperature data is to calculate weighted mean of stations in and around the catchment. When different elevation zones are used temperature will be corrected for elevation above sea level with usually -0.6^{o}C per 100 m (parameter TCALT)

$$T(h) = To \left[1 + \frac{TCALT(h-h_o)}{10000}\right] \text{---------- (4.6)}$$

Where, To= mean daily areal temperature [^{o}C], h=height of elevation zone amsl [m], T (h)=areal temperature at the center of elevation zone [^{o}C], ho-height of temperature observation amsl [m], TCALT=rate of temperature decrease over 100 m.

Potential evaporation

Estimates of the potential evaporation may be provided by calculations using, for instance, the Penman formula or measurements by evaporimeters. Normally monthly mean values are assumed to be sufficient. The long-term mean evaporation can be corrected by using the deviations of the temperature from its long-term mean.

$$E_{pot}(t) = \lceil 1 + C_{ET}(T(t) - T_M) \rceil E_{pot,m} \text{ --- ---------- (4.7)}$$

(BUT: 2 $E_{pot,M} \geq E_{pot\,(t)} \geq 0$)

Where Epot(t)= potential evaporation at day t [mm d^{-1}]

CET correction factor [°C-1]

T(t)= temperature at day t [°C]

T_M= long-term mean temperature for this day of the year [°C]

$E_{pot,M}$ long-term mean evaporation for this day of the year [mm $^{d-1}$]

Catchment Data

Watershed delineation is the first step in hydrological modeling and is followed by discretization of the catchment into hydrologic response units. Elevation zones were considered as primary hydrological units of the catchment and were divided into different vegetation zones. The version of HBV model used for this study allows dividing the catchment up to 20 elevation zones and into three vegetation zones per elevation zone (Seibert, 2002). The zonings were completely done based on elevation and land cover data of the areas using ArcGIS.

4.4. ArcSWAT Model

The Soil and Water Assessment Tool (SWAT) model (Arnold et al., 1998; Arnold and Fohrer, 2005) has proven to be an effective tool for assessing water resource and non point source pollution problems for a wide range of scales and environmental conditions across the globe. SWAT is a basin scale, continuous time model that operates on a daily time step and is designed to predict the impact of management on water, sediment, and agricultural chemical yields in un-gauged watersheds.

4.4.1. SWAT Model Structure

Watersheds can be subdivided into subwatersheds and further into hydrologic response units (HRUs) to account for differences in soils, land use, crops, topography, weather, etc. The model has a weather generator that generates daily values of precipitation, air temperature, solar radiation, wind speed, and relative humidity from statistical parameters derived from average monthly values. The model computes surface runoff volume either by using modified SCS curve number method or the Green & Ampt infiltration method. Flow is routed through the channel using a variable storage coefficient method or the Muskingum routing method. SWAT has three options for estimating potential evapotranspiration: Hargreaves, Priestley-Taylor, and Penman-Monteith. The model also includes controlled reservoir operation and groundwater flow model. A complete description of the SWAT model components is found in Arnold et al. (1998) and Neitsch et al. (2002). A brief description of the SWAT hydrologic component is given here.

4.4.1.1. Hydrologic Water Balance

Water balance is the driving force behind everything that happens in the watershed. In SWAT simulation of hydrology of the watershed can be separated in to two major divisions. The first division is the land phase of hydrologic cycle controls the amount of water, sediment, nutrient and pesticide loadings in to the main channel in each sub basin. The second division is the routing phase of hydrological cycle which can be defined as the movement of water, sediments, etc through the channel network of the watershed to the outlet. As far as this research work is concerned the hydrologic cycle largely dealt with on the movement of water, which is the runoff generation.

The land phase of the hydrologic processes (figure 4.9) is simulated based on water balance equation:

$$SW_t = SW_o + \sum_{i=1}^{t}\left[R_{day} - Q_{surf} - E_a - W_{seep}\right] \text{---------- (4.8)}$$

Where: SWt is the final soil water content (mm water),

SW_0 is the initial soil water content on day (mm water),
t is the time (days),
Rday is the amount of precipitation on day i (mm water),
Qsurf is the amount of surface runoff on day i (mm water),
Ea is the amount of evapotranspiration on day i (mm water),
Wseep is the amount of percolation and bypass flow exiting the soil profile bottom on day i (mm water).

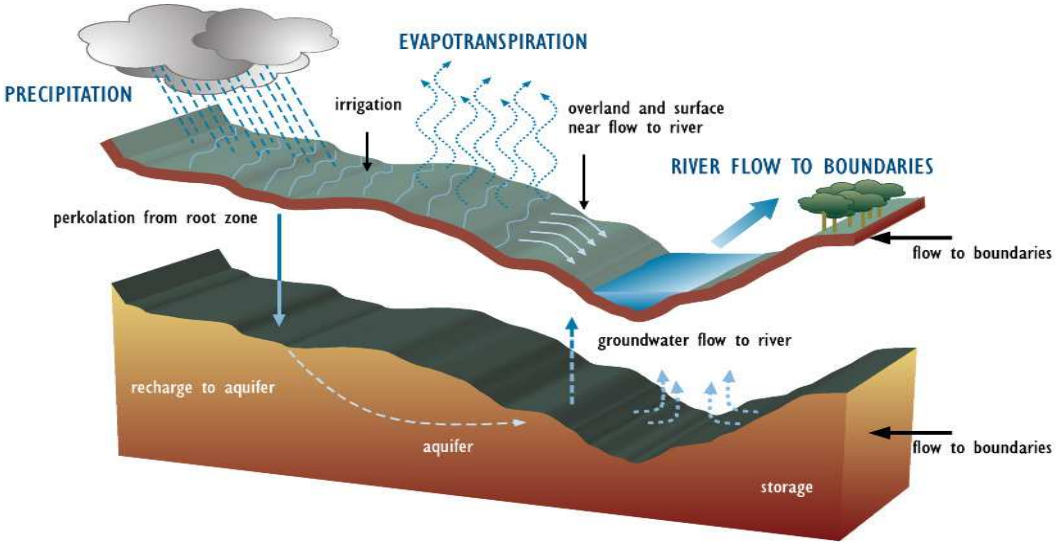

Figure 4.8*: Schematic representation of the hydrologic cycle in SWAT*

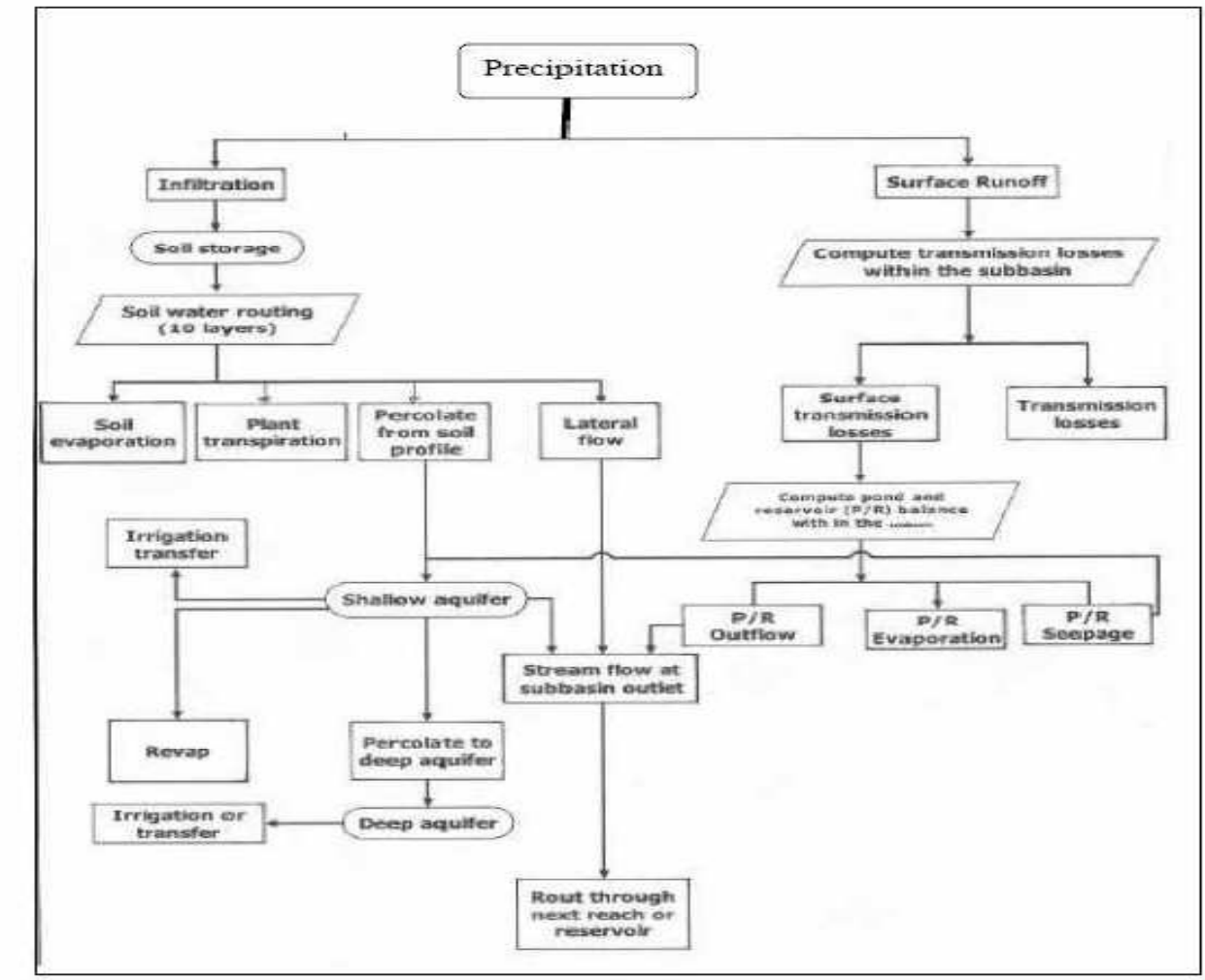

Figure 4.9*: over view of SWAT hydrologic component (Adapted from Arnold et.al, 1998)*

4.4.1.2. Weather Generator

Lack of full and realistic long period climatic data is the problem of developing countries. Weather generators solve this problem by generating data having the same statistical properties as the actual ones (Danuso 2002). SWAT requires daily values of precipitation, maximum and minimum temperature, solar radiation, relative humidity and wind speed. The climatic data collected from the twenty-nine meteorological stations in the study areas have; however, too many missing data. Since SWAT has a built in weather generator called WGEN (Richardson *et al.*, 1984) that is used to fill the gaps, all the missing values were filled with a missing data identifier, -99.

The weather generator first independently generates precipitation for the day. Maximum and minimum temperature, solar radiation and relative humidity are then generated based on the presence or absence of rain for the day while wind speed is finally generated independently. For the sake of data generation, weather parameters were developed by using the weather parameter calculator pcpSTAT and dew point temperature calculator DEW02 (Liersch, 2003), which were downloaded from the SWAT website (http://www.brc.tamus.edu/swat/soft_links.html). The pcpSTAT program reads daily values of rainfall, then it calculates monthly daily averages and standard deviations of all variables as well as probability of wet and dry days, skew coefficient, and average number of precipitation days in the month. The DEW02 programs reads daily values of relative humidity, and maximum and minimum temperature values and calculates monthly average dew point temperatures. The weather generator parameters used in this study and their values are shown in *Appendix A.*

The daily precipitation generator is a Markov chain-skewed (Nicks, 1974) or Markov chain exponential model (Williams, 1995). A first-order Markov chain is used to define the day as wet or dry. When a wet day is generated, a skewed distribution or exponential distribution is used to generate the precipitation amount. In this research work an exponential distribution has been used.

4.4.1.3. Sub watershed Discretization and Determination of HRUs.

The sub watershed discretization divides the watershed into sub-basins based on topographic features of the watershed. This technique preserves the natural flow paths, boundaries, and

channels required for realistic routing of water, sediment and chemicals. All of the GIS interfaces developed for SWAT use the sub watershed discretization to divide a watershed. The number of sub-basins chosen to model the watershed depends on the size of the watershed, the spatial detail of available input data and the amount of detail required to meet the goals of the project. When subdividing the watershed, topographic attributes (slope, slope length, channel length, channel width, etc.) are calculated or summarized at the sub-basin level. The-sub basin delineation should be detailed enough to capture significant topographic variability within the watershed.

The subbasin delineation was followed by the determination of HRUs, which are unique soil and land use combinations within a subbasin modelled regardless of their spatial positioning. This describes better hydrologic water balance and increases the accuracy of load predictions (Luzio *et al.* 2002). SWAT predicts the land phases of the hydrologic cycle separately for each HRU and routes to obtain the total loadings of the subwatershed.

The HRUs can be determined either by assigning only one HRU for each subwatershed considering the dominant soil/landuse combinations, or by assigning multiple HRUs for each subwatershed considering the sensitivity of the hydrologic process based on a certain threshold values of soil/landuse/slope combinations. For this study, the latter method was adopted as it better describes the heterogeneity within the watershed and as it accurately simulates the hydrologic processes. The ArcSWAT manual (Luzio *et al.* 2002) recommends the threshold levels for multiple HRUs to be set based on the project goal and the amount of detail desired. Default threshold values of 20% landuse, 10% soil and 20% slope type are recommended to be adequate for most applications.

4.4.1.4. Surface Runoff Simulation

a) Surface Runoff Volume

SWAT provides two methods for estimating surface runoff: the SCS curve number method (SCS) and the Green & Ampt infiltration method. Even though the latter method is better in estimating runoff volume accurately, its sub-daily time step data requirement makes it difficult to be used for this study. Hence, the SCS curve number method was adopted. The method is an empirical model, which is based on the following equation:

$$Q_{surf} = \frac{(R_{day} - I_a)^2}{(R - I_a + S)} \text{---------- (4.9)}$$

Where: Q_{surf} *is* accumulated runoff or rainfall excess (mm water),
R_{day} *is* rainfall depth for the day (mm water),
Ia is an initial abstraction which includes surface storage, interception and infiltration prior to runoff (mm water), *S is a* retention parameter (mm water).

The retention parameter varies spatially due to changes in soils, land use, management and slope, and temporally due to changes in soil water content. It is mathematically expressed as:

$$S = 25.4 * \left(\frac{1000}{CN} - 10\right) \text{---------- (4.10)}$$

Where: *CN* is the curve number for the day which is f (land use, practice, soil permeability, soil hydrologic group)

For the definition of the soil hydrologic groups, the model uses the U.S. Natural Resource Conservation Service (NRCS) classification, which classifies soils into four hydrologic groups (A, B, C, & D) based on infiltration characteristics of the soils. Group A, B, C and D soils have high, moderate, slow, and very low infiltration rates with low, moderate, high, and very high runoff potential, respectively. The initial abstraction, Ia, is commonly approximated as 0.2*S* and the equation becomes:

$$Q_{surf} = \frac{(R_{day} - 0.2S)^2}{(R_{day} + 0.8S)} \text{---------- (4.11)}$$

b) *Peak Discharge*

The peak discharge or the peak surface runoff rate is the maximum volume flow rate passing a particular location during a storm event. SWAT calculates the peak runoff rate with a modified rational method. In rational method it assumed that a rainfall of intensity *I* begins at time *t = 0* and continues indefinitely, the rate of runoff will increase until the time of concentration, *t* = t_{conc}. The modified rational method is mathematically expressed as:

$$q_{peak} = \frac{\alpha_{tc} * Q_{surf} * Area}{3.6 * t_{conc}} \text{---------- (4.12)}$$

Where: *qpeak* is the peak runoff rate (m3/s),
αtc is the fraction of daily rainfall that occurs during the time of concentration,
Qsurf is the surface runoff (mm),

Area is the sub-basin area (km²),
*t*conc is the time of concentration (hr), and 3.6 is a conversion factor.

SWAT estimates the value of α using the following equation:

$$\alpha_{tc} = 1 - exp[2 * t_{conc} * ln(1 - \alpha_{0.5})] \text{---------- (4.13)}$$

Where: $\alpha_{0.5}$ is the fraction of daily rain falling in the half-hour highest intensity rainfall.

Time of Concentration

The time of concentration, $t_{conc,}$ is a time within which the entire subbasin area is discharging at the outlet point. It is calculated by summing up both the overland flow time of the furthest point in the subbasin to reach a stream channel (t_{ov}) and the upstream channel flow time needed to reach the outlet point (t_{ch}):

$$t_{conc} = t_{ov} + t_{ch} \text{---------- (4.14)}$$

The overland flow time (t_{ov}) is computed as:

$$t_{ov} = \frac{L_{slp}}{3600 * V_{ov}} \text{---------- (4.15)}$$

Where: *Lslp* is the average subbasin slope length (m),
Vov is the overland flow velocity (m/s), and 3600 is a unit conversion factor.

The overland flow velocity for a unit width along the slope is calculated by using the Manning's equation:

$$V_{ov} = \frac{{q_{ov}}^{0.6} * slp^{0.3}}{n^{0.5}} \text{---------- (4.16)}$$

Where: *qov* is the average overland flow rate (m^3/s),
slp is the average slope of the subbasin (m/m),
n is Manning's roughness coefficient of the subbasin.

Assuming an average flow rate of 6.35 mm/hr and substituting the equation of V_{ov} into t_{ov}, the simplified equation of the overland flow becomes:

$$t_{ov} = \frac{{L_{slp}}^{0.6} * n^{0.5}}{18 * slp^{0.3}} \text{---------- (4.17)}$$

Channel flow time is computed as:

$$t_{ch} = \frac{L_c}{3.6 * V_c} \text{---------- (4.18)}$$

Where: *Lc* is the average flow channel length (km),
Vc is the average flow velocity (m/s), and 3.6 is a unit conversion factor.

The average flow channel length is calculated as:

$$L_c = \sqrt{l * L_{cen}} \text{---------- (4.19)}$$

Where: *L* is the channel length from the furthest point to the subbasin outlet (km),
L*cen* is the distance along the channel to the subbasin centroid (km).

Assuming $L_{cen} = 0.5L$, and using the Manning's equation for V_c for a trapezoidal channel with side slope of 2:1 and bottom width to depth ratio of 10:1, channel flow time becomes:

$$t_{ch} = \frac{0.62 * L * n^{0.75}}{Area^{0.125} * slp_{ch}{}^{0.375}} \text{---------- (4.20)}$$

Where: *tch* is the time of concentration for channel flow (hr),
L is channel length from the most distant point to the sub basin outlet (km),
n is Manning's roughness coefficient for the channel,
Area is the sub basin area (km2), and
S*lpch* is the channel slope (m/m).

Surface Runoff Lag

In large subbasins with a time of concentration greater than 1 day, only a portion of the surface runoff will reach the main channel on the day it is generated. SWAT incorporates a surface runoff storage feature to lag a part of the surface runoff release to the main channel. Once surface runoff is calculated, the amount of surface runoff released to the main channel is calculated as:

$$Q_{sutf} = \left(Q'_{surf} + Q_{stor,i-1}\right) * \left[1 - exp\left|\frac{-surlag}{t_{conc}}\right|\right] \text{---------- (4.21)}$$

Where: *Qsurf* is amount of surface runoff discharged to main channel in a day (mm),
Q'surf is amount of surface runoff generated in a sub basin in a day (mm),
Qstor,*i*-1 is the surface runoff stored or lagged from the previous day (mm),
surlag is the surface runoff lag coefficient, and
tconc is the time of concentration for the sub-basin (hrs).

4.4.1.5. Potential Evapotranspiration (PET)

According to Penman (1956), PET is defined as "*the amount of water transpired by a short green crop, completely shading the ground, of uniform height and never short of water*". Even though, there are numerous methods for PET estimation, SWAT provides three alternatives for

its calculation: Penman-Monteith (Monteith 1965, Allen 1986, Allen *et al.* 1989), Priestley-Taylor (Priestley and Taylor 1972), and Hargreaves (Hargreaves *et al.* 1985) methods. As an option, measured values can also be used as an input data. The methods have various needs for a number and type of climate variables: Penman-Monteith method requires solar radiation, air temperature, relative humidity and wind speed; Priestley-Taylor method requires solar radiation, air temperature and relative humidity; whereas Hargreaves method requires air temperature only. In this study Penman-Monteith method was considered for PET estimation.

Penman-Monteith Method

The Penman-Monteith equation combines components that account for energy needed to sustain evaporation, the strength of the mechanism required to remove the water vapor and aerodynamic and surface resistance terms. The penman-Monteith equation is:

$$\lambda E = \frac{\Delta*(H_{net}-G)+\rho_{air}*C_p*[e_z^o-e_z]/r_a}{\Delta+\gamma*(1+r_c/r_a} \text{---------- (4.22)}$$

Where: λ E is the latent heat flux density (MJ m-2 d-1), E is the depth rate evaporation (mm d-1), Δ is the slope of the saturation vapor pressure-temperature curve, de/dT (kPa °C-1), Hnet is the net radiation (MJ m-2 d-1), G is the heat flux density to the ground (MJ m-2 d-1), ρ air is the air density (kg m-3), Cp is the specific heat at constant pressure (MJ kg-1 °C-1), is the saturation vapor pressure of air at height z (kPa), e^oz -ez is the water vapor pressure of air at height z (kPa), γ is the psychrometric constant (kPa °C-1), rc is the plant canopy resistance (s m-1), and ra is the diffusion resistance of the air layer (aerodynamic resistance) (s m-1).

For well-watered plants under neutral atmospheric stability and assuming logarithmic wind profiles, the Penman-Monteith equation may be written (Jensen et al., 1990):

$$\lambda E_t = \frac{\Delta*(H_{net}-G)+\gamma*K_1*\left(0.622*\lambda*\frac{\rho_{air}}{P}\right)*[e_z^o-e_z]/r_a}{\Delta+\gamma*(1+r_c/r_a} \text{---------- (4.23)}$$

Where: λ is the latent heat of vaporization (MJ kg-1), Et is the maximum transpiration rate (mm d-1), K_1 is a dimension coefficient needed to ensure the two terms in the numerator have the same units (for uz in m s-1, K1 = 8.64 x 104), and P is the atmospheric pressure (kPa).

4.4.1.6. Soil Water - Percolation, Bypass Flow, and Lateral Flow

Soil water may follow different paths of movement: vertically upward (plant uptake), vertically downward (percolation), or laterally-contributing to stream flow. The vertical movement as plant

uptake removes the largest portion of water that enters the soil profile. Percolation is the downward movement of water in the soil. SWAT calculates percolation for each soil layer in the profile. Water is allowed to percolate if only the water content exceeds the field capacity of that layer (Neitsch *et al.* (A) 2002).

Bypass flow is the vertical movement of free water along macropores through unsaturated soil horizons and occurs in areas dominated by Vertic soils when the rate of rainfall or irrigation exceeds the vertical infiltration rate. While simulating the bypass flow, SWAT calculates the crack volume of the soil matrix for each day of simulation by layer. On days in which precipitation events occur, infiltration and surface runoff are first calculated for the soil peds. Part of the surface runoff equivalent to the cracks volume enters the soil profile as bypass flow, and the rest remains overland flow. Cracks are filled in accordance with their presence in the consecutive layers: those at the bottom layers are filled first (Neitsch *et al.* (A) 2002).

Lateral flow is common in areas with high hydraulic conductivities in surface layers and an impermeable or semi-permeable layer at a shallow depth. Rainfall will percolate vertically up to the impermeable layer and develops a saturated zone stored above this layer. This is called a perched water table, which is the source of water for lateral subsurface flow. SWAT incorporates a kinematic storage model for subsurface flow (Neitsch *et al.* (A) 2002).

4.4.1.7. Groundwater System

SWAT assumes two layers of aquifers while simulating the groundwater balance; namely a shallow unconfined aquifer, and a deep-confined aquifer. The unconfined shallow aquifer is contributes to flow in the main channel or reach of the sub-basin, whereas the deep confined aquifer assumed to contribute to stream flows outside the watershed (Arnold *et al.* 1993).

The volume of water available in the shallow aquifer is governed by the recharge from the top soil profile (recharge), the flow into the main stream channels or reach (base flow), the movement into the overlying unsaturated zone (revap), and the flow to the deep aquifer (deep percolation). The details of the methodology are described in the SWAT Theoretical Documentation, version 2000 (Neitsch *et al.* (A) 2002). Evaporation, pumping withdrawals,

seepage to the deep aquifer, and water uptake from the shallow aquifer by deep rooted plants are also components of the groundwater.

Shallow Aquifer

The water balance for a shallow aquifer in SWAT is calculated with:

$$aq_{sh,i} = aq_{sh,i-1} + w_{rchrg} - Q_{gw} - w_{revap} - W_{deep} - W_{pump,sh} \text{---------- (4.24)}$$

Where: *aqsh,i* is the amount of water stored in the shallow aquifer on day *i* (mm),
aqsh,i-1 is the amount of water stored in the shallow aquifer on day *i*-1 (mm),
wrchrg is the amount of recharge entering the aquifer on day *i* (mm),
Qgw is the groundwater flow, base flow, into the main channel on day *i* (mm),
wrevap is the amount of water moving into the soil zone in response to water deficiencies on day *i* (mm),
wdeep is the amount of water percolating from the shallow aquifer into the deep aquifer on day *i* (mm), and
wpump,sh is the amount of water removed from the shallow aquifer by pumping on day *I* (mm).

Deep Aquifer

The water balance for the deep aquifer is:

$$aq_{dp,i} = aq_{dp,i-1} + W_{deep} - W_{pump,dp} \text{---------- (4.25)}$$

Where: qdp, i is the amount of water stored in the deep aquifer on day i (mm),
aqdp, i-1 isthe amount of water stored in the deep aquifer on day i-1 (mm),
wdeep is the amount of water percolating from the shallow aquifer into the deep aquifer on day i (mm), and
wpump,dp is the amount of water removed from the deep aquifer by pumping on day I (mm).

Base flow occurs only when the amount of water stored in the shallow aquifer exceeds a threshold volume of water. Similarly, deep percolation happens only when the amount of water stored in the shallow aquifer exceeds a threshold value.

4.4.1.8. Channel Routing

The second phase of the SWAT hydrologic simulation, the routing phase, consists of the movement of water, sediment and other constituents (e.g. nutrients, pesticides) in the stream network. As an optional process, the change in channel dimensions with time due to down cutting and widening is also included.

Similar to the case for the overland flow, the rate and velocity of flow is calculated by using the Manning's equation. The main channels or reaches are assumed to have a trapezoidal shape by the model. Two options are available to route the flow in the channel networks: the variable storage and Muskingum methods. Both are variations of the kinematic wave model. While calculating the water balance in the channel flow, the transmission and evaporation are also well considered by the model.

The variable storage method uses a simple continuity equation in routing the storage volume, whereas the Muskingum routing method models the storage volume in a channel length as a combination of wedge and prism storages. In the latter method, when a flood wave advances into a reach segment, inflow exceeds outflow and a wedge of storage is produced. As the flood wave recedes, outflow exceeds inflow in the reach segment and a negative wedge is produced. In addition to the wedge storage, the reach segment contains a prism of storage formed by a volume of constant cross-section along the reach length.

For this research, the variable storage method was adopted. The method was developed by Williams (1969) and used in ROTO (Arnold *et al.* 1995) models. Storage routing is based on the continuity equation:

$$\Delta V_{stored} = V_{in} - V_{out} \text{---------- (4.26)}$$

Where: V_{in} is the volume of inflow during the time step (m^3 water),
Vout is the volume of outflow during the time step (m^3 water), and
$\Delta Vstored$ is the change in volume of storage during the time step (m^3 water).

This equation can also be detailed as follows:

$$V_{stored,2} - V_{stored,1} = \Delta t * \left[\frac{q_{in,1}+q_{in,2}}{2}\right] - \Delta t * \left[\frac{q_{out,1}+q_{out,2}}{2}\right] \text{---------- (4.27)}$$

Where: Δt is the length of the time step (s),
$q_{in,1}$ is the inflow rate at the beginning of the time step (m^3/s),
$q_{in,2}$ is the inflow rate at the end of the time step (m^3/s),
$q_{out,1}$ is the outflow rate at the beginning of the time step (m^3/s),
$q_{out,2}$ is the outflow rate at the end of the time step (m^3/s),
$V_{stored,1}$ is the storage volume at the beginning of the time step (m^3 water),and
$V_{stored,2}$ is the storage volume at the end of the time step (m^3 water).

Travel time is computed by dividing the volume of water in the channel by the flow rate.

$$TT = \frac{V_{stored}}{q_{out}} = \frac{V_{stored,1}}{q_{out,1}} = \frac{V_{stored,2}}{q_{out,2}} \text{---------- (4.28)}$$

Where: *TT* is the travel time (s),
Vstored is the storage volume (m^3 water), and
qout is the discharge rate (m^3/s)

4.4.2. SWAT Model Inputs

Digital Elevation Model

The digital elevation model (DEM) data was used to delineate the sub-watersheds in the ArcSWAT interface. DEM of the study areas were masked from Ehio-DEM with datum GCS_WGS_1984 and format type of USGSDEM. Before the DEM data was loaded in to ArcSWAT interface, it was projected into coordinate system parameters of Ethiopia (study area) is: UTM-WGS 1984-UTM zone 37N.prj.

Land Use/Land Cover

The land use/land cover map of the study area was collected from MoWR GIS department which was obtained in shape file format. The land use/cover data reclassified according to the SWAT land use/cover type. A look up table that identifies the 4-letter SWAT code for the different categories of land cover/land use were prepared so as to relate the grid values to SWAT land cover/land use classes; and SWAT calculated the area covered by each land use.

Soil Data

Soil data was also collected from the Ethiopian MoWR GIS department; however, this data was only in shape file format and the characteristics of the soils needed by the SWAT couldn't be found. The soil data used for this study was instead collected from the Master Plan of Abbay Basin which is available at MoWR. The basic characteristics of the soils and the look up table which links the grid size with the soil type was prepared to make understandable by SWAT. The characteristic soil parameter values were enclosed in *Appendix B*.

Meteorological Data

Meteorological data is needed by the SWAT model to simulate the hydrological conditions of the basin. The meteorological data required for this study were collected from the Ethiopian National Meteorological Services Agency (NMSA). The meteorological data collected were precipitation, maximum and minimum temperature, relative humidity, wind speed and sunshine hours. Data

from twenty-nine principal and nonclass-1 stations, which are within and around the study area, were collected.

Hydrological Data

The hydrological data was required for performing sensitivity analysis, calibration and validation of the model. The hydrological data was also collected from the Ethiopian MoWR hydrological section for the selected five catchments: Gilgel Abbay, Chemoga, Muger, Guder and Didessa stream flows.. For calibration of simulated flows, the total gauged stream flow data should be separated into surface and base flow components. The automated base flow separation and recession analysis techniques (Arnold *et al.* 1999), and the Web-based Hydrograph Analysis Tool (WHAT) (http://pasture.ecn.purdue.edu/~what/) are among the several methods available to separate base flows. However, due to its simplicity, the former technique was applied.

---

[7]http://www.brc.tamus.edu/swat/soft_baseflow.html

4.5. Sensitivity Analysis

Sensitivity analysis is a simple technique for assessing the effect of uncertainty on the system performance. It is also a measure of the effect of change of one parameter on another. While there are a number of techniques available for conducting SA (Saltelli, 2000), all can be broadly grouped as local and global approaches (Saltelli et al., 1999). In local techniques, output responses are determined by sequentially varying each of the input factors and by fixing all other factors to constant nominal values. The further the perturbation moves away from the nominal value, the less reliable the analysis results become (Helton, 1993). Also, the more nonlinear the relationship between inputs and output variables, which is typical in hydrologic models, the more difficult and unreliable it is to employ local techniques. Furthermore, since sampling is performed for one input at a time by fixing all other inputs at constant values, local approaches do not account for any interaction between inputs, if any exists. Unlike the local techniques, global SA methods explore the entire range of input factors, and all input factors can be simultaneously varied, allowing investigation of output variation as a result of all inputs and their possible interaction (i.e. output uncertainty is averaged over all input factors). Therefore sensitivity analysis as an instrument for the assessment of the input parameters with respect to

their impact on model output is useful not only for model development, but also for model validation and reduction of uncertainty (Hamby, 1994 cited in Lenhart *et al.* 2002).

The sensitivity analysis was undertaken by using a built-in tool in SWAT2005 that uses the Latin Hypercube One-factor-At-a-Time (LH-OAT) design method of Morris (1991). The OAT design appeared to be a very useful method for SWAT modeling as it is able to analyze sensitivity on high number of parameters. The LHOAT sensitivity analysis method combines thus the robustness of the Latin Hypercube sampling that ensures that the full range of all parameters has been sampled with the precision of an OAT designs assuring that the changes in the output in each model run can be unambiguously attributed to the input changed in such a simulation leading to a robust and efficient sensitivity analysis method. Using the built in tool in SWAT model sensitivity analysis has been performed for all gauged stream flow and the result is found in modeling section of this report.

In HBV modelling, unlike swat model it has no built-in program for sensitivity analysis, local sensitivity technique was applied that output responses are determined by sequentially varying each of the input parameters and by fixing all other factors to constant nominal values; and the sensitivity result is found in modeling section of this report.

4.6. Models Calibration

Calibration is a major aspect of hydrological modeling and is aimed at fitting the simulated outputs of the model to the observed outputs of the watershed by adjusting the model parameters. A measure of the fit between the simulated and observed outputs is called calibration. The goal of calibration is to find those values for the model parameters that minimize (Maximize) the specified calibration criterion.

Parameter estimation follows the decision of which parameters of the simulation model to calibrate. Manual calibration and automatic calibration are two types of parameter estimation approaches. There are three calibration approaches widely used by the scientific community. These are the manual calibration, automatic calibration and a combination of the two. Manual calibration is by far the most widely used approach for complex models, including those of the distributed type (Refsgaard and Knudsen, 1996; Refsgaard, 1997; Senarath et al., 2000). Manual

calibration, however, is time consuming and very subjective, and its success highly depends on the experience of the modeler and their knowledge of the study watershed, along with model assumptions and its algorithms. Automatic calibration involves the use of a search algorithm to determine best-fit parameters, and it offers a number of advantages over the manual approach. Automatic calibration is fast, it is less subjective, and since it makes an extensive search of the existing parameter possibilities, it is highly likely that results would be better than that which could be manually obtained. Senarath et al. (2000) and Eckhardt and Arnold (2001) have implemented automatic calibration for distributed models.

4.6.1. HBV-Light Model Parameter Estimation

HBV-Light has built-in Monte-Carlo calibration tool. The Monte-Carlo autocalibration technique is used to obtain an optimal fit of process parameters which is based on the coefficient of efficiency, R_{eff}.

$$R_{eff} = 1 - \frac{\sum[Q_{sim}(t) - Q_{obs}(t)]^2}{\sum[Q_{obs}(t) - \bar{Q}_{obs}]^2} \quad \text{(4.29)}$$

R_{eff} compares the prediction by the model with the simplest possible prediction, a constant value of the observed mean value over the entire period.

Where: R_{eff} = 1 Perfect fit, $Q_{Sim}(t) = Q_{obs}(t)$ t

R_{eff} = 0 Simulation as good (or poor) as the constant-value prediction

R_{eff} < 0 Very poor fit

The calibration period should include a variety of hydrological events and normally 5 to 10 years sufficient to calibrate the HBV model.

4.6.2. ArcSWAT Model Parameter Estimation

SWAT has two built-in calibration tools: the manual calibration helper and the autocalibration. The manual calibration approach helps to compare the measured and simulated values, and then to use the expert judgment to determine which variable to adjust, how much to adjust them, and ultimately assess when reasonable results have been obtained. The autocalibration technique is used to obtain an optimal fit of process parameters which is based on a multi-objective calibration and incorporates the Shuffled Complex Evolution Method algorithms (Green and van

Griensven, 2007). In this study both of the techniques were employed to get the best model parameters.

First, the manual calibration was performed and when the model evaluation parameters reached to an unchanged level, the model was run automatically. Parameter changes in SWAT affecting hydrology were done in a distributed way for selected sub-basins and HRU's. They were modified by replacement, by addition of an absolute change and by multiplication of a relative change depending on the nature of the parameter. However, a parameter was never allowed to go beyond the predefined parameter ranges during the calibration process. In the manual calibration, first the water balance was calibrated followed by temporal flow calibration. SWAT developers in Santhi et.al, (2001) assumed an acceptable calibration for hydrology with coefficient of determination (R^2) >0.6 and Nash-Sutcliffe efficiency (E_{NS})>0.5 and these values were also considered in this study as adequate statistical values for acceptable calibration.

4.7. Models Validation

The predictions of the model are directly compared with measurements for two purposes. First, most water Resource models include "free parameters," i.e. variables used in the mathematical formulation for which direct measurements do not exist. These can be estimated by adjusting their values until the resulting model prediction agrees with measurements, a process referred to as model "calibration." Second, the model is operated under the same external conditions as encountered during collection of a set of field data, and the model predictions compared to the field measurements, without any adjustment or "fitting" of the model, to evaluate the performance of the model, a process referred to as model "verification." (Ward, G., Benamen, 1999).

Once calibration has been conducted to estimate the best values for model parameters, the outcome needs to be verified to determine if the results provide adequate information for answering the questions that face decision-makers. Thus; validation is the process of testing model performance of the calibrated model parameter set against an independent set of measured data. For this research work an independent validation period was taken as 5 years beginning Jan. 1st, 2001 to Dec. 31, 2005 for both HBV and SWAT models.

4.8. Model Efficiency Evaluation Criteria Used

No single index of goodness-of-fit is suitable for describing how well a particular model performs. Therefore, I used a number of quantitative indices for model evaluation. Over seven performance evaluation criteria have been considered in the study:

- The coefficient of efficiency [Nash and Sutcliffe,1970], is defined by the dimensionless expression

$$NSE = 1 - (\frac{MSE}{Fo}) \text{---------- (4.30)}$$

With $Fo = \frac{1}{N}\sum_1^N[(Qo)i - \overline{Qo}]^2$; and

$$NSE = \frac{1}{N}[(Qo)i - (Qs)i]^2$$

Where: MSE being the mean square error, (Qo)i is the observed discharge and (Qs)i the simulated discharge at the ith time step, N is the total number of discharge values, and $\overline{Qo}$ is the mean of the (Qo)i series over the calibration or verification period.

- The index of agreement, IoA, is defined as [Willmott, 1981]

$$IoA = 1 - \frac{\sum_1^N[(Qo)i-(Qs)i]^2}{\sum_{i=1}^N\{|(Qo)i-\overline{Qo}|+|(Qs)i-\overline{Qo}|\}^2} \text{---------- (4.31)}$$

In which the numerator is N times the MSE and the denominator is called the potential error. The other symbols have the same meaning as for Nash and Sutcliffe.

- The coefficient of determination, r^2, is given by

$$r^2 = \frac{\{\sum_{i=N}^N(Qo-\overline{Qo})(Qs-\overline{Qs})\}^2}{\sum_{i=N}^N(Qo-\overline{Qo})^2\sum_{i=N}^N(Qs-\overline{Qs})^2} \text{---------- (4.32)}$$

Where: all symbols have the same meanings as given above.

- The index of volumetric fit, IVF, the ratio of the total volume of (Qs)i to the total volume of (Qo)i, is

$$IVF = \frac{\sum_{i=1}^N(Qs)i}{\sum_{i=1}^N(Qo)i} \text{---------- (4.33)}$$

- The relative error of the peak (RE) is defined as

$$RE = \frac{|(Qp)s-(Qp)o|}{(Qp)o} \text{---------- (4.34)}$$

In which (Qp)o and (Qp)s being the observed and simulated peak flows respectively

- Efficiency using ln

$$\log R_{eff} = 1 - \frac{\sum(\ln Qo - \ln Qs)^2}{\sum(\ln Qo - \overline{\ln Qo})^2} \text{---------- (4.35)}$$

- Mean Difference

$$meandiff = \frac{\sum(Qo - Qs)}{\text{No of days}} 365 \text{-------- (4.35)}$$

- Percentage of Deviation

$$D = 100 \cdot \left[\frac{\left(\sum_{i=1}^{n} q_{si} - \sum_{i=1}^{n} q_{oi} \right)}{\sum_{i=1}^{n} q_{oi}} \right] \text{ ---------- (4.36)}$$

Table 4.2*: Objective functions*

Performance Criteria	Definition	Value for 'perfect' fit
Nash and Sutcliffe	$\text{NSE} = 1 - \frac{\sum(\text{Qo} - \text{Qs})^2}{\sum \text{Qo} - \overline{\text{Qo}})^2}$	1
Coefficient of Determination	$r^2 = \frac{\{\sum_{i=N}^{N}(\text{Qo}) - \overline{\text{Qo}})(\text{Qs} - \overline{\text{Qs}})\}^2}{\sum_{i=N}^{N}(\text{Qo} - \overline{\text{Qo}})^2 \sum_{i=N}^{N}(\text{Qs} - \overline{\text{Qs}})^2}$	1
Index of Agreement	$\text{IoA} = -\frac{\sum_{1}^{N}[(\text{Qo})i - (\text{Qs})i]^2}{\sum_{i=1}^{N}\{\lvert(\text{Qo})i - \overline{\text{Qo}}\rvert + \lvert(\text{Qs})i - \overline{\text{Qo}}\rvert\}^2}$	1
Index of Volumetric Fit	$\text{IVF} = \frac{\sum_{i=1}^{N}(\text{Qs})i}{\sum_{i=1}^{N}(\text{Qo})i}$	1
Relative Error of the Peak	$\text{RE} = \frac{\lvert(\text{Qp})s - (\text{Qp})o\rvert}{(\text{Qp})o}$	0
Ln Efficiency	$logR_{eff} = 1 - \frac{\sum(lnQo - lnQs)^2}{\sum(lnQo - \overline{lnQo})^2}$	1
Mean Difference	$meandiff = \frac{\sum(Qo - Qs)}{No\ of\ days} 365$	0
% Deviation	$D = 100. \left\lvert \frac{(\sum_{i=1}^{N} Qs - \sum_{i=1}^{N} Qo)}{\sum_{i=1}^{N} Qo} \right\rvert$	0

5. Modelling of the Gauged Catchments

5.1. Modelling of Catchments with HBV

Input data for HBV model are daily rainfall, daily temperature, long-term monthly evaporation and daily river flow data for calibration.

Hydrometrological Data

A total of twenty-nine stations inside and around the gauged catchments are used to estimate areal rainfall by Thiessen polygon method.

Table 5.1*: Weights of rainfall stations by Thiessen polygon method for the respective catchments.*

Catchmets	**Metrological Stations**					
Gilgel Abbay	Dangila	Bahir Dar	Abay Sheleko	Wetet Abay		Kidmaja
	0.138	0.324	0.018	0.292		0.228
Chemoga	Debre Markos	Rob Gebya				
	0.240	0.760				
Muger	A.A Observatory	Sululta	Shola Gebya			
	0.250	0.500	0.250			
Guder	Ambo	Guder	Tikur Inchini			
	0.110	0.110	0.780			
Didessa	Arjo	Nekemte	Seko	Yafna	Jimma	Limu Genet
	0.260	0.094	0.213	0.237	0.089	0.107

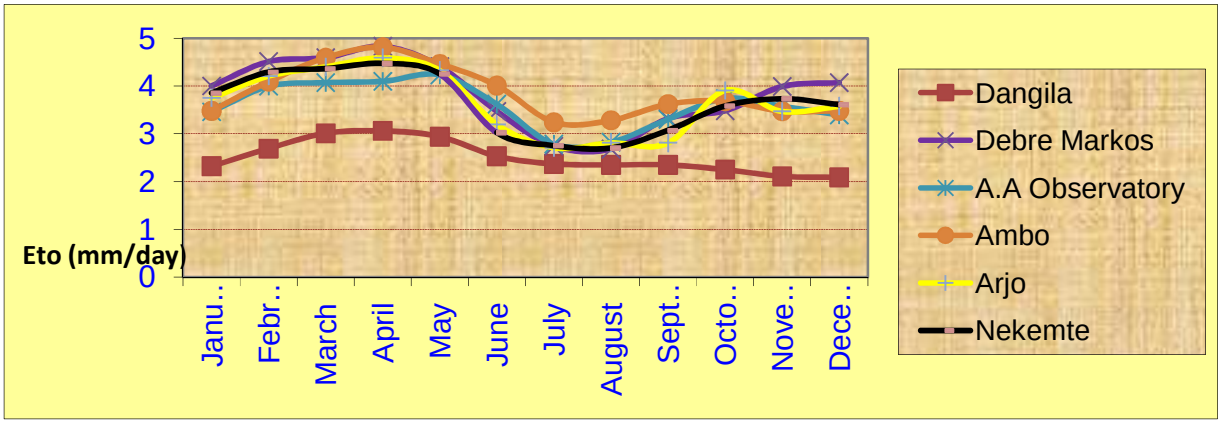

Figure 5.1*: Long-term monthly potential evapotranspiration in mm/day (1990-2005)*

Catchment Data

The model was set up by using elevation and vegetation cover data. Elevation zones were considered as primary hydrological units of the catchment and were divided into different vegetation zones. The version of HBV model used for this study allows dividing the catchment up to 20 elevation zones and into three vegetation zones per elevation zone (Seibert, 2002). The zonings were completely done based on elevation and land cover data of the area using ArcGIS as presented in Table 5.2.

Table 5.2: ***Semi-distributed representation of the five catchments in to various elevation and vegetation zones***

Catchment	Elevation Zone	Mean Elevation	Vegetation Zone (%)		
			Agriculture	**Agro-pastoral**	**Agro-sylvicultural**
Gilgel Abbay	Very Low Elev.	2005.0	0.1525	0.1575	0.0
	Low Elev.	2214.0	0.0948	0.1330	0.0032
	Medium Elev.	2401.5	0.0713	0.1528	0.0089
	High Elev.	2624.0	0.0509	0.1359	0.0031
	Very High Elev.	3136.0	0.0029	0.0332	0.0
			Agro-pastoral	**Agro-sylvicultural**	**Pastoral**
Chemoga	Very Low Elev.	2416.5	0.3402	0.0003	0.1015
	Low Elev.	2717.0	0.2155	0.0072	0.0
	Medium Elev.	2998.0	0.1325	0.0	0.0005
	High Elev.	3306.5	0.0718	0.0	0.0440
	Very High Elev.	3710.0	0.0067	0.0001	0.0797
			Agriculture	**Pastoral**	**Sylvicultural**
Muger	Very Low Elev.	2582	0.0775	0.2907	0.0
	Low Elev.	2661	0.1536	0.1163	0.0116
	Medium Elev.	2753	0.1642	0.0657	0.0311
	High Elev.	2886	0.0016	0.0437	0.0233
	Very High Elev.	3169	0.0	0.0176	0.0031
			Agriculture	**Pastoral**	**Urban**
Guder	Very Low Elev.	2163.5	0.0269	0.0431	0.0246
	Low Elev.	2409.5	0.2013	0.2936	0.0057
	Medium Elev.	2567.5	0.0011	0.2474	0.0002
	High Elev.	2725.0	0.0	0.1117	0.0
	Very High Elev.	3009.5	0.0	0.0445	0.0
			Agriculture	**Pastoral**	**Sylvicultural**

Didessa	Very Low Elev.	1425.0	0.0869	0.2866	0.0044
	Low Elev.	1678.0	0.1479	0.0804	0.0189
	Medium Elev.	1922.5	0.1198	0.0425	0.0455
	High Elev.	2178.5	0.1424	0.0100	0.0608
	Very High Elev.	2730.5	0.0301	0.0053	0.0184

5.2. Modelling of Catchments with SWAT

5.2.1. Modelling Gilgel Abay Catchment

In order to model this gauged river using SWAT, the spatial input which is shown in Figure 5.1 have been used. For modelling purpose a catchment is partitioned in to a number of sub-watersheds. According to (Luzio *et al.* 2002) user manual, the threshold levels set for multiple HRUs is a function of the project goal and the amount of detail desired by the modeler. For most applications, the settings for land use threshold (20 %) and soil threshold (10 %) and slope threshold (20%) are adequate and applied in this research work. In the delineation process this catchment is partitioned in to sixteen sub-watersheds by taking a threshold value of 20% for land use, 10 % for soil and 20% for slope; and 51 HRU's have been derived from the overlay analysis.

Table 5.3*: Soil type of Upper Gilgel Abbay catchment as per FAO-UNESCO soil classification system*

No.	Soil Type	Soil Classes defined in SWAT	Coverage Area (Km^2)	% of Total Area
1	Halpic Luvisols	H. Luvisols	13.50	0.81
2	Halpic Alisols	H. Alisols	31.57	1.90
3	Eutric vertisols	E.vertisols	672.33	40.40
4	Halpic Nitisols	H. Nitisols	937.09	56.32
5	Eutric Rigosols	E.Rigosols	9.51	0.57
Total			1664	100

Table 5.4*: Land use classification of Upper Gilgel Abbay catchment used in SWAT*

No.	Land use	SWAT Land use Class	Coverage Area (Km^2)	% of Total Area
1	Agriculture	AGRC	620.83	37.31
2	Agro-pastoral	SPAS	1018.30	61.20
3	Agro-sylvicultural	AGRL	24.87	1.49
Total			1664	100

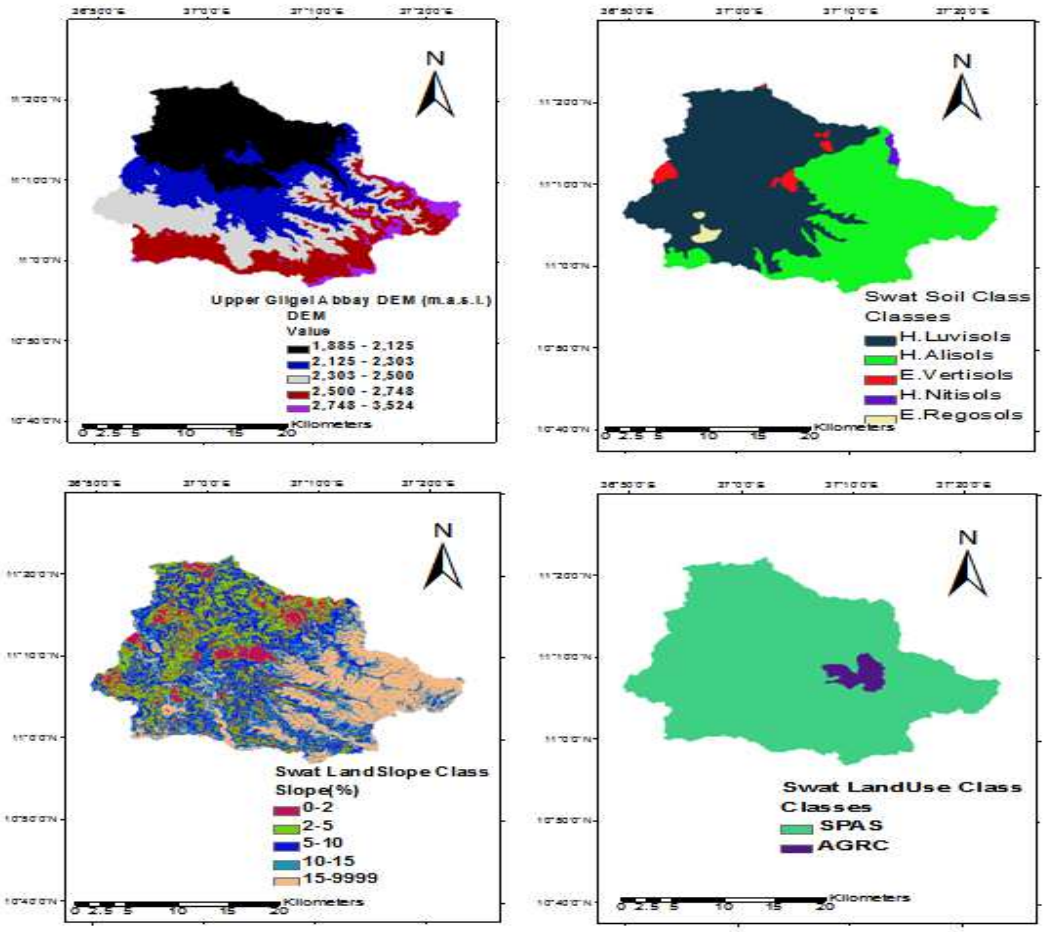

Figure 5.2*: SWAT model Spatial inputs data for Upper Gilgel Abay Catchment.*

5.2.2. Modelling Chemoga Catchment

It has a catchment area of 364 km^2 and the elevation ranging from 2246-3956 m +MSL. Modelling work has been carried out to delineate the catchment, the first spatial input DEM grid was processed by SWAT; and the watershed is partitioned in to nine HRU units.

Table 5.5*: Soil type of Gauged Chemoga catchment as per FAO-UNESCO soil classification system*

No.	Soil Type	Soil Classes defined in SWAT	Coverage Area (Km^2)	% of Total Area
1	Eutric Cambisols	E. Cambisols	13.29	3.65
2	Eutric Leptosols	E. Leptosols	49.38	13.56
3	Eutric Vertisols	E. Vertisols	43.09	11.84
4	Haplic Alisols	H.c Alisols	144.22	39.62
5	Haplic Luvisols	H. Luvisols	114.04	31.33
Total			364	100

Table 5.6*: Land use classification of Gauged Chemoga catchment used in SWAT*

No.	Land use	SWAT Land use Class	Coverage Area (Km^2)	% of Total Area
	Agriculture	AGRC	0.05	0.01
	Agro-pastoral	SPAS	280.33	77.01
	Agro-sylvicultural	AGRL	2.10	0.58
	Pastoral	PAST	81.52	22.40
Total			364	100

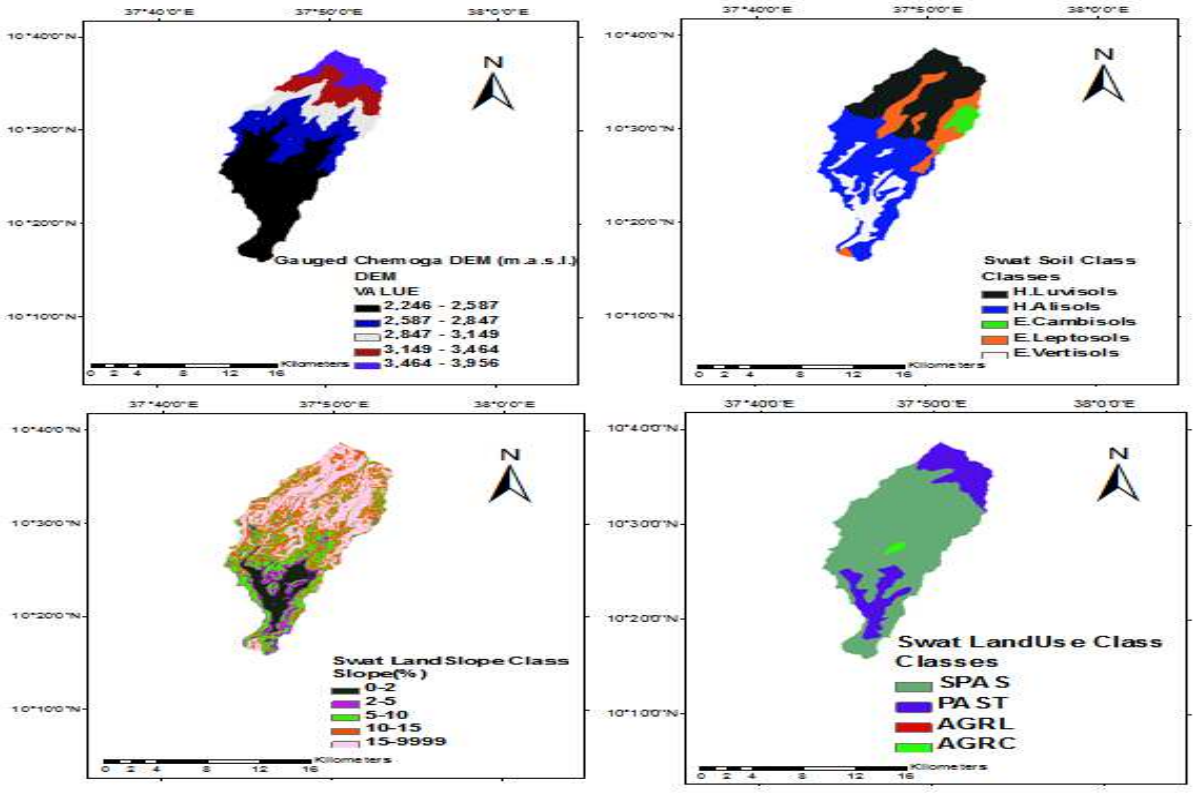

Figure 5.3*: SWAT model Spatial input data for Gauged Chemoga catchment.*

5.2.3. Modelling Muger Catchment

Taking the recommendations (Luzio *et al.* 2002) in to consideration, 20%, 10%, and 20% threshold levels for the land use, soil and slope classes were applied, respectively so as to encompass most of spatial details; and thirty-one HRUs were produced.

Table 5.7*: Soil type of Gauged Muger catchment as per FAO-UNESCO soil classification system*

No.	Soil Type	Soil Classes defined in SWAT	Coverage Area (Km^2)	% of Total Area
1	Chromic Luvisols	C. Luvisols	95.82	19.60
2	Eutric Cambisols	E. Cambisols	156.02	31.91
3	Eutric Leptosols	E. Leptosols	59.52	12.17

4	Eutric Vertisols	E. Vertisols	177.64	36.33
Total			489	100

Table 5.8*: Land use classification of Gauged Muger catchment used in SWAT*

No.	Land use	SWAT Land use Class	Coverage Area (Km^2)	% of Total Area
1	Agriculture	AGRC	185.66	37.97
2	Agro-pastoral	SPAS	89.87	18.38
3	Pastoral	PAST	159.92	32.70
4	Sylvicultural	AGRL	53.55	10.95
Total			489	100

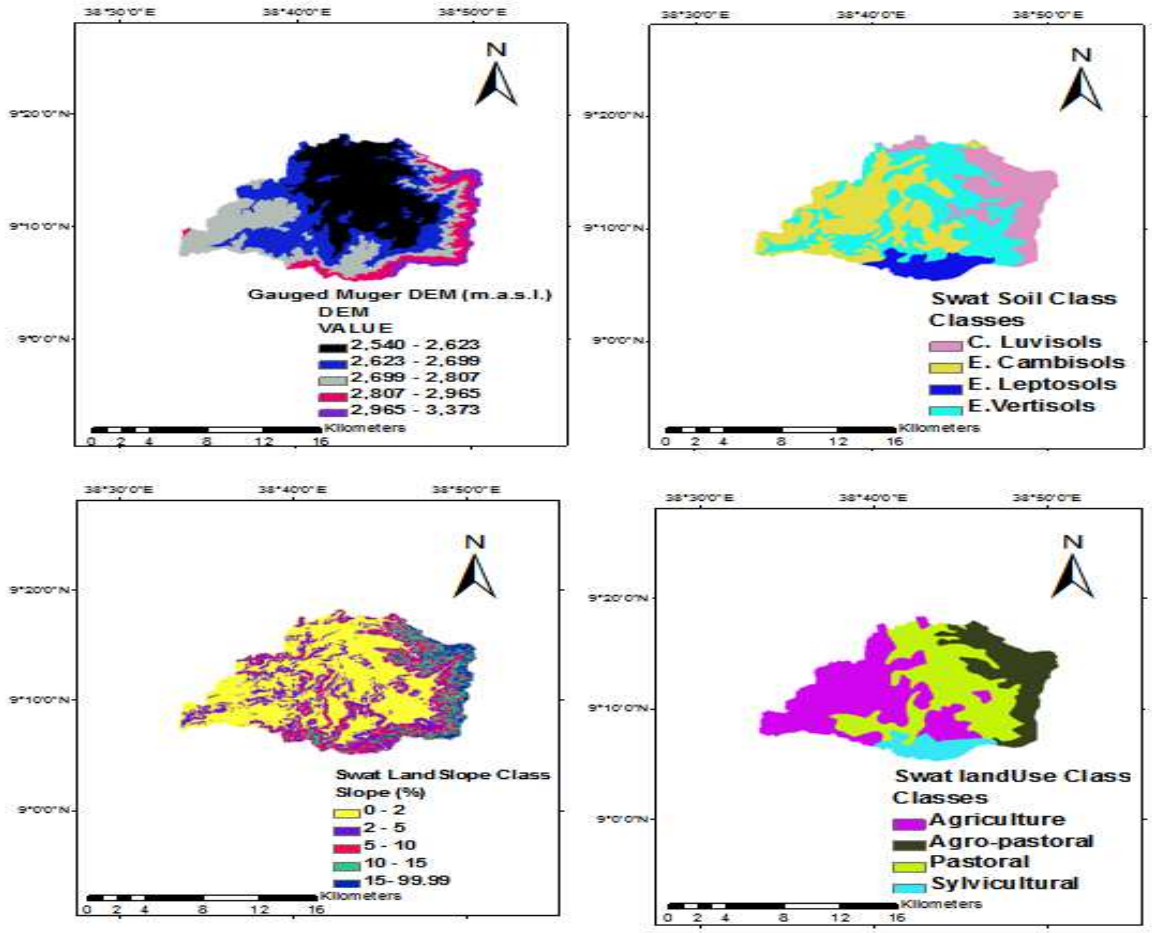

Figure 5.4 *: SWAT model spatial input data for Gauged Muger Watershed.*

5.2.4. Modelling Guder Catchment

To simulate the runoff at the outlet of this catchment, DEM, land use and Soil map of the watershed used are clearly shown here below in fig 5.5 and table 5.9 & 5.10. The threshold

values of 20%, 10%, and 20% (Luzio *et al.* 2002) for the land use, soil and slope classes were applied, respectively to divide the watershed in to 32 HRUs.

Table 5.9*: Soil type of Gauged Guder catchment as per FAO-UNESCO soil classification system*

No.	Soil Type	Soil Classes defined in SWAT	Coverage Area (Km^2)	% of Total Area
1	Calcic Vertisols	C. Vertisols	0.82	0.16
2	Chromic Luvisols	C. Luvisols	92.84	17.72
3	Eutric Fluvisols	E. Fluvisols	152.06	29.02
4	Eutric Leptosols	E. Leptosols	3.09	0.59
5	Eutric Vertisols	E. Vertisols	20.62	3.94
6	Haplic Alisols	H. Alisols	192.62	36.76
7	Haplic Luvisols	H. Luvisols	47.34	9.03
8	Haplic Nitisols	H. Nitisols	12.84	2.45
9	Urban	Urban Land	1.77	0.34
Total			524	100

Table 5.10*: Land use classification of Gauged part Guder catchment used in SWAT*

No.	Land use	SWAT Land use Class	Coverage Area (Km^2)	% of Total Area
1	Agriculture	AGRC	14.03	2.68
2	Agro-pastoral	SPAS	291.57	55.64
3	Agro-sylvicultural	AGRL	103.16	19.69
4	Pastoral	PAST	33.48	6.39
5	Sylvo-pastoral	WPAS	78.77	15.03
6	Urban	URLD	2.98	0.57
Total			524	100

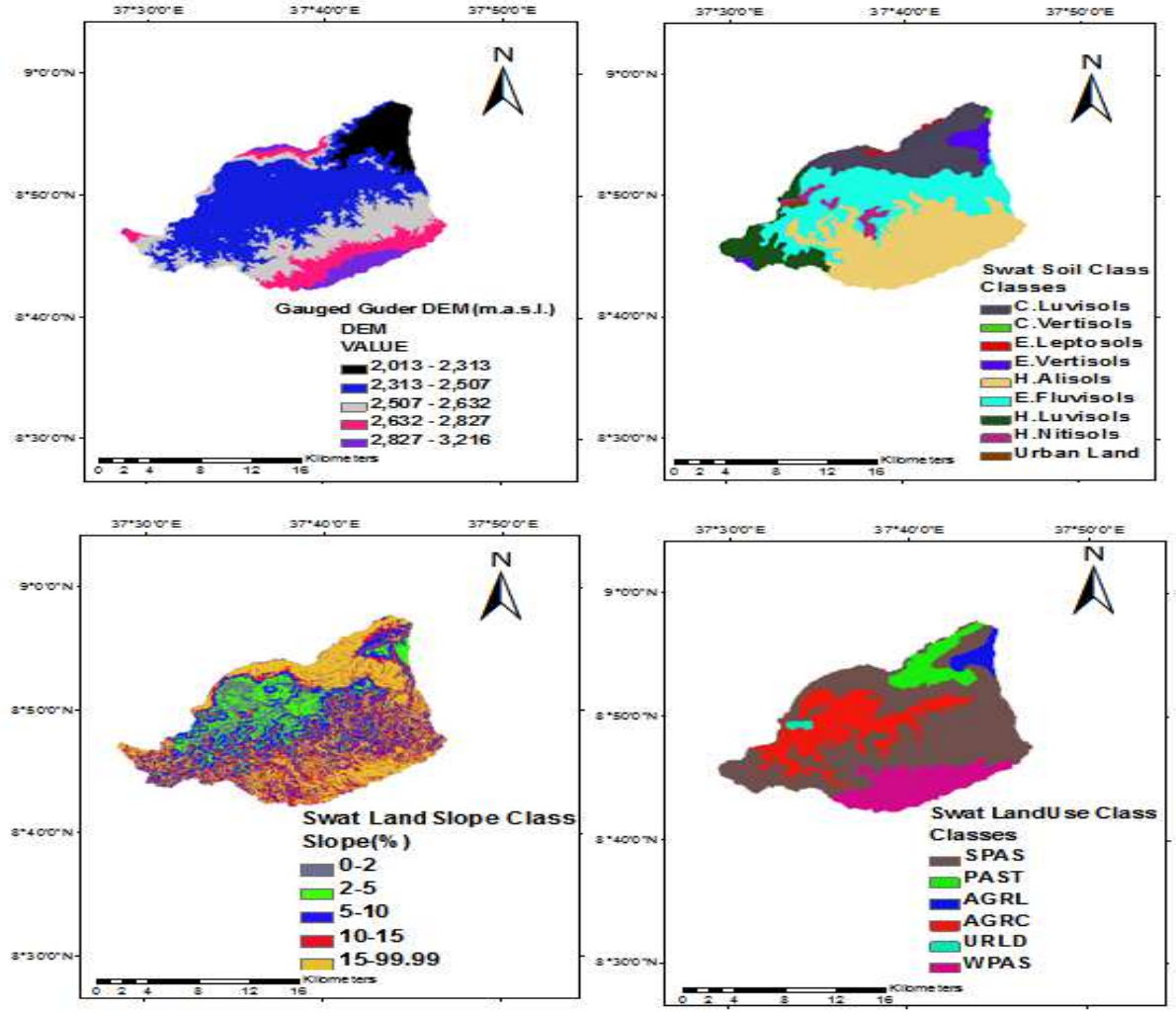

Figure 5.5*: SWAT model Spatial input data for Gauged Guder Catchment.*

5.2.4. Modelling Didessa Catchment

The threshold values of 20%, 10%, and 20% (Luzio *et al.* 2002) for the land use, soil and slope classes were applied, respectively to get 295 HRUs.

Table 5.11*: Soil type of Gauged Didessa catchment as per FAO-UNESCO soil classification system*

No.	Soil Type	Soil Classes defined in SWAT	Coverage Area (Km^2)	% of Total Area
1	Eutric Fluvisols	C. Vertisols	86.11	0.86
2	Eutric Leptosols	C. Luvisols	7.14	0.07
3	Eutric Regosols	E. Fluvisols	3.37	0.03
4	Eutric Vertisols	E. Leptosols	1355.38	13.58
5	Haplic Acrisols	E. Vertisols	1120.76	11.23

6	Haplic Alisols	H. Alisols	6334.21	63.46
7	Haplic Nitisols	H. Luvisols	835.90	8.37
8	Rhodic Nitisols	H. Nitisols	238.14	2.39
Total			9981	100

Table 5.12*: Land use classification of Gauged Didessa catchment used in SWAT*

No.	Land use	SWAT Land use Class	Coverage Area (Km^2)	% of Total Area
1	Agriculture	AGRC	3116.78	31.23
2	Agro-pastoral	SPAS	24.78	0.25
3	Agro-sylvicultural	AGRL	2316.21	23.21
4	Pastoral	PAST	292.07	2.93
5	State Farm	AGRR	29.44	0.29
6	Sylvicultural	AGRL	1385.76	13.88
7	Sylvo-pastoral	WPAS	2807.13	28.12
8	Urban	URLD	8.83	0.09
Total			9981	100

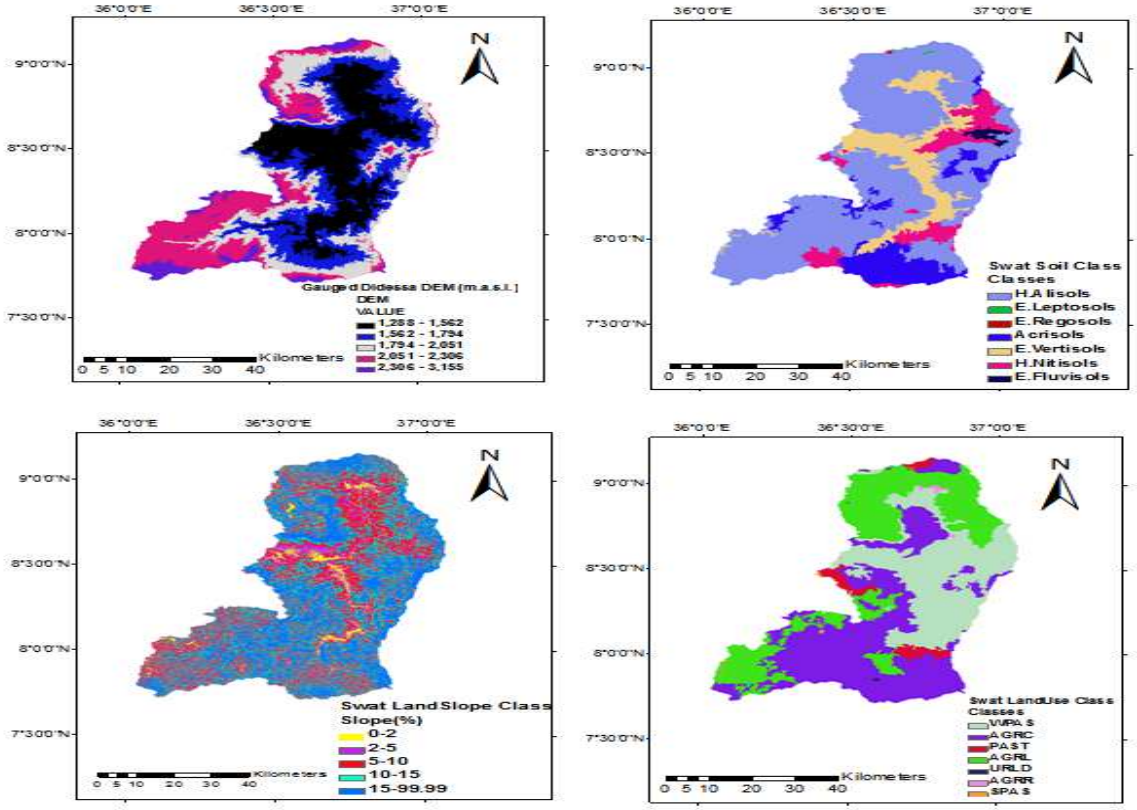

Figure 5.6*: SWAT model Spatial input data for Gauged Didessa Watershed.*

5.3. Parameter Identification

As a distributed model, SWAT allows for subdivision of a watershed into smaller subwatersheds and HBV-Light also allows partition of watershed in to different elevation and vegetation zones. Each of these subbasins and vegetation zones are represented by a number of parameters that could be derived by calibration. Determining parameter values that are both realistic and 'optimal' for such a large number of parameters is not feasible, calling for a necessary reduction of the number of calibrable parameters. In this study, three hierarchical methods are applied to achieve this reduction.

5.3.1. Screening

Screening, as applied in this study, refers to identification of model parameters that could be estimated with reasonable accuracy based on field data alone. A detailed investigation of the literature related to HBV and SWAT has assisted in identifying the parameters in Tables 5.13 and 5.14 that are integrally related to the model's streamflow prediction; whose estimation from readily available data alone may pose significant uncertainty; and for which there exists insufficient information from which the parameters could be directly estimated. Thus, if screening is the only parameter reduction mechanism used, the parameter estimation algorithm is left to identify best-fit values for over one thousand parameters, which is still quite a daunting task (Misgana, 2004).

Table 5.13: ***Swat model parameters involved in the streamflow prediction process*** (van Griensven, 2002)**.**

No.	Parameter	Description	Range of Value	
			Min	Max
1	Alpha_Bf	Base flow alpha factor (days)	0	1
2	Biomix	Biological mixing efficiency	0	1
3	Blai	Maximum potential leaf area index	0	1
4	Canmx	Maximum canopy storage [mm]	0	10
5	Ch_K2	Channel effective hydraulic conductivity [mm/hr]	0	150
6	Ch_N2	Manning's n value for main channel	0	1
7	Cn2	Initial SCS CN II value	35	98
8	Epco	Plant uptake compensation factor	0	1
9	Esco	Soil evaporation compensation factor	0	1
10	Gw_Delay	Groundwater delay [days]	0	50

11	Gw_Revap	Groundwater "revap" coefficient	0.02	0.2
12	Gwqmn	Threshold water depth in the shallow aquifer for flow [mm]	0	5000
13	Revapmn	Threshold water depth in the shallow aquifer for "revap" [mm]	0	500
14	Sftmp	Snowfall temperature [ºC]	0	5
15	Slope	Average slope steepness [m/m]	0	1
16	Slsubbsn	Average slope length [m]	10	150
17	Smfmn	Melt factor for snow on June 21 [mm H2O/ºC-day]	0	10
18	Smfmx	Melt factor for snow on December 21 [mm H2O/ºC-day]	0	10
19	Smtmp	Snow melt base temperature [ºC]	0	5
20	Sol_Alb	Moist soil albedo	0	0.25
21	Sol_Awc	Available water capacity [mm H20/mm soil]	0	1
22	Sol_K	Saturated hydraulic conductivity [mm/hr]	0	100
23	Sol_Z	Soil depth [mm]	0	3000
24	Surlag	Surface runoff lag time (days)	0	10
25	Timp	Snow pack temperature lag factor	0	1
26	Tlaps	Temperature lapse rate [°C/km]	0	10

Table 5.14*: HBV model parameters involved in the streamflow prediction process* (Seibert, 2005)**.**

No.	**Parameter**	**Description**	**Range of Value**	
			Min	**Max**
1	FC	Max. soil moisture storage (mm)	50	1500
2	LP	soil moisture value above which ET_{act} reaches ET_{pot} (mm)	0.3	1
3	BETA	parameter that determines the relative contribution to runoff from rain or snowmelt (-)	1	6
4	PERC	Max. Percolation to lower zone (mm day^{-1})	0	6
5	UZL	threshold parameter (mm)	0	100
6	Ko	Recession coefficient (day^{-1})	0.05	0.5
7	K1	Recession coefficient (day^{-1})	0.01	0.3
8	K2	Recession coefficient (day^{-1})	0.01	0.1
9	MAXBAS	Routing, length of weighting function	1	5

In an attempt to further reduce the number of calibrable parameters, some spatially varying inputs (e.g. ground water flow parameters) are forced to assume uniform values over the watershed and some others (e.g. Manning's coefficient for channels) are broadly grouped. For several other parameters, including the Curve Number, Manning's roughness coefficient for

overland flow, and maximum water holding capacity of a soil, a concept referred to in this study as parameterization was applied.

5.3.2. Parameterization

Parameters affecting hydrology can be changed either in a lumped way (over the entire catchment), or in a distributed way (for selected subbasins or HRU's).Parameterization is a technique for transferring model parameters of a given spatial unit to other spatial units in the watershed. For this study, a 'representative subbasin' is selected, upon which the model assumes homogeneity of parameters and variables. A relationship between required parameters of this representative modeling unit and corresponding parameters of other homogeneous units (e.g. subbasins) is developed using available information about the parameters. In this way, the definition of variables in the representative subbasin enables determination of a corresponding parameter in other subbasins. For parameterization of the Curve Number, CN, for example, a hypothetical subbasin covered with pasture lands that is grown under treatment conditions and soil group 'A' was considered to be representative. Then, the relationship between the CN of the representative virtual subbasin and other subbasins that have the same land use and treatment conditions as the representative subbasin, but belonging to a different soil group, were derived based on CN values recommended in the literature. So, some parameters were allowed to vary spatially and others assume uniform values over the watersheds.

Parameter changes in SWAT affecting hydrology were done in a distributed way for selected sub-basins and HRU's while in HBV lumped parameter changes were applied for various elevation and vegetation zones.

A combination of the screening and parameterization reduced the number of parameters that need to be calibrated. Yet, it may still not be necessary or wise to apply a search algorithm to all remaining parameters. Particularly for watersheds that lack long years of recorded data, it is essential to reduce the number of calibrable parameters as much as possible. Fortunately, model outputs are not equally sensitive to all parameters of a model. If an output is not appreciably sensitive to certain parameters, it would be reasonable to assign nominal estimates for those parameters and consider only the parameters to which the model is sensitive during the calibration effort, calling for a parameter sensitivity analysis.

5.3.3. Parameter Sensitivity Analysis

Sensitivity analysis is one of valuable tools for identifying important parameters of the model which has significant impact on model response and reduces the computational time of the model run. It is also important to assess parameter identifiability and sources of uncertainty (Muleta and Nicklow, 2005; Sieber and Uhlenbrook, 2005). The SWAT model sensitivity analysis was undertaken by using a built-in tool in ArcSwat that uses the Latin Hypercube One-factor-At-a-Time (LH-OAT) design method of Morris (1991). Details of this method are explained in Huisman et al. (2004). After the analysis, the mean relative sensitivity (MRS) of the parameters was used to rank the parameters, and their category of sensitivity was also defined based on the Lenhart et al. (2002) classification. He divided sensitivity into four classes: small to negligible ($0 \leq MRS < 0.05$), medium ($0.05 \leq MRS < 0.2$), high ($0.20 \leq MRS < 1.0$), and very high ($MRS \geq 1.0$). Dilnesaw (2006) indicated that there can be a significant variation of hydrological processes between individual watersheds; therefore, this justified the need for the sensitivity analysis made to each of the five watersheds in the study area.

The SWAT sensitivity analysis had been carried out for all modelled watershed, generally, sensitivity of parameters varies (table 5.5) from catchment to catchment in Upper Blue Nile Basin. CN is the most sensitive parameter in all catchments, indicating the importance of this parameter during calibration. Threshold water depth in the shallow aquifer for flow (Gwqmn) was the second highest sensitive parameter which governs the base flow in Gilgel Abbay, Chemoga and Muger catchments. This is an indication that these three catchments have highest ground water contribution to the flow. While Sol_Z and Esco are the second most sensitive parameters in Guder and Didessa catchments, respectively.

Table 5.15*: Result of SWAT parameter sensitivity analysis of flow in test watersheds.*

Rank	Parameter	Lower Bound	Upper Bound	Sensitivity	
				MRS Value	Sensitivity Class
Gilgel Abbay					
1	Cn2	35	98	0.56	Highly sensitive
2	Gwqmn	0	5000	0.22	Highly sensitive
3	Canmx	0	10	0.16	Medium
4	Blai	0	1	0.15	Medium

5	Sol_Z	0	3000	0.15	Medium
6	Sol_Awc	0	1	0.14	Medium
7	Esco	0	1	0.11	Medium
8	Gw_Revap	0.02	0.2	0.07	Medium
9	Ch_K2	0	150	0.02	Low
10	Epco	0	1	0.01	Low
11	Alpha_Bf	0	1	0.01	Low
Chemoga					
1	Cn2	35	98	0.32	Highly sensitive
2	Gwqmn	0	5000	0.22	Highly sensitive
3	Esco	0	1	0.18	Medium
4	Sol_Z	0	3000	0.16	Medium
5	Canmx	0	10	0.14	Medium
6	Sol_Awc	0	1	0.09	Medium
7	Blai	0	1	0.088	Medium
8	Gw_Revap	0.02	0.2	0.05	Medium
9	Slope	0	1	0.01	Low
Muger					
1	Cn2	35	98	0.66	Highly sensitive
2	Gwqmn	0	5000	0.31	Highly sensitive
3	Esco	0	1	0.29	Highly sensitive
4	Blai	0	1	0.26	Highly sensitive
5	Canmx	0	10	0.14	Medium
6	Sol_Z	0	3000	0.11	Medium
7	Gw_Revap	0.02	0.2	0.05	Medium
8	Epco	0	1	0.02	Low
9	Alpha_Bf	0	1	0.02	Low
10	Sol_Awc	0	1	0.01	Low
11	Ch_K2	0	150	0.01	
Guder					
1	Cn2	35	98	0.27	Highly sensitive
2	Sol_Z	0	3000	0.18	Medium
3	Esco	0	1	0.15	Medium
4	Gwqmn	0	5000	0.13	Medium
5	Blai	0	1	0.09	Medium
6	Canmx	0	10	0.06	Medium

7	Sol_Awc	0	1	0.05	Medium
8	Gw_Revap	0.02	0.2	0.03	Low
9	Epco	0	1	0.01	Low
10	Ch_K2	0	150	0.01	Low
11	Alpha_Bf	0	1	0.01	Low
Didessa					
1	Cn2	35	98	0.55	Highly sensitive
2	Esco	0	1	0.30	Highly sensitive
3	Gwqmn	0	5000	0.19	Medium
4	Sol_Awc	0	1	0.19	Medium
5	Sol_Z	0	3000	0.08	Medium
6	Blai	0	1	0.05	Medium
7	Alpha_Bf	0	1	0.04	Low
8	Gw_Revap	0.02	0.2	0.03	Low
9	Canmx	0	10	0.03	Low
10	Ch_K2	0	150	0.02	Low
11	Epco	1	2	0.02	Low

Unlike swat model, HBV has no built-in program tool for sensitivity analysis, local sensitivity technique was applied that output responses are determined by sequentially varying each of the input parameters by fixing all other factors to constant nominal values; and fig. 5.7; thus, displays the result of HBV sensitivity analysis. The graph demonstrates that LP, BETA and FC, in that order, are the most sensitive parameter in all catchments.

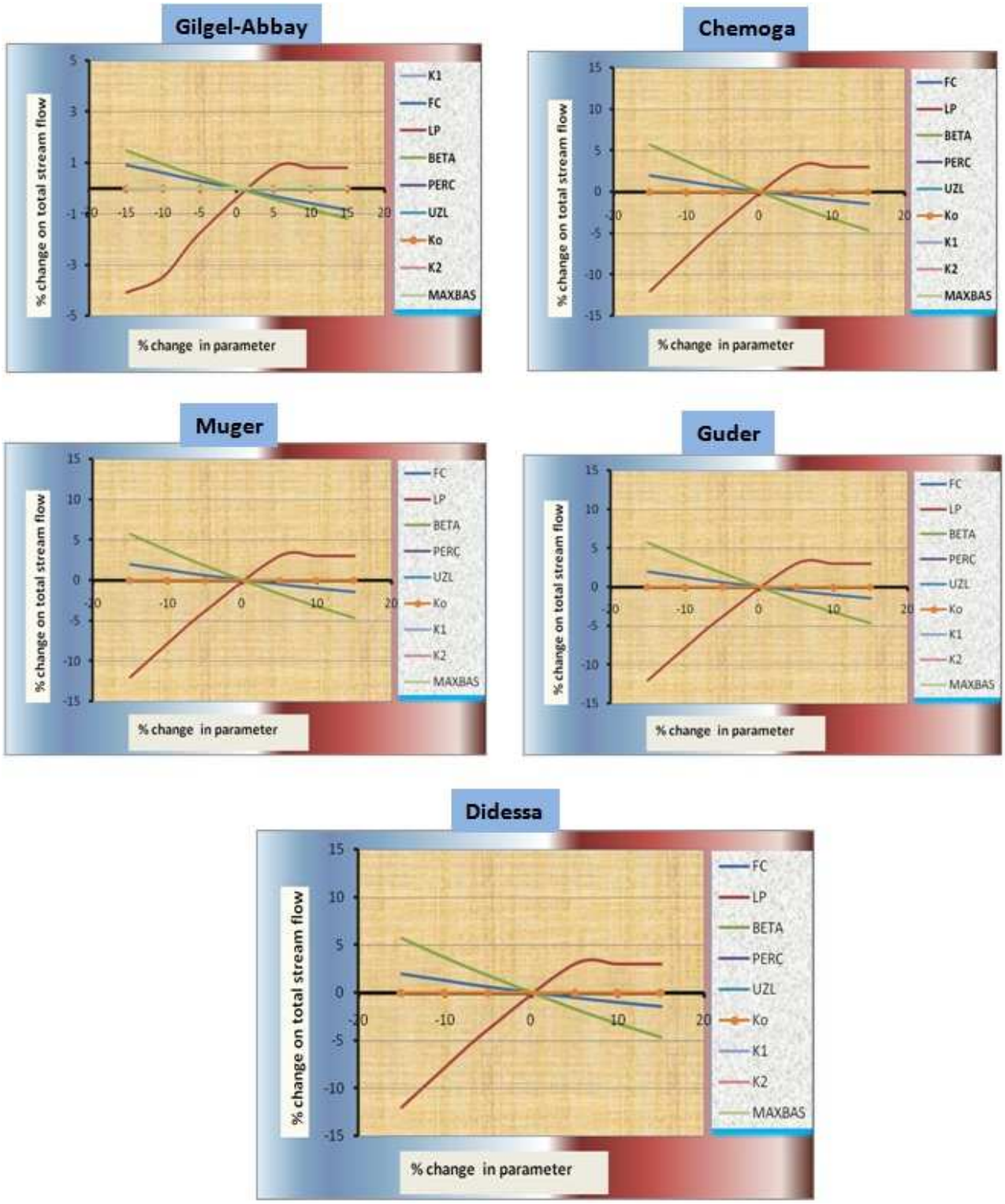

Figure 5.7: ***Result of HBV parameter sensitivity analysis of flow in test watersheds***

6. Results and Discussion

Both the basic models are applied to each of the five test catchments, operating in continuous river-flow simulation mode, involving the use of calibration and verification periods (about two-thirds for calibration and one-third for verification) (Seibert, 2005). In terms of increasing complexity, the HBV is the simplest, followed by the SWAT. Both HBV-Light and ArcSWAT models have built-in auto-calibration tools (see methodology section for more detail); henceforth, automatic searching algorithms were used to determine best parameters and to estimate the simulations.

6.1. Monthly Auto-Calibration and Validation

The best basis for judging model performance is a comparison of model estimates with observations both quantitatively (numerically) and qualitatively (visually) (Willmott, 1984). Even if a model is based on the best available knowledge, comparison of the results with observations is the only way of establishing confidence in the simulation.

Table 6.1*: Monthly time step goodness-of-fit indices of the two substantive models.*

Model	Gilgel-Abbay (1664km^2)							
	r^2	N_{SE}	IoA	IVF	RE	$meandiff$	D	Remark
Calibration								
HBV-Light	0.900	0.891	0.969	0.893	0.208	0.197	-10.675	Very Good
ArcSWAT	0.860	0.824	0.944	0.836	-0.055	5.238	-16.390	Very Good
Verification								
HBV-Light	0.865	0.846	0.956	0.831	0.243	0.145	-16.926	Very Good
ArcSWAT	0.851	0.754	0.908	0.773	-0.438	3.318	-22.735	Very Good
	Chemoga (364 km^2)							
Calibration								
HBV-Light	0.693	0.693	0.902	0.998	-0.379	0.002	-0.237	Good
ArcSWAT	0.634	0.202	0.834	1.730	0.09	-1.921	72.953	Good
Verification								
HBV-Light	0.752	0.710	0.895	0.787	-0.328	0.251	-21.317	Very Good
ArcSWAT	0.540	0.46	0.638	0.603	-0.506	0.467	-39.669	Good
Model	**Muger (489km^2)**							
	r^2	N_{SE}	IoA	IVF	RE	$meandiff$	D	Remark
Calibration								
HBV-Light	0.797	0.793	0.936	0.92	-0.168	0.052	-7.974	Very Good

ArcSWAT	0.608	0.598	0.872	1.047	0.020	-0.175	4.723	Good
Verification								
HBV-Light	0.888	0.868	0.968	1.111	0.039	-0.04	11.062	Very Good
ArcSWAT	0.575	0.571	0.839	0.880	-0.232	0.245	-11.979	Good
Guder (524 km^2)								
Calibration								
HBV-Light	0.825	0.823	0.951	1.000	0.112	0.000	-0.010	Very Good
ArcSWAT	0.706	0.634	0.891	0.724	-0.158	2.680	-27.552	Good
Verification								
HBV-Light	0.847	0.832	0.957	1.083	0.079	-0.283	8.290	Very Good
ArcSWAT	0.801	0.515	0.886	1.633	0.423	-2.158	63.259	Good
Didessa (1998 km^2)								
Calibration								
HBV-Light	0.786	0.784	0.938	0.987	-0.261	0.007	-1.342	Very Good
ArcSWAT	0.729	0.499	0.547	3.438	1.030	-125.459	243.831	Fair
Verification								
HBV-Light	0.891	0.852	0.9600	0.795	-0.257	5.089	-20.524	Very Good
ArcSWAT	0.311	0.347	0.509	1.157	-0.049	-34.905	115.749	Not Good

Gilgel Abay

The calibrations of the models were performed for eleven years including warming up period (1990 to 2000) and validation for a period of five years (2001-2005) using Gilgel Abay river flow data at Merawi stream gauging station. After monthly calibration of models parameters, the simulation showed good results for the monthly average discharge values with a slope of the simulated versus measured values close to unity, with high coefficient of determination r^2, Nash-Sutcliffe efficiency N_{SE} and Index of Agreement IoA for both models. As indicated in calibration and validation results: r^2, N_{SE} and IoA values for the monthly stream flow of validation and calibration ranges from 0.851 - 0.9, 0.754-0.891 and 0.908-0.969 respectively. According to the model evaluation guide lines, both models simulated the stream flow very good in both calibration and validation period. Both HBV and SWAT models; therefore, able to capture monthly and seasonal patterns with increasingly secured performance. For catchments characterized by strong seasonality, such as Gilgel Abbay, the SWAT, with its inherent

component of seasonal variation, equivalently outperforms the HBV. The calibrated parameters for both models are reported in Appendix-D.

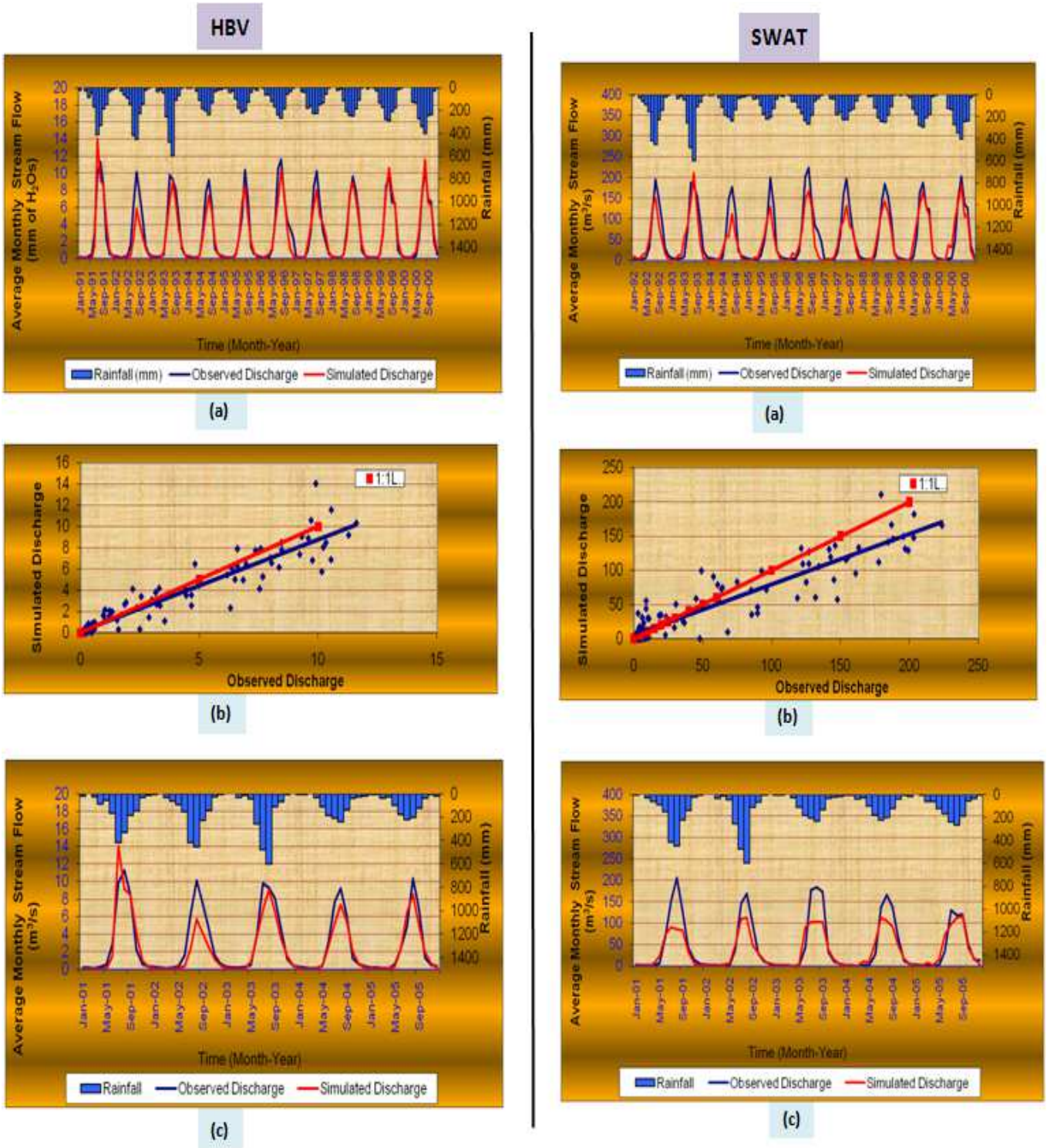

Figure 6.1*: Monthly Auto- Calibration and Validation results of upper Gilgel Abay River gauged near Merawi. (a)Observed and simulated flow hydrograph for both models during calibration. (b) Scatter plot of simulated versus observed discharge during calibration period. (c) Validation of observed and simulated flow hydrographs.*

Chemoga

From the performance results for this catchment (table 6.1), it is clear that the simulation performance of the SWAT is, in each case, inferior to that of the HBV model, which is an indication of the poor performance of the SWAT model as the size of the catchment gets smaller a behavior shared by other studies (e.g. Yared, 2009). The validation and calibration results of HBV demonstrate that r^2, N_{SE} and IoA for monthly stream flow values ranges from 0.693 to 0.901. Based on the model performance criteria, the HVB model simulated the stream flow trend as good to very good performance. HBV model; therefore, able to handle monthly and seasonal patterns with better efficiency than the SWAT model for the Chemoga watershed. For relatively smaller catchments, however, such as Chemoga and Muger, the HBV model performs consistently better than the SWAT model.

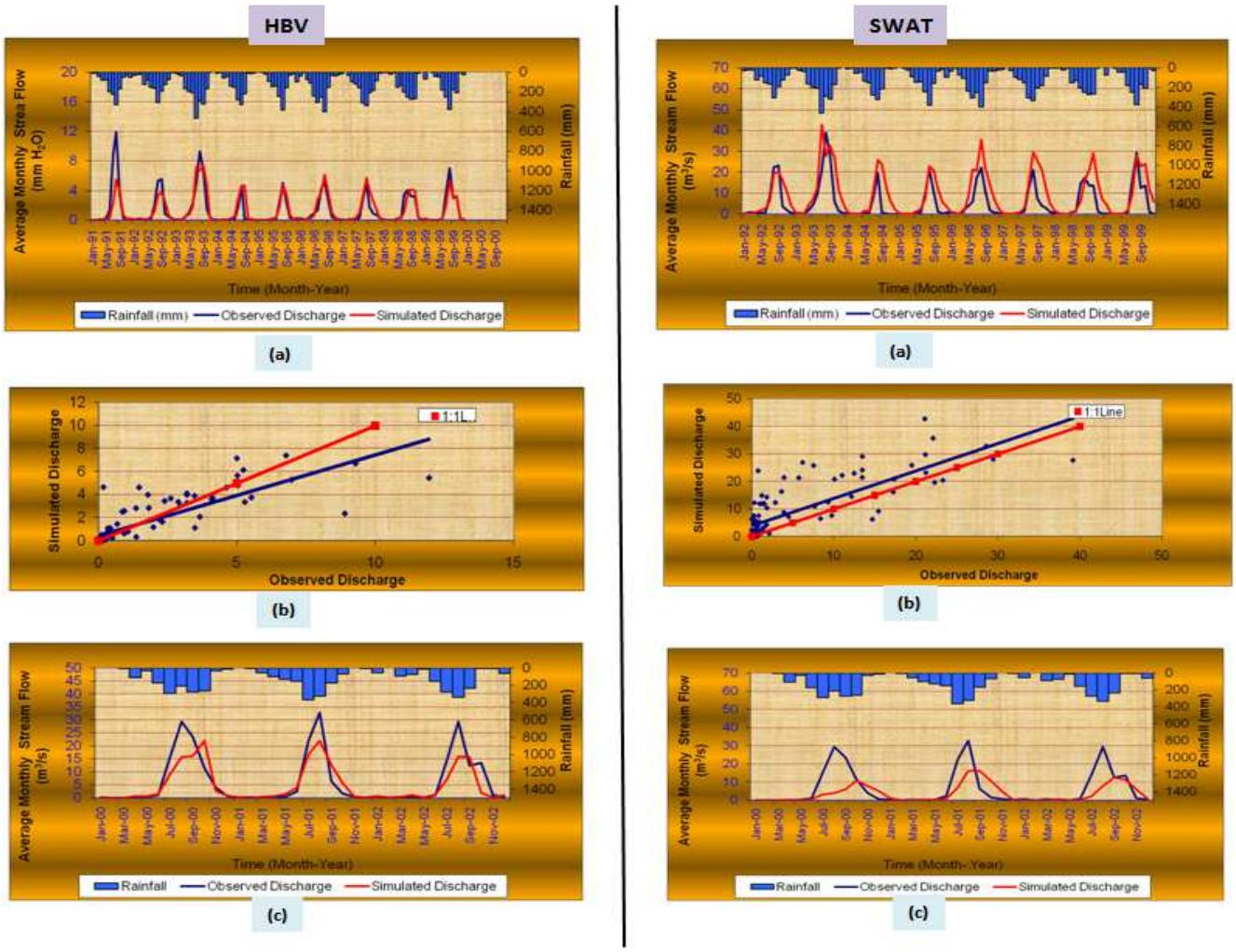

Figure 6.2*: Graphical representations of monthly Auto- Calibration and Validation results of Chemoga River gauged near Debre Markos. (a)Observed and simulated flow hydrograph for both models during calibration. (b) Scatter plot of simulated versus observed discharge during calibration period. (c) Validation of observed and simulated flow hydrographs.*

Muger

The calibration results show that there is a good agreement between the simulated and gauged monthly flows in both two models. This is demonstrated by the correlation coefficient r^2 and the Nash-Suttcliffe simulation efficiency N_{SE}values. The results fulfilled the requirements suggested by Santhi & et al. (2001) for $r^2 > 0.6$ and $N_{SE} > 0.5$. Comparable to the calibration runs, the two models performed sufficiently in terms of efficiency criteria's when validated, with the quasi-semi-distributed HBV model simulating the overall hydrograph better than the physically based distributed SWAT model in this catchment. Though the SWAT model can sufficiently handle the monthly hydrological patterns of Muger, in the case of smaller catchments, such as Chemoga and Muger, the HBV performs better than SWAT model.

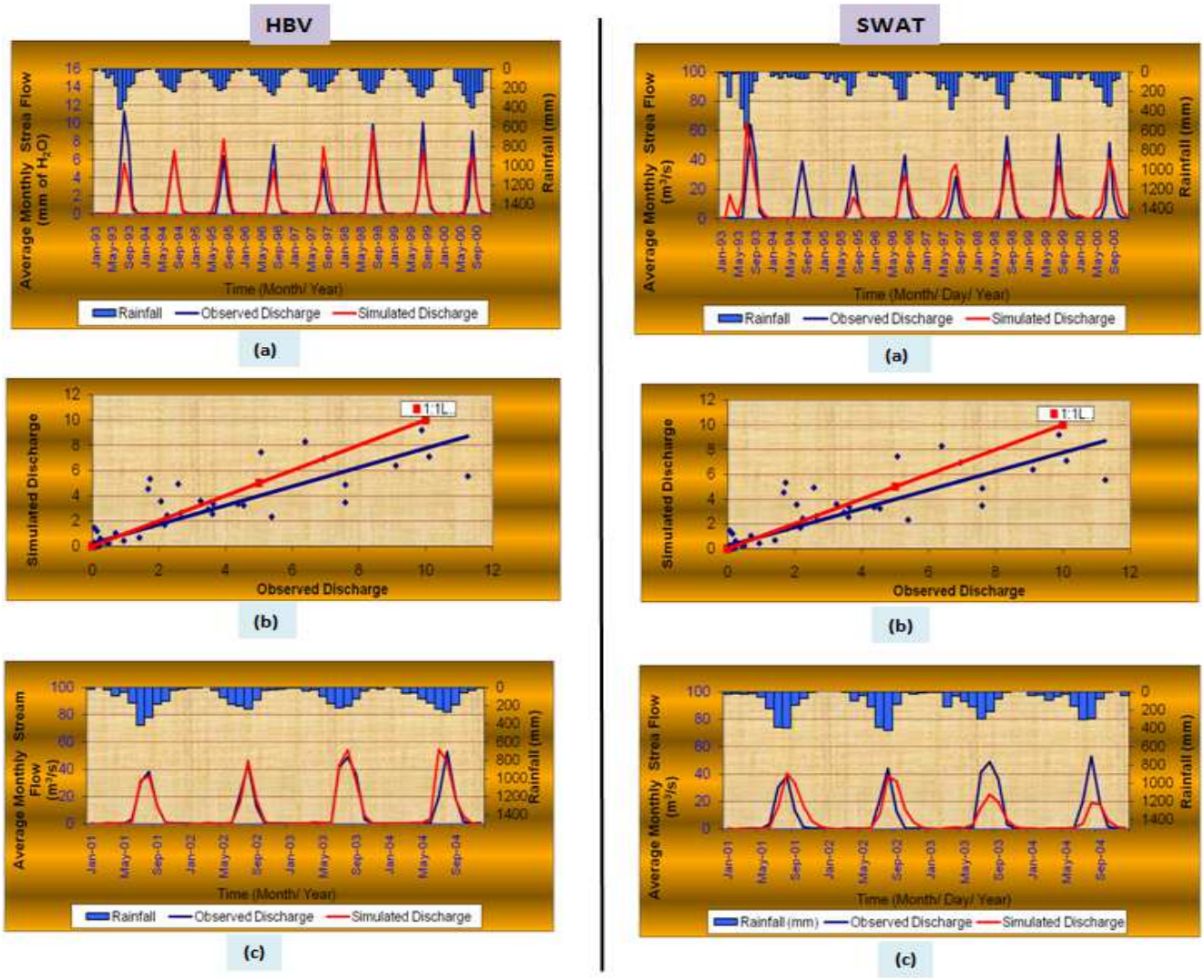

Figure 6.3*: Monthly Auto- Calibration and Validation results of Muger River. (a)Observed and simulated flow hydrograph for both models during calibration. (b) Scatter plot of simulated versus observed discharge during calibration period. (c) Validation of observed and simulated flow hydrographs.*

Guder

The calibrations of the models were performed for eleven years including warming up period (1990 to 2000) and validation for a period of five years (2001-2005) using Guder stream flow data at Guder instantaneous steam flow gauging station. When calibrated, the two models fit the observed values efficiently in terms of the overall r^2, N_{SE} and IoA values; although the conceptual HBV mode1 yielded a slightly better fit for this catchment. Both HBV and SWAT models; therefore, able to capture monthly and seasonal patterns with good efficiency for this catchment.

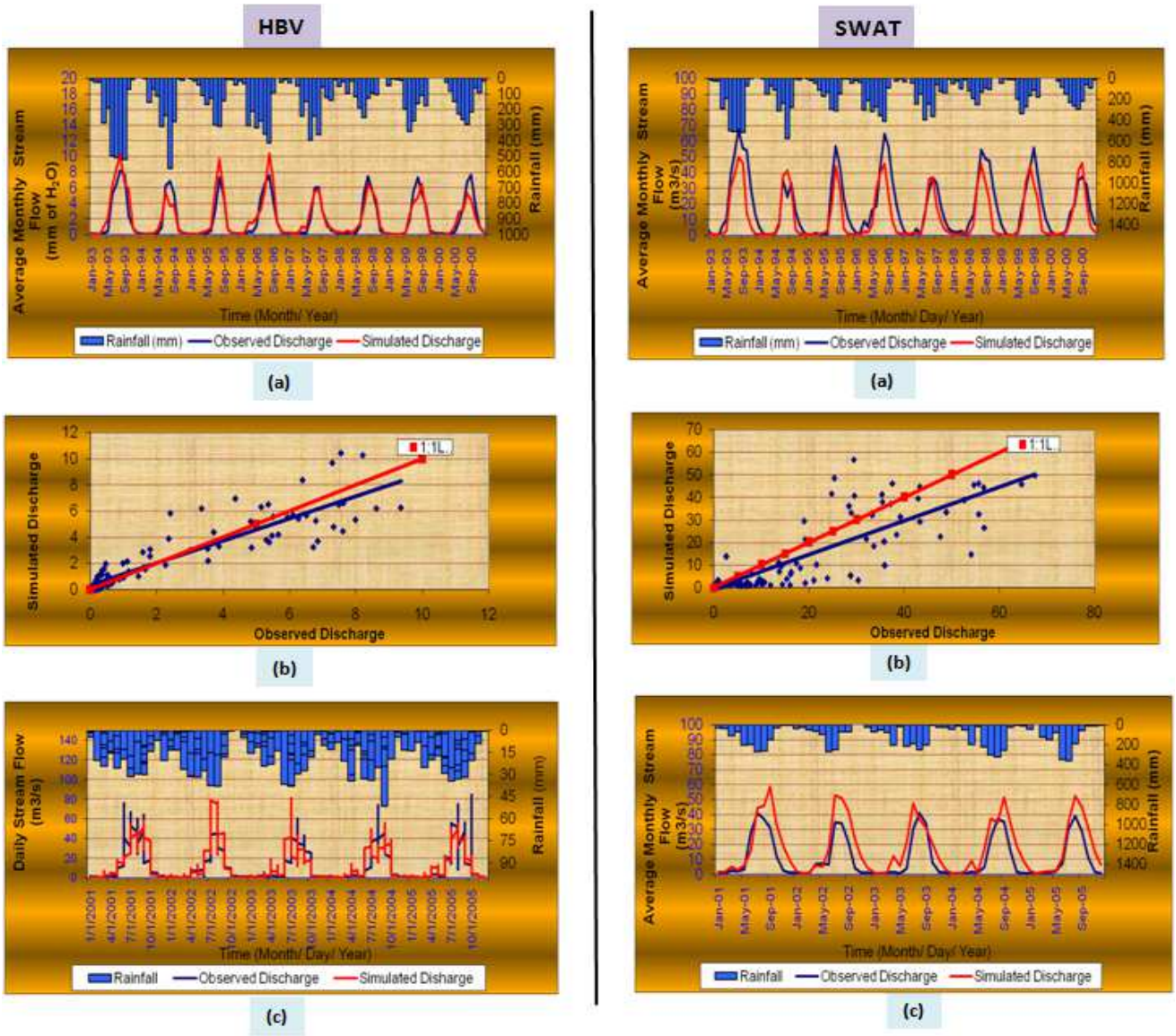

Figure 6.4: ***Monthly Auto- Calibration and Validation results of Guder River. (a)Observed and simulated flow hydrograph for both models during calibration. (b) Scatter plot of simulated versus observed discharge during calibration period. (c) Validation of observed and simulated flow hydrographs.***

Didessa

In the case of large catchments such as Gilgel Abbay, having a catchment area 1664 km^2, SWAT performs nearly equal to HBV model. However; Didessa, having a catchment area of 9981km^2, and characterized by physiographical and hydro-meteorological variability, the SWAT, with its inherent component of seasonal variation, can not sufficiently simulate monthly discharges with nice performance rating criteria (table 6.1). The hydrographs (Figure 6.4) allow for a graphical comparison of simulated to observed monthly discharge rates for the calibration and the validation data sets within each catchment. The SWAT model provided a better fit of the hydrograph in calibration period than that of validation. The simulated peak values were too high, but the peak positions were generally correct. This may be due to unreliable precipitation, soil, landuse and other data given as an input to the model or gauged flow used for the calibration. From the shape of hydrograph of HBV it was noticed that systematic and dynamic errors emanating from unknown catchment response pattern unaccounted by structure of the HBV model were very less. As indicated in calibration and validation results for HBV model: r^2, N_{SE} and IoA values for the monthly stream flow of validation and calibration ranges from 0.786 - 0.891, 0.784-0.852 and 0.938-0.960 respectively. According to the model evaluation guide lines, HBV model simulated the stream flow very good in both calibration and validation period. Therefore, unlike the SWAT model, this model able to capture monthly and seasonal patterns with secured performance in the Didessa catchment.

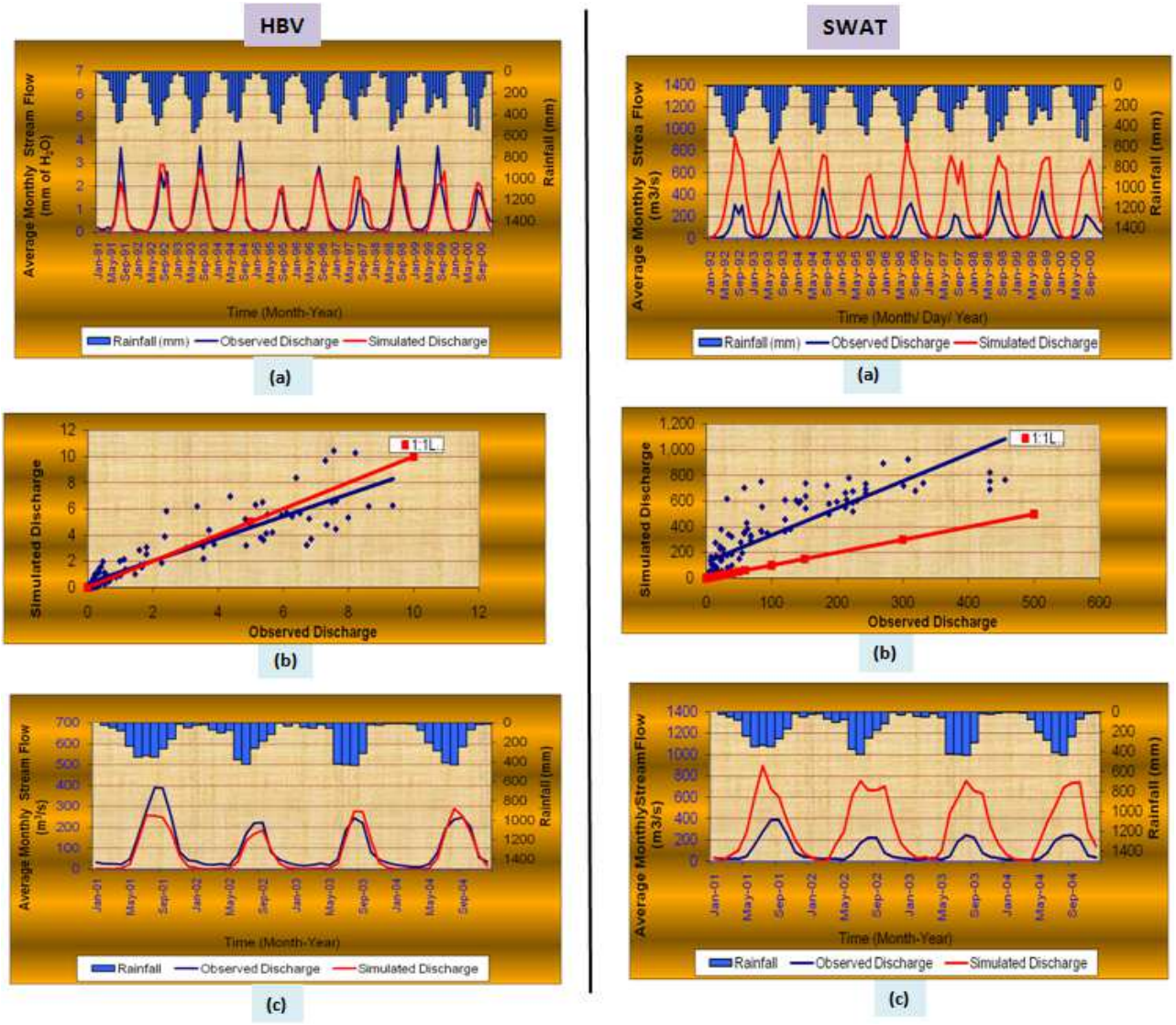

Figure 6.5*: Graphical representations of monthly Auto- Calibration and Validation results of Didessa River gauged near Arjo. (a) Observed and simulated flow hydrograph for both models during calibration. (b) Scatter plot of simulated versus observed discharge during calibration period. (c) Validation of observed and simulated flow hydrographs.*

6.2. Daily Auto-Calibration and Validation

From calibration and validation results on daily time step (table 6.2), the performance of the SWAT is clearly inferior to that of the HBV model. In the case of SWAT daily discharge generally, however, showed less accurate simulation with some major discrepancies, which is a common attribute shared by many other studies (Lewarne, 2009; Yared, 2010) and r^2 of only less than 0.6 and Nash-Sutcliffe efficiency N_{SE} of only less than 0.5 automatically were determined for all the test catchments. The peak values were at times too high or too low, but the peak positions were generally correct. The SWAT, although characterized by a large number of

Table 6.2*: Daily time step Calibration and verification results of the two substantive models*

Model	r^2	R^2	IoA	IVF	RE	$meandiff$	D	Rank
	Gilgel-Abbay (1664km^2)							
Calibration								
HBV-Light	0.724	0.714	0.916	0.898	0.536	111.925	-10.247	1
ArcSWAT	0.408	0.402	0.740	1.462	1.867	-99.59	46.207	
Verification								
HBV-Light	0.810	0.770	0.943	1.174	0.065	-77.631	17.350	1
ArcSWAT	0.40	0.402	0.676	1.473	2.249	-77.689	74.316	
	Chemoga (364 km^2)							
Calibration								
HBV-Light	0.540	0.540	0.826	1.010	-0.318	-0.238	2.912	1
ArcSWAT	0.302	0.254	0.650	0.631	0.023	29.162	-36.924	
Verification								
HBV-Light	0.523	0.505	0.709	0.808	-0.102	6.960	-19.219	1
ArcSWAT	0.496	0.468	0.803	0.771	0.111	102.392	-22.884	
	Muger (489km^2)							
Calibration								
HBV-Light	0.704	0.700	0.895	0.990	-0.607	3.899	-1.027	1
ArcSWAT	0.429	0.420	0.772	1.044	-0.624	-5.059	4.430	
Verification								
HBV-Light	7.12	0.699	0.913	1.172	-0.511	-208.66	17.214	1
ArcSWAT	0.409	0.406	0.726	0.876	-0.635	7.792	-12.381	
	Guder (524 km^2)							
Calibration								
HBV-Light	0.744	0.741	0.924	1.001	-0.111	-0.053	-0.137	1
ArcSWAT	0.408	-0.22	0.740	1.462	1.867	-99.593	46.207	
Verification								
HBV-Light	0.706	0.609	0.912	1.081	-0.127	-8.455	8.088	1
ArcSWAT	0.390	-1.00	0.676	1.743	2.249	-77.829	74.316	
	Didessa (1998 km^2)							
Calibration								
HBV-Light	0.700	0.693	0.905	0.986	-0.465	0.209	-1.375	1
ArcSWAT	0.203	0.247	0.622	1.821	1.661	37.120	82.120	
Verification								

HBV-Light	0.790	0.757	0.928	0.796	-0.365	54.828	20.412	1
ArcSWAT	0.396	0.368	0.803	0.771	0.111	21.392	52.884	

weights (parameters), does not generally perform better than the simpler conceptual model HBV. The HBV model variants, having eighth, nine or ten parameters, adequately simulate the hydrological behavior of the small to large catchments on daily time step. These results indicate the simpler HBV model, involving fewer parameters or weights to be evaluated are often better in discharge forecasting than the SWAT model which involve a significantly larger number of parameters or weights to be evaluated and which rely on complex mathematical computations.

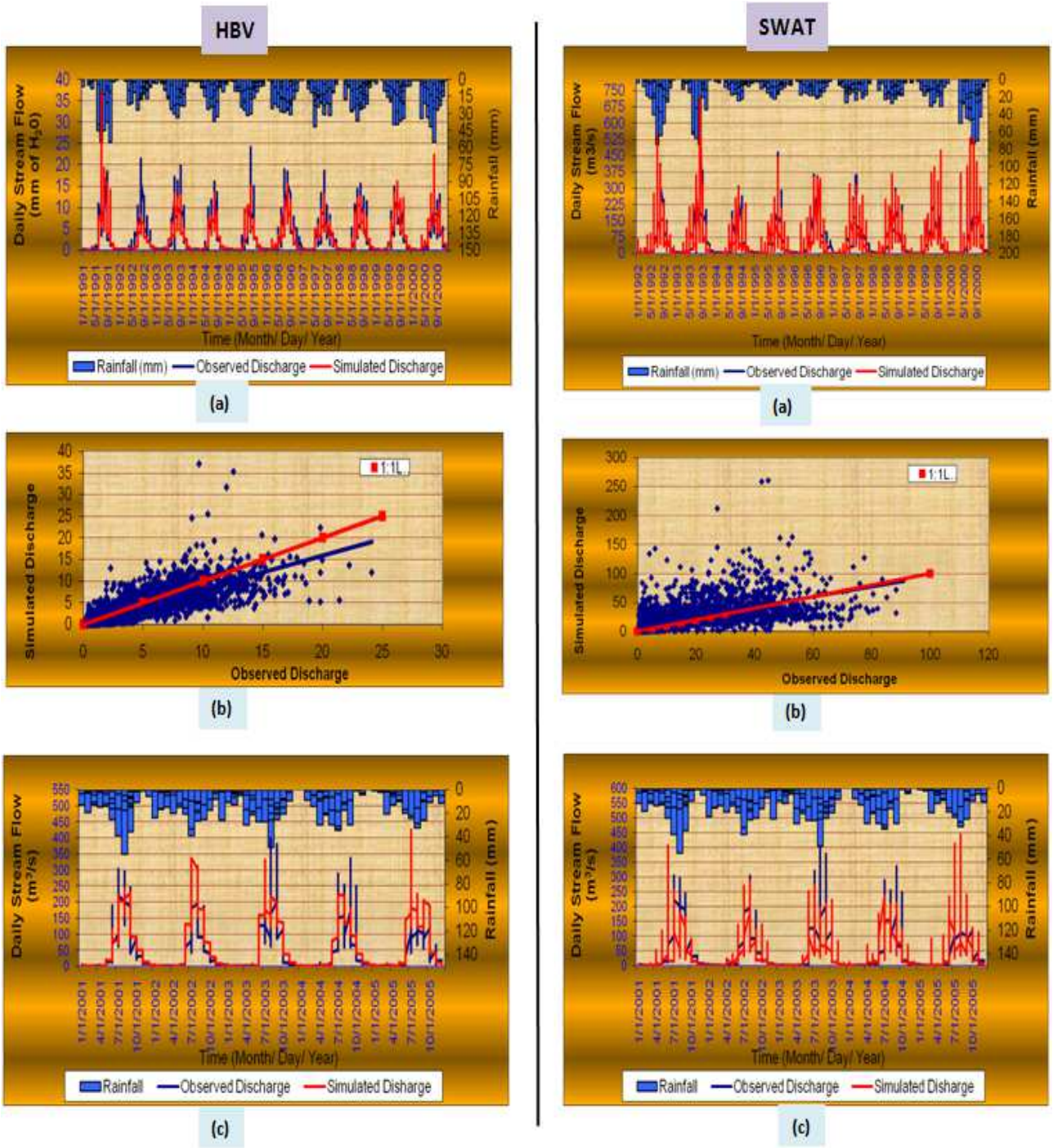

Figure 6.6: ***Daily Auto- Calibration and Validation results of upper Gilgel Abay River gauged near Merawi. (a)Observed and simulated flow hydrograph for both models during calibration. (b) Scatter plot of simulated versus observed discharge during calibration period. (c) Validation of observed and simulated flow hydrographs.***

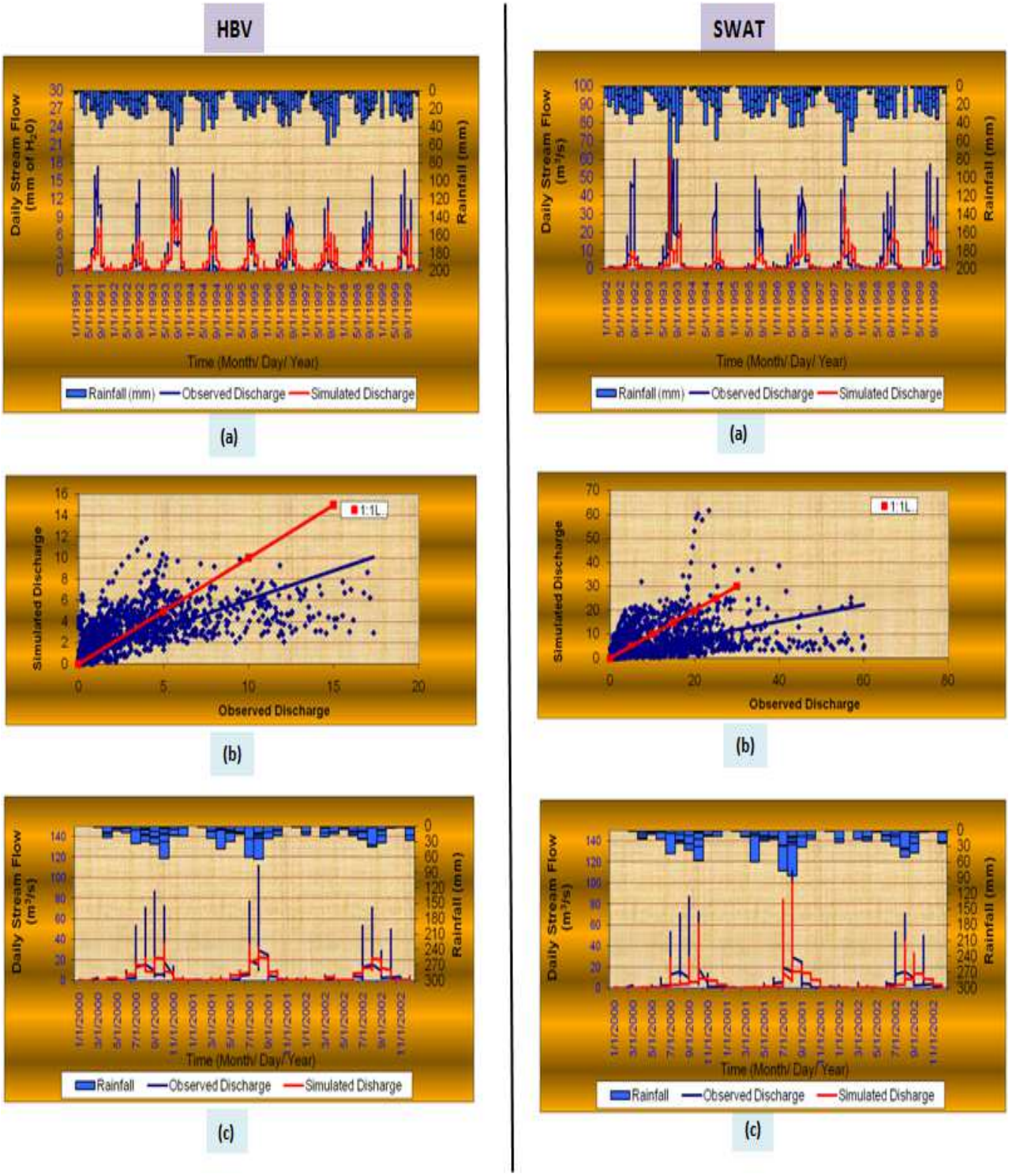

Figure 6.7*: Graphical representations of daily Auto- Calibration and Validation results of Chemoga River gauged near Debre Markos. (a)Observed and simulated flow hydrograph for both models during calibration. (b) Scatter plot of simulated versus observed discharge during calibration period. (c) Validation of observed and simulated flow hydrographs.*

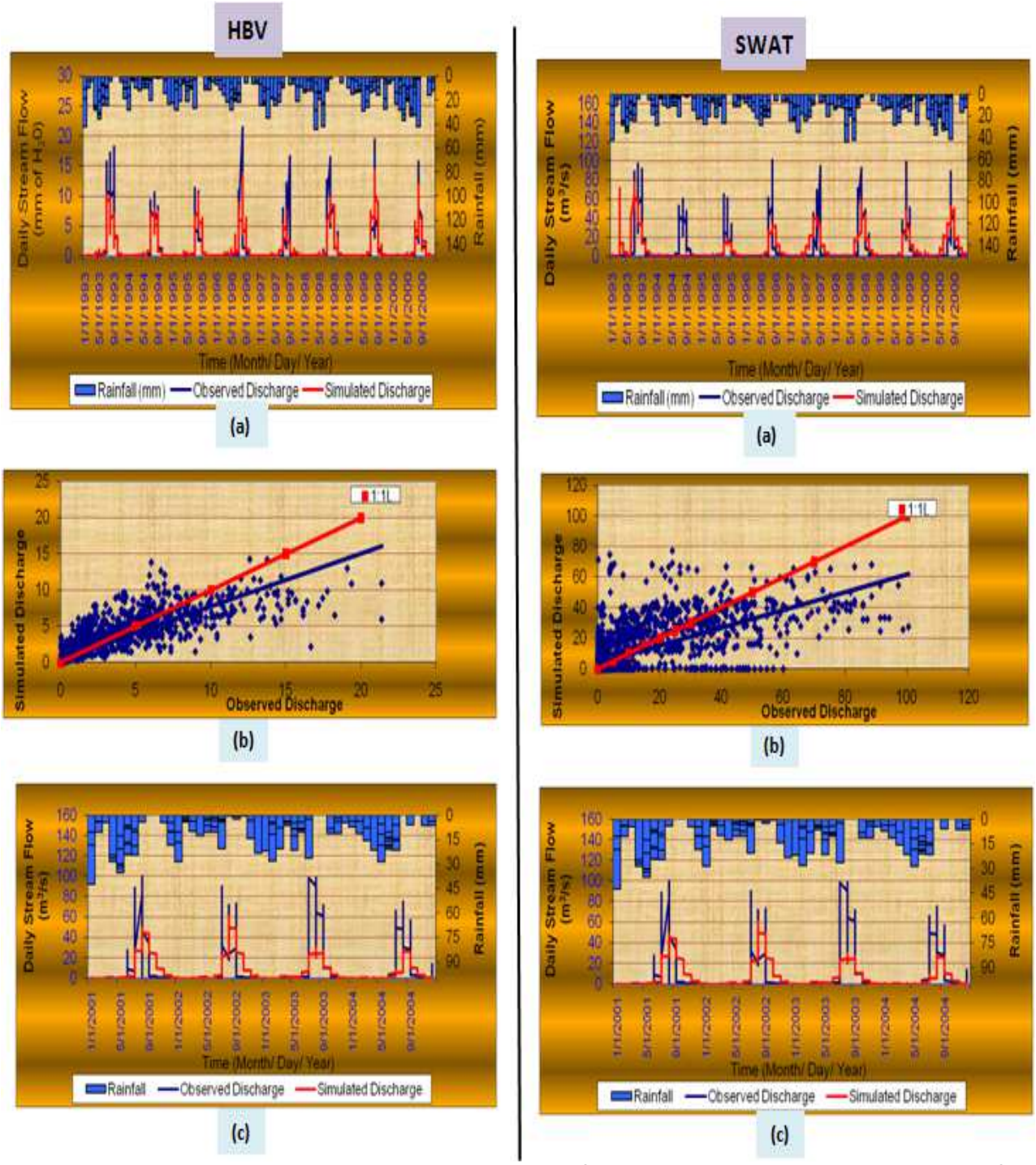

Figure 6.8: ***Daily Auto- Calibration and Validation results of Muger River. (a)Observed and simulated flow hydrograph for both models during calibration. (b) Scatter plot of simulated versus observed discharge during calibration period. (c) Validation of observed and simulated flow hydrographs.***

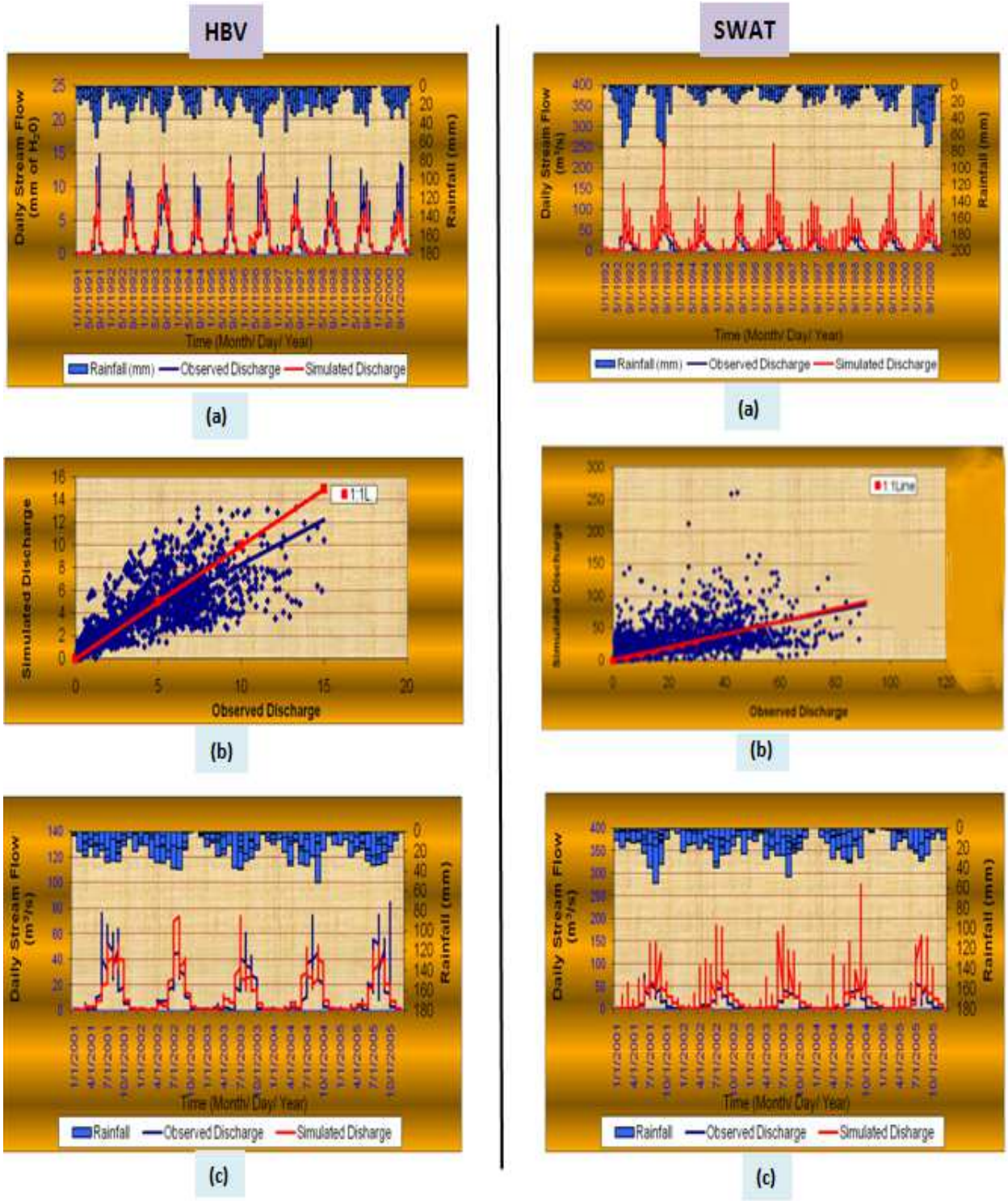

Figure 6.9: ***Daily Auto- Calibration and Validation results of Guder River. (a)Observed and simulated flow hydrograph for both models during calibration. (b) Scatter plot of simulated versus observed discharge during calibration period. (c) Validation of observed and simulated flow hydrographs.***

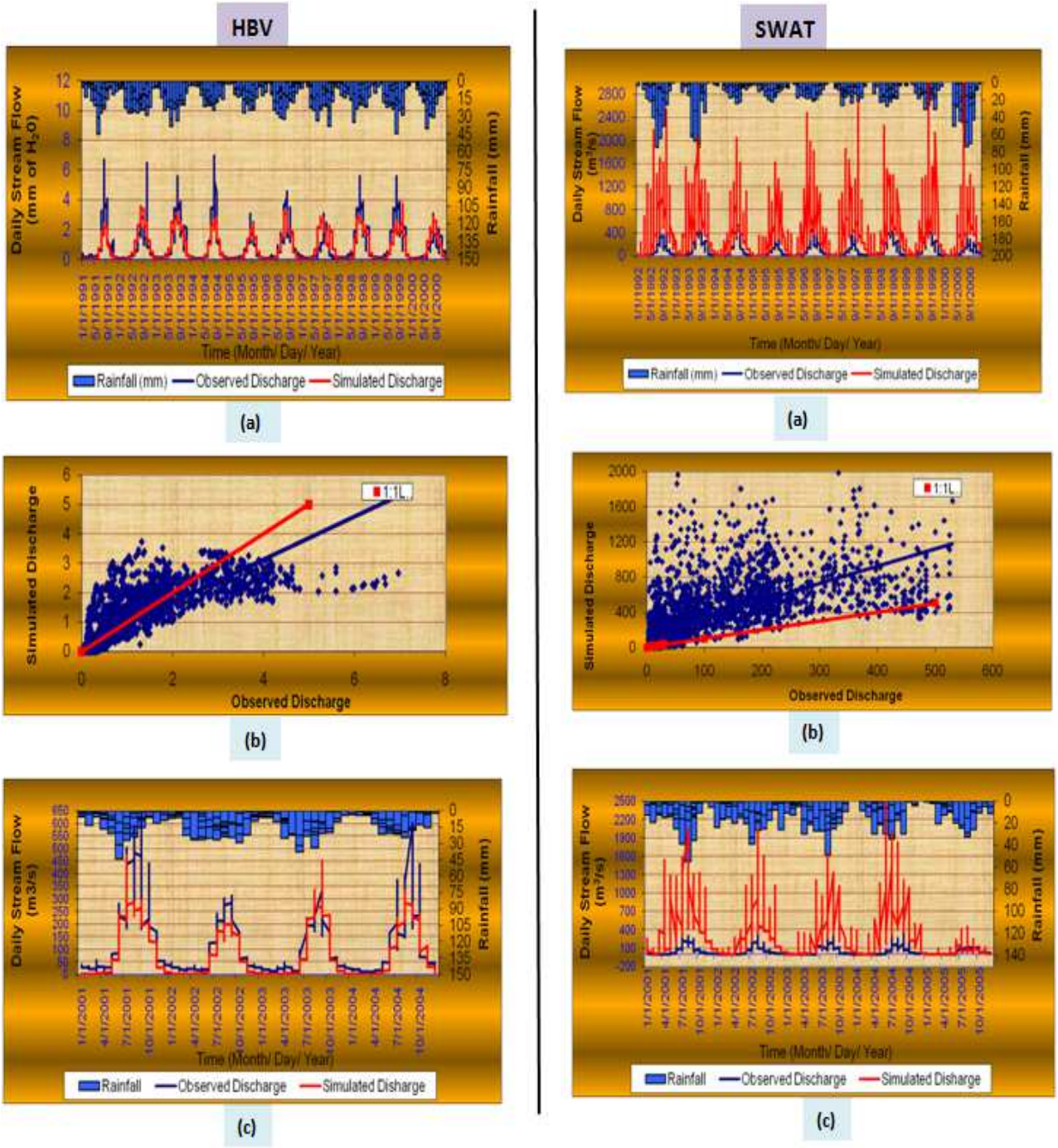

Figure 6.10: ***Daily Auto- Calibration and Validation results of Didessa River. (a)Observed and simulated flow hydrograph for both models during calibration. (b) Scatter plot of simulated versus observed discharge during calibration period. (c) Validation of observed and simulated flow hydrographs.***

7. Conclusions and Recommendations

It was somewhat difficult to get high quality input data to perform the modelling works; however every single effort was exerted to produce good output. A cascade of models was used in this study and the result was satisfactory. However, there are some uncertainties due to unavoidable assumptions taken. The catchments modelling were conducted with the object of understanding hydrologic functioning and basically for performance evaluation of the two substantive models; and the following conclusions were drawn.

7.1. Conclusions

- The result of HBV model parameter sensitivity analysis showed that LP, BETA and FC, in that order, are the most sensitive parameter in all catchments. SWAT sensitivity analysis revealed CN is the most sensitive parameter in all catchments. Except CN, the rest parameters level of sensitivity to runoff differs from one catchment to another catchment. Thus, this is an indication that the hydrological processes in the basin differ from one catchment to another catchment. In most of the gauged part of catchments after calibration it can be seen that base flow contribution is more; and this also a clear indication of the ground water component is the second dominant hydrological process in the basin.

- The values of three performance evaluation criteria namely: the coefficient of determination, the coefficient of efficiency [Nash and Sutcliffe, 1970] and the Index of Agreement are very consistent especially in case of monthly auto-calibration and validation. The Index of Volumetric Fit, the Relative error of Peak, The Mean Difference and % Deviation auxiliary indices were used, when the performances of two models are indistinguishable on the basis of the first three.

- The verification exercise of the ArcSWAT model indicated good performance on simulating average monthly and seasonal discharges. The model is able to capture monthly and seasonal patterns, especially in such cases of the study area where rainfall is bimodal in nature and temporal variability is quite significant. The two rainfall seasons, *Kiremt* and *Belg*, which contribute the largest share of the total rainfall, are well explained. Efficiency evaluation criteria values obtained proved this fact. However,

SWAT exhibits, on daily time step, poor efficiency of the calibrated model for streamflow, a behavior shared by other research works (e.g Lewarne, 2009; Yared, 2010). Factors of this could be that the model is physically based, but remains full of assumptions and some of the parameters required are often not measurable, or hardly so. These make very strong assumptions of the system under investigation because of the lack of options to describe variability. This model performs, generally, better for large catchments than smalls. Hence, it can be concluded that SWAT can able to reliably explain the monthly and seasonal hydrological characteristics of the larger watersheds (having an area of apporoximately ≥ 450km2) in the Abbay Basin with sufficient evaluation efficiencies.

- According to the auto-calibration and validation analysis carried out, HBV-Light has proved to very well simulate daily and monthly discharges; therefore, the model is able to capture daily, monthly and seasonal patterns with satisfactory performance rating criteria.

- In conclusion, the performance of the ArcSWAT is clearly inferior to that of HBV-Light hydrologic model; and this study confirms that simpler models for continuous river-flow simulation can surpass their complex counterparts in performance. There is a strong justification, therefore, for the claim that increasing the model complexity, thereby increasing the number of parameters, does not necessarily enhance the model performance. It is suggested that, in practical hydrology, the simpler models, "based largely on exercises in pattern recognition and curve fitting, through analysis of the available data" (O'Connor, 1998), can still play a significant role as effective simulation tools, and that performance enhancement is not guaranteed by the adoption of complex model structures.

7.2. Recommendations

Based on the findings and limitations noted while doing this study, the following outlooks towards the direction of future works and a model output are suggested:

- It is believed that the results of this study give a clue and increase awareness on the possible lower performance of complex models than their simple counterparts. Hence,

such studies should continue at its kernel on different Abbay watersheds for better representation of hydrological processes in Upper Blue Nile River Basin by a given rainfall-runoff model. This will contribute partly to the long-way towards sustainability if best models output are considered at all levels (from planning to execution and management) of water resource development projects instead of simply implementing one available model.

- The study did, however, rely upon a relatively short duration of recorded data due to the lack of availability of sufficient data for the study watersheds. The capability of the automatic calibration algorithm and the uncertainty analysis methodology, as well as the behavior of the simulation model could be more effectively tested if the calibration and the verification analysis efforts could be applied to a 'data rich' watershed.

- The result of any model depends on the quality of the input data. Input data should, therefore, be checked for missing and unrealistic values in order to come up with good results. Lack of reliable land-use and soil characteristic parameter data were one of the challenges in this study; hence, responsible bodies should give due attention to the acquisition and recording of reliable data.

- In addition to increasing the number of models tested and the number of tests used; an increase in the number of catchments used in the testing would provide an improvement to mode1 comparison studies. Testing the models on more than five catchments, if possible, would be beneficial. With regard to operational modelling, more rigorous analysis should be done on larger watersheds since most engineering hydrology decisions are on larger catchments.

- Future studies should include the evaluation of models at all four levels of testing, as opposed to just the first or second level, especially when evaluating new models against existing models. Future research should extend the hierarchical testing approach with statistical testing, providing a better relative comparison. These models should be of varying complexity and type so that more information is collected regarding where future model development efforts could be concentrated.

- The SWAT documentation is a vast growing collection of knowledge built up over the time that the software has been developed. Good support exists for user groups in Europe and America, but Ethiopia still has a small user base and is not well supported due to lack of direct contact with regular users and support groups. It has been one of the largest obstacles to overcome in this study. Supposing that a larger user and support base for SWAT is developed in Ethiopia, it would be viable to investigate the possibility of an integrated modelling suite, with SWAT at its end.

- The study recommends that SWAT is more useful for comparative scenarios than for absolute results. One reason for this is that when using the SCS method, the curve number remains constant for all simulations, along with the retention factor (F). The conditions in the test catchments and the particular problems needing focused study will require that SWAT be used in conjunction with other software, for instance, to assess groundwater and surface water interaction in greater detail. This research found that the most useful results from SWAT were for monthly and seasonal estimations, but for daily analyses the results are increasingly less secure.

- Due to less number of model parameter requirements, the HBV model can be used for Ethiopian conditions with data usually less available without too much calibration work for simulating and predicting the daily, monthly and annual discharge. This study eventually recommends, HBV model has be to checked for extending runoff data series (or filling gaps), for data quality control, for runoff forecasting (flood warning and reservoir operation), and also to simulate discharge from ungauged catchments.

References

Abeyou, (2008), Hydrological balance of Lake Tana, upper Blue Nile, Ethiopia, ITC Enschede, MSc Thesis.

Arnold, J.G., P.M Allen, R. Muttiah, and G. Bernhardt, November- December (1995): Automated base flow separation and recession analysis techniques. Ground Water vol 33(6): 1010-1018pp.

Arnold, J. G., and P. M. Allen. (1996). Estimating hydrologic budgets for three Illinois watersheds. J. Hydrol. 176(1-4): 57-77.

Arnold, J.G., Sirinivasan, R., Muttiah, R.S, Williams, J.R. (1998).Large area hydrologic modelling and assessment, Part 1: Model development. Journal of the American water resources association, 34(1).

Arnold, J.G., R. Srinivasan, R.S. Muttiah, and P.M. Allen, (1999): Continental scale simulation of the hydrologic balance. J. Am. Water Resource Association 35(5), 1037-1051

Arnold, J. G., and N. Fohrer. (2005). SWAT 2000: Current capabilities and research opportunities in applied watershed modeling. *Hydrol. Process*. 19(3): 563-572.

BCEOM (1999), Abay River Basin integrated master plan, main report, MoWR, Addis Ababa, Ethiopia.

BCEOM & Associates (1999): Abbay Basin Integrated Master Plan Studies, Volume VI Part 2- Large Dams and Hydropower, Part 3 Dams and Reservoirs.

Conway, D. and M. Hulme (1993), Recent Fluctuations in Precipitation and Runoff over the Nile sub-basins and their impact on main Nile drainage, Climatic Change 25: 127-151.

Conway, D. and M. Hulme (1996), The impacts of climate variability and future climate change in the Nile Bain on water resources in Egypt, Water Resources Development Vol. 12, No. 3, pp 277-296.

Conway, D., (2000). The climate and hydrology of the Upper Blue Nile River. The Geographical Journal 166, 49–62.

Dingman, S.L. (2002), Physical Hydrology (2nd ed.), Prentice Hall Inc., USA.

Dupuis, C.E. (1936), Lake Tana and The Nile, Journal of Royal African Society, 35 (138): 18-25.

El-Khodari, N. (2003), The Nile River: challenges to sustainable development Presentation to the River symposium 2003.

Goswami, M., K.M. O'connor, K.P. Bhattarai And A.Y. Shamseldin (2005), Assessing the performance of eight real-time updating models and procedures for the Brosna River, Hydrology and the Earth System Sciences. 9 (4): 394-411

Green, W.H. and G.A. Ampt, (1911). Studies on soil physics, 1. The flow of air and water through soils. Journal of Agricultural Sciences 4:11-24.

Hargreaves, G.H. and Z.A. Samani. (1985). Reference crop evapotranspiration from temperature. Applied Engineering in Agriculture 1:96-99.

IHMS, (2006). " Integrated Hydrological modeling System manual. "Version 5.1.

Jensen, M.E., R.D. Burman, and R.G. Allen (ed). (1990). Evapotranspiration and irrigation water requirements. ASCE Manuals and Reports on Engineering Practice No. 70, ASCE, N.Y. 332 pp.

Kebede. S., Travi, Y., Alemayehu, T., Marc, V., 2005 Water balance of Lake Tana and its sensitivity to fluctuations in rainfall, Blue Nile basin Ethiopia, pp, 233-247 Journal of Hydrology 316.

Kebede, S., Y. Travi, T. Alemayehu, T. Ayenew (2006), Water balance of Lake Tana and its sensitivity to fluctuations in rainfall, Blue Nile Basin, Ethiopia, Journal of Hydrology, 316: 233-247.

Krause P. And F. Base (2006), Sensitivity and uncertainty analysis of the Hydrological model J2000, Geophysical Research Abstracts, Vol. 8, 02510.

Lenhart, T., K. Eckhardt, N. Fohrer, H.-G. Frede, (2002). Comparison of two different approaches of sensitivity analysis, Physics and Chemistry of the Earth 27 (2002), Elsevier Science Ltd., 645–654pp

Liden, R. and J. Harlin (2000), Analysis of conceptual rainfall-runoff modeling performance in different climates, Journal of Hydrology, 238: 231-247.

Liersch S., August (2003). Dew02 Users' Manual, Berlin, 5pp.

Luzio, M. Di, R. Srinivasan, J.G. Arnold, S.L. Neitsch, (2002). ArcView Interface for SWAT2000 (AVSWAT2000), User's Guide, Grassland Soil and Water Research Laboratory, Blackland Research Center, Texas Agricultural Experiment Station, Texas Water Resources Institute, Texas Water Resources Institute, College Station, Texas TWRI Report TR-193, 345pp.

Mishra, A., T. Hata, A.W. Abdelhadi, A. Tada, and H. Tanakamaru (2003), Recession flow analysis of the Blue Nile River, Hydrol. Process. 17, 2828-2835.

Mishra, A., T. Hata, and A.W. Abdelhadi (2004), Models for recession flows in the Blue Nile River, Hydrol. Process. 18, 2773-2786

Moriasi, D.N, J. G. Arnold, M. W. Van Liew, R. L. Bingner, R. D. Harem,T. L.Veith, (2007). Model evaluation guidelines for systematic quantification of accuracy in Watershed simulations. Vol. 50(3), 850-900pp. American society of Agricultural and Biological Engineers ISSN 0001-235

Morris.M.D., (1991). Factorial sampling plans for preliminary comp experiments. Tecnometrics. Vol.33 nr2

Nash, J. E., and J. V. Sutcliffe. (1970). River flow forecasting through conceptual models: Part 1. A discussion of principles. *J. Hydrology* 10(3): 282-290.

Neitsch (A), S.L., J.G. Arnold, J.R. Kiniry, J.R. Williams, K.W. King , (2002). Soil and Water Assessment Tool (SWAT) Theoretical Documentation, Version 2000, Grassland Soil and Water Research Laboratory, Black land Research Center, Texas Agricultural Experiment Station, Texas Water Resources Institute, Texas Water Resources Institute, College Station, Tex as, 506pp.

Nicks, A.D. (1974). Stochastic generation of the occurrence, pattern and location maximum amount of daily rainfall. p. 154-171. In Proc. Symp.Statistical Hydrology, Tucson, AZ. Aug.-Sept. 1971. USDA Misc. Publ. 1275. U.S. Gov. Print. Office, Washington, DC

O'Connor, K.M., (1998) . 'The Education and Training of Hydrologists', A Discussion Paper submitted to the Unesco Steering Committee of IHPV Project 8.1 in the context of its Draft Education Policy Document.(unpublished).

Penman, H.L. (1956). Evaporation: An introductory survey. Netherlands Journal Agricultural Science 4:7-29.

Ponce, V.M, (1998). Engineering Hydrology. Principles and practice. Prentice Hall 640p.

Priestley, C.H.B. and R.J. Taylor. (1972). On the assessment of surface heat flux and evaporation using large-scale parameters. Mon. Weather. Rev. 100:81-92.

Refsgaard, J.C. and Storm, B., (1996), Construction, calibration and validation of hydrological models, Distributed Hydrological Modelling (eds. M.B.Abbott and J.C. Refsgaard), Kluwer Academic Publishers, 41-54.

Rozanski, K., K. Froehlich and W.G. Mook (2000), Environmental isotopes in the hydrological cycle, Vol III, UESCO/IAEA, Paris/ Vienna.

Rosenthal, W. D., R. Srinivasan, and J. G. Arnold. (1995). Alternative river management using a linked GIS-hydrology model. *Trans. ASAE* 38(3): 783-790.

Saleh, A., J. G. Arnold, P. W. Gassman, L. W. Hauck, W. D. Rosenthal, J. R. Williams, and A. M. S. McFarland. (2000). Application of SWAT for the upper North Bosque River watershed. *Trans. ASAE* 43(5): 1077-1087.

Santhi, C., J.G. Arnold, J.R. Williams, W.A. Dugas, and L. Hauck. (2001). "Validation of the SWAT Model on a Large River Basin with Point and Non point Sources." *J. Am. Water Resour. Assoc.* 37(5): 1169-88.

Shahin, M., (1988). Hydrology of the Nile basin, International Institute for Hydraulic and Environmental Engineering. Elsevier, The Netherlands.

Sharpley, A.N. and J.R. Williams, eds. (1990). EPIC-Erosion Productivity Impact Calculator, 1. Model documentation. U.S. Department of Agriculture, Agricultural Research Service, Tech. Bull. 1768.

S.L., J.G. Arnold, J.R. Kiniry, R. Srinivasan, J. R. Williams, (2005). Soil and Water Assessment Tool (SWAT) User's Manual, Version 2005, Grassland Soil and Water Research Laboratory, Blackland Research Center, Texas Agricultural Experiment Station, Texas Water Resources Institute, Texas Water Resources Institute, College Station, Texas, 520pp.

SMEC I.P (2007) Hydrological study of the Tana Beles sub-basins part –I

Soil Conservation Service, (1972). Section 4: Hydrology *In* National Engineering Handbook. SCS.

Srinivasan, R., and J. G. Arnold. (1994). Integration of a basin-scale water quality model with GIS. *Water Resour. Bull.* (30)3: 453-462.

Srinivasan, R., T. S. Ramanarayanan, J. G. Arnold, and S. T. Bednarz. (1998). Large-area hydrologic modeling and assessment: Part II. Model application. *J.* American Water Resour. Assoc. 34(1): 91-101.

Uhlenbrook, S. (2004), Quantifying the impact of land-use changes at the event and seasonal time scale using a process-oriented catchment model, Hydrology and
Earth System Sciences 8 (1): 62-78.

Van Griensven A., Francos A. and Bauwens W. (2002). Sensitivity analysis and auto-calibration of an integral dynamic model for river water quality, Water Science and Technology, 45(5), 321-328.

Ward, G., and J. Benaman, (1999): Models for TMDL application in Texas water courses: screening and model review. Report to Texas Natural Resource Conservation Commission, Center for Research in Water Resources, University of Texas at Austin.

Williams, J. R. (1969). Flood routing with variable travel time or variable storage coefficients. *Trans. ASAE* 12(1): 100-103

Williams,J.R. and R.W.Hann. (1973). HYMO, problem oriented language for hydrologic modeling-user manual USDA, ARS-5-9

Williams, J.R. (1995). Chapter 25: The EPIC model. p. 909-1000. In V.P. Singh (ed). Computer models of watershed hydrology. Water Resources Publications, Highlands Ranch Co.

Yohanse, (2007). Remote sensing based assessment of water resource Potential for Lake Tana basin. Addis Ababa University. MSc Thesis.

Web site sources:

http://www.brc.tamus.edu/swat/soft_links.html

APPENDICES

Appendix-A: Weather generator (WGN) parameters used by the SWAT Model

Table –A-1

Legend of the parameters used in the weather generation		
	Symbol	**Description**
A	TMPMX	Average or mean daily maximum air temperature for month (ºC).
B	TMPMN	Average or mean daily minimum air temperature for month (ºC).
C	TMPSTDMX	Standard deviation for daily maximum air temperature in month (ºC).
D	TMPSTDMN	Standard deviation for daily minimum air temperature in month (ºC).
E	PCPMM	Average or mean total monthly precipitation (mm H2O).
F	PCPSTD	Standard deviation for daily precipitation in month (mm H2O/day).
G	PCPSKW	Skew coefficient for daily precipitation in month.
H	PR_W1	Probability of a wet day following a dry day in the month.
I	PR_W2	Probability of a wet day following a wet day in the month.
J	PCPD	Average number of days of precipitation in month.
K	SOLARAV	Average daily solar radiation for month (MJ/m2/day).
L	DEWPT	Average daily dew point temperature in month (ºC).
M	WNDAV	Average daily wind speed in month (m/s).

TMPMX (mon): Average or mean daily maximum air temperature for month (ºC). Calculated based on following formula:

$$\mu mx_{mon} = \frac{\sum_{d=1}^{N} T_{mx,mon}}{N}$$

Where: μmax_{mon} is the mean daily maximum temperature for the month (^{0}C), *Tmx,mon* is the daily maximum temperature on record *d* in month *mon* (^{0}C), and *N* is the total number of daily maximum temperature records for month *mon*.

TMPMN (mon): Average or mean daily minimum air temperature for month (ºC).Calculated based on following formula:

$$\mu mn_{mon} = \frac{\sum_{d=1}^{N} T_{mn,mon}}{N}$$

Where: μmn_{mon} is the mean daily minimum temperature for the month (^{0}C), $T_{mn,mon}$ is the daily minimum temperature on record *d* in month *mon* (^{0}C), and *N* is the total number of daily minimum temperature records for month *mon*.

TMPSTDMX (mon): Standard deviation for daily maximum air temperature in month (ºC) Calculated based on following formula:

$$\sigma mx_{mon} = \sqrt{\frac{\sum_{d=1}^{N} (T_{mx,mon} - \mu mx_{mon})^2}{N-1}}$$

Where: σmx_{mon} is the standard deviation for daily maximum temperature in month *mon* (ºC), $T_{mx,mon}$ is the daily maximum temperature on record *d* in month *mon* (^{0}C), $\mu_{mx,\ mon}$ is the average daily maximum temperature for the month (^{0}C), and *N* is the total number of daily maximum temperature records for month *mon*.

TMPSTDMN (mon): Standard deviation for daily minimum air temperature in month (ºC). Calculated based on following formula:

$$\sigma mn_{mon} = \sqrt{\frac{\sum_{d=1}^{N} (T_{mn,mon} - \mu mn_{mon})^2}{N-1}}$$

Where: σmn_{mon} is the standard deviation for daily minimum temperature in month *mon* (ºC), *Tmn,mon* is the daily minimum temperature on record *d* in month *mon* (^{0}C), μ*mnmon* is the average daily minimum temperature for the month ^{0}C), and *N* is the total number of daily minimum temperature records for month *mon.*

$$\overline{R}_{mon} = \frac{\sum_{d=1}^{N} R_{day,mon}}{yrs}$$

PCPMM (mon): Average or mean total monthly precipitation (mm H2O). Calculated based on following formula:

Where: $\overline{R}_{mon}$ is the mean monthly precipitation (mm H2O), $R_{day,mon}$ is the daily precipitations for record *d* in month *mon* (mm H2O), *N* is the total number of records in month *mon* used to calculate the average, and *yrs* is the number of years of daily precipitation records used in calculation.

PCPSTD (mon): Standard deviation for daily precipitation in month (mm H2O/day).Calculated based on following formula:

$$\sigma_{mon} = \sqrt{\frac{\sum_{d=1}^{N} (R_{day,mon} - \overline{R}_{mon})^2}{N-1}}$$

Where: σ_{mon} is the standard deviation for daily precipitation in month *mon* (mm H2O), $\overline{R}_{mon}$ is the mean monthly precipitation (mm H2O), $R_{day,mon}$ is the daily precipiation for record *d* in month *mon* (mm H2O), *N* is the total number of records in month *mon* used to calculate the average, and *yrs* is the number of years of daily precipitation records used in calculation.

PCPSKW (mon): Skew coefficient for daily precipitation in month. Calculated based on following formula:

$$g_{mon} = \frac{N \cdot \sum_{d=1}^{N} (R_{day,mon} - \overline{R}_{mon})^3}{(N-1) \cdot (N-2) \cdot (\sigma_{mon})^3}$$

Where: g_{mon} is the skew coefficient for precipitation in the month, *N* is the total number of daily precipitation records for month *mon*, $R_{day,mon}$ is the amount of precipitation for record *d* in month *mon* (mm H2O), $\overline{R}_{mon}$ is the average precipitation for the month (mm H2O), and σ_{mon} is the standard deviation for daily precipitation in month *mon* (mm H2O).

PR_W1 (mon) : Probability of a wet day following a dry day in the month. Calculated based on following formula:

$$P_i(W/D) = \frac{days_{W/D,i}}{days_{dry,i}}$$

Where: *Pi(W/D)* is the probability of a wet day following a dry day in month *i*, $days_{W/D,i}$ is the number of times a wet day followed a dry day in month *i* for the entire period of record, and $days_{dry,i}$ is the number of dry days in month *i* during the entire period of record. A dry day is a day with 0 mm of precipitation. A wet day is a day with > 0 mm precipitation.

PR_W2 (mon) : Probability of a wet day following a wet day in the month. Calculated based on following formula:

$$P_i(W/W) = \frac{days_{W/W,i}}{days_{wet,i}}$$

Where: *Pi(W/W)* is the probability of a wet day following a wet day in month *i*, $days_{W/W,i}$ *i* is the number of times a wet day followed a wet day in month *i* for the entire period of record, and $days_{wet,i}$ is the number of wet days in month *i* during the entire period of record. A dry day is a day with 0 mm of precipitation. A wet day is a day with > 0 mm precipitation.

PCPD (mon): Average number of days of precipitation in month. Calculated based on following formula:

$$\bar{d}_{wet,i} = \frac{days_{wet,i}}{yrs}$$

Where: $\bar{d}_{wet,i}$, is the average number of days of precipitation in month *i*, $days_{wet,i}$ is the number of wet days in month *i* during the entire period of record, and *yrs* is the number of years of record.

SOLARAV (mon): Average daily solar radiation for month (MJ/m2/day). Calculated based on following formula:

$$\mu rad_{mon} = \frac{\sum_{d=1}^{N} H_{day,mon}}{N}$$

Where: μrad_{mon} is the mean daily solar radiation for the month (MJ/m^2/day), $H_{day,mon}$ is the total solar radiation reaching the earth's surface for day *d* in month *mon* (MJ/m^2/day), and *N* is the total number of daily solar radiation records for month *mon*.

DEWPT (mon): Average daily dew point temperature in month (ºC). Calculated based on following formula:

$$\mu dew_{mon} = \frac{\sum_{d=1}^{N} T_{dew,mon}}{N}$$

Where: μdew_{mon} is the mean daily dew point temperature for the month (ºC), *Tdew,mon* is the dew point temperature for day *d* in month *mon* (ºC), and *N* is the total number of daily dew point records for month *mon*.

WNDAV (mon): Average daily wind speed in month (m/s). Calculated based on following formula:

$$\mu wnd_{mon} = \frac{\sum_{d=1}^{N} \mu_{wnd,mon}}{N}$$

Where: μwnd_{mon} is the mean daily wind speed for the month (m/s), $\mu_{wnd,mon}$ is the average wind speed for day *d* in month *mon* (m/s), and *N* is the total number of daily wind speed records for month *mon*.

The numbers 1 through 12 in the following tables represent the months from January to December and the alphabets A, B, C….M, indicate the description of weather generator parameters as per in appendix-A, Table A-1.

Table –A-2

STATION	LAT	LONG	ELEV	RAIN YEARS	A1	A2	A3	A4	A5	A6	A7	A8
Bahirdar	11.60	37.42	1770	16.00	26.77	28.41	29.39	29.95	29.30	27.05	24.36	24.39
Dangila	11.12	36.90	2140	16.00	25.88	27.02	27.49	27.52	25.87	23.43	21.66	21.88
Markos	10.333	37.667	2515	16.00	23.99	25.30	25.31	24.98	24.41	21.04	18.84	18.97
Arjo	8.750	36.500	2565	16.00	21.38	21.95	22.11	21.66	21.27	20.02	19.19	19.27
Nekemte	9.083	36.450	2080	16.00	25.90	27.29	27.25	26.24	24.60	22.24	20.92	21.16
Ambo	8.97	37.87	2130	16.00	26.68	27.47	27.45	27.23	26.95	25.29	24.15	24.09
Fitche	9.80	38.70	2750	14.00	19.96	21.55	21.84	22.15	22.69	21.88	17.86	17.53
Addis Ababa	9.033	38.75	2408	14.00	24.13	25.65	25.60	25.12	25.48	23.61	21.31	21.18

STATION	A7	A8	A9	A10	A11	A12	B1	B2	B3	B4	B5	B6
Bahirdar	24.36	24.39	25.63	26.59	26.76	26.74	9.11	10.98	13.28	15.27	15.48	14.88
Dangila	21.66	21.88	22.87	23.22	23.76	24.53	4.65	6.10	8.10	10.24	10.90	11.26
Markos	18.84	18.97	20.51	21.78	22.85	23.49	9.06	10.18	11.14	11.93	11.78	10.80
Arjo	19.19	19.27	19.80	20.61	20.77	21.08	10.85	11.20	11.58	11.41	11.18	10.78
Nekemte	20.92	21.16	22.53	23.69	24.36	25.18	12.29	13.25	13.99	14.30	13.78	12.82
Ambo	24.15	24.09	24.81	25.74	26.25	26.27	11.34	11.92	12.52	12.52	11.85	11.64
Fitche	17.86	17.53	18.49	19.16	19.38	19.79	7.25	7.93	9.09	9.55	9.84	9.55
Addis Ababa	21.31	21.18	22.02	23.12	23.40	23.63	9.24	9.95	11.65	12.31	12.46	11.49

STATION	B7	B8	B9	B10	B11	B12	C1	C2	C3	C4	C5	C6
Bahirdar	14.49	14.36	13.78	13.73	11.82	9.67	1.55	1.81	1.74	1.99	1.92	1.69
Dangila	11.32	11.20	10.05	9.36	6.95	4.74	1.34	1.80	1.89	2.31	2.25	1.58
Markos	10.96	10.91	10.19	9.81	8.98	8.60	1.25	1.49	1.84	2.17	2.38	1.97
Arjo	10.60	10.72	10.81	10.94	10.97	10.96	1.24	1.94	1.76	1.74	1.63	1.21
Nekemte	12.62	12.73	12.69	12.82	12.65	12.31	1.41	1.85	1.91	2.30	2.08	1.53
Ambo	11.82	11.75	11.17	10.80	10.62	10.87	1.18	1.77	2.17	1.84	1.61	1.51
Fitche	9.19	9.34	8.86	6.87	5.84	6.12	1.23	1.56	1.81	1.83	1.86	2.03
Addis Ababa	11.44	11.67	11.36	10.27	8.71	8.12	1.56	1.90	1.82	2.15	1.97	2.24

STATION	C7	C8	C9	C10	C11	C12	D1	D2	D3	D4	D5	D6
Bahirdar	1.50	1.43	1.28	1.18	1.05	1.16	2.18	2.35	2.70	2.45	1.83	1.25
Dangila	1.74	1.63	1.74	2.28	2.61	2.75	2.40	2.94	3.04	2.65	2.14	1.75
Markos	1.48	1.44	1.33	1.27	1.29	1.01	1.68	1.72	1.60	1.60	1.49	1.06
Arjo	1.92	1.79	1.31	0.79	0.88	0.94	0.85	0.87	1.17	0.97	0.90	0.80
Nekemte	1.77	1.73	1.33	1.39	1.39	1.17	1.43	1.58	1.37	1.37	1.21	0.75
Ambo	2.07	2.12	1.48	0.95	0.86	1.36	1.71	1.55	1.53	1.57	1.35	1.04
Fitche	1.86	1.44	1.09	0.96	1.04	0.93	1.75	1.80	1.52	1.36	1.13	0.93
Addis Ababa	1.65	1.64	1.46	1.35	1.30	1.20	2.06	1.93	1.58	1.23	1.24	1.04

STATION	D7	D8	D9	D10	D11	D12	E1	E2	E3	E4	E5	E6
Bahirdar	1.03	1.06	1.13	1.53	2.11	2.29	2.52	3.29	20.45	33.06	75.29	204.67
Dangila	1.57	1.59	2.21	1.93	2.19	2.06	18.96	18.59	41.47	51.92	139.61	255.07
Markos	0.85	0.95	1.15	1.38	1.57	1.54	16.56	11.90	50.86	88.45	95.72	171.90
Arjo	0.78	0.64	0.61	0.44	0.53	0.56	22.58	23.55	83.04	109.99	184.92	294.77
Nekemte	0.75	0.73	0.74	0.86	1.10	1.09	16.94	11.79	61.17	101.31	230.70	392.20
Ambo	0.95	1.00	1.18	1.75	1.96	1.79	49.19	45.62	58.38	75.71	79.95	123.78
Fitche	0.88	0.89	1.02	1.80	1.88	1.87	21.63	31.06	63.00	66.96	42.14	95.54
Addis Ababa	0.91	1.04	1.34	1.88	1.95	1.84	18.14	25.43	63.29	88.21	82.50	154.86

STATION	E7	E8	E9	E10	E11	E12	F1	F2	F3	F4	F5	F6
Bahirdar	420.88	378.74	192.3	94.93	13.51	3.11	0.62	1.09	3.11	3.70	6.65	11.23
Dangila	329.64	341.25	238.6	127.01	46.95	15.22	1.51	1.57	3.90	4.02	7.00	9.61
Markos	277.72	310.58	220.7	102.51	32.68	28.99	2.64	1.88	3.54	6.00	5.87	6.66
Arjo	320.84	300.19	235.7	121.15	54.86	47.04	2.27	2.84	5.45	7.66	8.51	10.73
Nekemte	420.75	397.27	269.8	150.83	44.16	16.79	2.32	1.74	5.48	7.25	11.32	14.87
Ambo	153.14	146.41	89.9	56.72	33.04	38.64	3.19	4.36	3.48	4.56	4.44	5.30
Fitche	335.59	326.13	124.7	19.64	5.89	8.98	2.85	4.52	5.15	5.52	3.29	6.84
Addis Ababa	275.50	283.00	175.9	38.57	6.57	9.43	2.85	3.99	6.79	7.26	6.60	6.72

STATION	F7	F8	F9	F10	F11	F12	G1	G2	G3	G4	G5	G6
Bahirdar	16.18	15.04	10.00	7.13	2.33	0.79	9.10	14.38	13.29	5.78	5.05	2.70
Dangila	10.36	10.12	8.84	7.49	4.14	1.78	0.02	0.03	0.09	0.14	0.28	0.60
Markos	11.61	10.67	9.12	7.34	3.37	3.41	8.37	7.03	3.39	3.76	3.10	2.16
Arjo	11.51	9.87	9.99	7.75	4.36	3.04	5.90	6.24	3.09	2.90	1.82	2.07
Nekemte	16.20	13.81	10.88	9.00	4.69	2.70	7.88	5.70	4.40	3.46	2.57	2.42
Ambo	6.65	5.62	3.95	4.00	1.50	1.47	7.47	8.48	5.07	4.39	5.13	3.84
Fitche	10.61	10.95	7.88	3.00	1.23	1.87	5.64	6.34	4.10	5.37	3.61	5.26
Addis Ababa	9.23	9.97	9.48	5.99	1.84	3.30	6.95	5.73	7.72	4.15	3.50	2.29

STATION	G7	G8	G9	G10	G11	G12	H1	H2	H3	H4	H5	H6
Bahirdar	2.33	2.63	2.77	3.29	7.16	9.79	0.01	0.03	0.08	0.10	0.20	0.48
Dangila	0.93	0.87	0.67	0.31	0.11	0.03	0.02	0.03	0.09	0.14	0.28	0.60
Markos	7.23	2.64	2.21	3.67	5.76	6.32	0.07	0.06	0.19	0.25	0.24	0.63
Arjo	2.16	1.42	1.44	3.89	3.97	3.67	0.08	0.05	0.24	0.20	0.35	0.68
Nekemte	1.91	1.67	1.89	2.73	4.68	8.10	0.07	0.06	0.17	0.23	0.37	0.88
Ambo	3.55	2.23	3.24	6.59	1.64	1.39	0.09	0.09	0.20	0.26	0.20	0.61
Fitche	1.31	1.30	4.48	8.52	9.54	10.84	0.09	0.11	0.22	0.26	0.17	0.37
Addis Ababa	1.57	2.16	2.43	8.52	10.65	14.21	0.06	0.05	0.16	0.25	0.22	0.54

STATION	H7	H8	H9	H10	H11	H12	I1	I2	I3	I4	I5	I6
Bahirdar	0.81	0.83	0.58	0.22	0.05	0.03	0.38	0.39	0.59	0.60	0.63	0.76
Dangila	0.93	0.87	0.67	0.30	0.11	0.03	0.84	0.82	0.74	0.69	0.79	0.90
Markos	0.85	0.83	0.57	0.14	0.10	0.08	0.48	0.45	0.64	0.71	0.73	0.88
Arjo	0.82	0.75	0.51	0.20	0.12	0.09	0.59	0.70	0.58	0.64	0.71	0.84
Nekemte	0.87	0.81	0.70	0.34	0.14	0.07	0.47	0.46	0.63	0.69	0.80	0.89
Ambo	0.73	0.71	0.51	0.11	0.04	0.04	0.87	0.83	0.79	0.80	0.85	0.88
Fitche	0.90	0.78	0.39	0.07	0.04	0.05	0.45	0.47	0.51	0.60	0.61	0.71
Addis Ababa	0.90	0.76	0.37	0.11	0.02	0.02	0.32	0.45	0.52	0.56	0.50	0.75

STATION	I7	I8	I9	I10	I11	I12	J1	J2	J3	J4	J5	J6
Bahirdar	0.92	0.90	0.78	0.58	0.33	0.18	0.81	1.13	5.31	6.19	11.56	20.81
Dangila	0.94	0.94	0.87	0.73	0.63	0.71	4.63	4.75	8.44	9.75	18.81	27.00
Markos	0.93	0.93	0.83	0.76	0.59	0.61	3.63	3.19	11.50	14.56	15.19	26.25
Arjo	0.82	0.86	0.75	0.73	0.65	0.76	5.31	4.31	11.81	11.06	17.63	25.31
Nekemte	0.90	0.90	0.86	0.73	0.47	0.31	3.63	3.38	10.25	13.13	20.94	27.50
Ambo	0.86	0.87	0.82	0.84	0.91	0.93	14.56	12.19	16.19	17.75	19.88	26.00
Fitche	0.89	0.88	0.71	0.51	0.36	0.43	4.69	5.56	10.25	12.38	10.13	17.38
Addis Ababa	0.85	0.83	0.72	0.39	0.29	0.09	2.64	3.00	7.86	11.29	10.07	21.07

STATION	J7	J8	J9	J10	J11	J12	K1	K2	K3	K4	K5	K6
Bahirdar	29.38	28.38	22.94	11.50	2.63	1.1	21.14	21.49	21.62	21.38	21.28	20.64
Dangila	30.06	30.06	26.38	17.63	8.19	3.19	19.45	19.44	19.44	18.47	18.53	18.24
Markos	29.75	29.56	24.44	12.81	6.69	5.50	20.6	20.9	19.8	21.5	19.5	17.9
Arjo	26.19	27.31	21.25	14.63	8.69	9.19	19.80	20.50	21.50	21.40	21.00	16.50
Nekemte	28.56	28.75	26.00	18.19	6.94	3.25	20.50	21.90	21.20	21.20	21.20	15.30
Ambo	27.25	27.13	23.38	15.06	12.31	14.56	18.30	19.40	20.20	20.20	19.90	18.80
Fitche	28.44	27.94	18.50	4.31	2.06	2.31	20.40	22.20	20.90	24.70	23.10	22.20
Addis Ababa	27.36	26.29	18.21	5.36	1.00	0.79	17.80	22.40	20.20	22.50	18.70	13.40

STATION	K7	K8	K9	K10	K11	K12	L1	L2	L3	L4	L5	L6
Bahirdar	20.09	20.09	20.71	20.83	20.93	20.71	9.88	9.24	9.94	10.88	12.77	15.24
Dangila	16.43	14.47	16.61	16.73	18.66	19.24	10.65	11.10	11.25	11.88	12.88	14.08
Markos	14.5	14.2	18.3	17.5	22.1	22.4	4.93	3.69	6.24	8.25	9.17	11.56
Arjo	13.80	15.00	15.40	23.30	20.40	21.20	5.89	3.30	6.04	5.22	6.85	11.14
Nekemte	14.50	14.10	16.20	19.40	20.40	19.80	6.51	4.50	7.83	9.91	11.59	14.26
Ambo	18.10	18.40	18.90	19.70	18.60	17.90	10.28	9.27	10.63	11.76	11.76	12.73
Fitche	18.70	21.30	21.30	23.30	22.50	18.70	5.69	4.46	7.63	8.35	7.57	9.05
Addis Ababa	21.80	13.90	17.00	23.00	21.70	15.80	4.71	3.21	6.09	7.66	7.50	10.10

STATION	L7	L8	L9	L10	L11	L12	M1	M2	M3	M4	M5	M6
Bahirdar	15.55	15.87	15.34	13.93	11.87	10.32	0.46	0.53	0.63	0.70	0.65	0.70
Dangila	13.44	13.93	13.72	13.19	11.93	10.66	0.95	1.07	1.16	1.13	1.30	1.20
Markos	12.02	12.27	11.52	8.84	6.65	5.10	1.37	1.61	1.80	2.05	1.95	1.43
Arjo	11.84	12.30	13.30	12.21	11.83	10.61	1.29	1.53	1.65	1.89	1.80	1.52
Nekemte	14.24	14.52	14.58	13.11	10.70	11.04	0.92	0.92	0.94	1.06	1.09	0.90
Ambo	12.11	13.17	13.30	11.78	10.34	9.10	2.40	2.40	2.40	2.40	2.40	2.40
Fitche	11.26	11.24	10.05	7.29	5.47	4.69	1.03	1.38	1.12	1.52	1.49	1.35
Addis Ababa	11.50	11.94	10.08	5.35	3.61	3.32	0.83	0.87	0.70	0.88	0.50	0.41

STATION	M7	M8	M9	M10	M11	M12
Bahirdar	0.59	0.60	0.60	0.60	0.51	0.46
Dangila	1.15	1.11	0.99	0.97	0.76	0.82
Markos	1.33	1.32	1.05	1.37	1.34	1.39
Arjo	1.55	1.43	1.22	1.05	1.09	1.06
Nekemte	0.84	0.94	0.87	0.76	0.86	0.81
Ambo	2.40	2.40	2.40	2.40	2.40	2.40
Fitche	1.09	0.94	1.12	1.32	1.18	0.90
Addis Ababa	0.27	0.28	0.46	0.72	0.74	0.64

Appendix-B: **Soil parameters used by the SWAT Model**

Table –B-1

Legend of the parameters used in Soil		
	Symbol	**Description**
1	SNAM	Soil name
2	NLAYERS	Number of layers in the soil
3	HYDGRP	Soil Hydrologic Group
4	SOL_ZMX	Maximum rooting depth of soil profile
5	SOL_Z	Depth from soil surface to bottom of layer
6	SOL_BD	Moist bulk density
7	AWC	Available water capacity of the soil layer
8	SOL_CBN	Organic carbon content
9	SOL_K	Saturated hydraulic conductivity
10	CLAY	Clay content
11	SILT	Silt content
12	SAND	Sand content
13	ROCK	Rock fragment content
14	SOL_ALB	Moist soil Albedo
15	USLE_K	USLE equation soil erodibilty (K) factor
16	SOL_EC	Electrical conductivity

The numbers 1 through 16 in the following table indicate soil parameters as per in appendix-B, Table B-1.

Table –B-2

1	**2**	**3**	**4**	**5**	**6**	**7**	**8**	**9**	**10**	**11**	**12**	**13**	**14**	**15**	**16**
			(m)	**(mm)**	**(g/cm)**	**mm/mm**	**(%)**	**(mm/hr)**	**(%)**	**(%)**	**(%)**	**(%)**			**(dS/)**
H.Alisols	1	C	2000	150	1.33	0.6	2.3	9.17	51	34	15	2	0.13	0.128	0.02
	2	C	2000	350	1.32	0.6	1.4	9.17	63	18	19	2	0.13	0.109	0.02
	3	C	2000	400	1.32	0.6	1.1	15.8	61	20	19	2	0.13	0.122	0.02
	4	C	2000	700	1.32	0.6	0.6	15.8	75	16	5	2	0.13	0.176	0.02
	5	C	2000	550	1.32	0.6	0.4	15.8	79	14	7	2	0.13	0.149	0.02
E.Fluvisols	1	C	2000	150	1.39	0.6	2.4	0.83	59	38	3	2	0.13	0.220	0.3
	2	C	2000	500	1.39	0.6	0.9	0.83	57	35	8	2	0.13	0.197	0.2
	3	C	2000	750	1.39	0.6	0.5	3.75	50	41	9	2	0.13	0.215	0.2
	4	C	2000	600	1.39	0.6	0.5	3.75	27	13	60	2	0.13	0.140	0.3
H.Luvisols	1	C	2000	200	1.38	0.6	2.4	14.6	41	42	17	2	0.13	0.138	0.06
	2	C	2000	400	1.33	0.6	0.9	14.6	67	20	13	2	0.13	0.134	0.02
	3	C	2000	500	1.33	0.6	0.5	14.2	83	16	7	2	0.13	0.152	0.01

	4	C	2000	900	1.33	0.6	0.5	14.2	45	12	5	2	0.13	0.184	0.06
C.Luvisols	1	C	2000	250	1.38	0.6	2.6	14.6	49	29	22	2	0.13	0.115	0.1
	2	C	2000	450	1.33	0.6	1.1	14.6	65	21	14	2	0.13	0.128	0.1
	3	C	2000	450	1.33	0.6	0.7	14.2	71	20	9	2	0.13	0.152	0.1
	4	C	2000	750	1.33	0.6	0.4	14.2	70	19	11	2	0.13	0.144	0.04
E.Vertisols	1	D	2000	150	1.22	0.6	3.7	0.83	52	34	14	2	0.13	0.130	0.03
	2	D	2000	250	1.21	0.6	1.1	0.83	72	18	10	2	0.13	0.131	0.02
	3	D	2000	500	1.21	0.6	0.9	3.75	74	20	6	2	0.13	0.170	0.02
	4	D	2000	900	1.21	0.6	0.5	3.75	72	18	10	2	0.13	0.144	0.1
C.Vertisols	1	D	2000	200	1.22	0.6	2	0.83	51	36	13	2	0.13	0.138	0.1
	2	D	2000	600	1.21	0.6	1.7	0.83	69	17	17	2	0.13	0.100	0.1
	3	D	2000	500	1.21	0.6	0.9	3.75	67	22	22	2	0.13	0.126	0.2
	4	D	2000	700	1.21	0.6	0.3	3.75	63	23	14	2	0.13	0.147	0.2
E.Leptosols	1	C	2000	300	1.42	0.6	0.39	14	73	25	5	2	0.13	0.209	0.1
H.Nitisols	1	D	2000	200	1.24	0.6	2	9.17	50	34	17	2	0.13	0.126	0.14
	2	D	2000	700	1.2	0.6	1.5	9.17	23	51	27	2	0.13	0.153	1.5
	3	D	2000	100	1.2	0.6	1.3	15.8	62	25	14	2	0.13	0.129	1.3
	4	D	2000	100	1.2	0.6	0.5	15.8	71	19	9	2	0.13	0.153	0.5
E.Regosols	1	B	2000	200	1.43	0.6	1.1	14	54	35	11	2	0.13	0.168	0.1
E.Cambisols	1	C	2000	250	1.34	0.6	2.43	0.83	88	11	1	2	0.13	0.171	0.1
	2	C	2000	550	1.33	0.6	1.08	0.83	85	14	1	2	0.13	0.221	0.1
	3	C	2000	750	1.33	0.6	0.7	3.75	73	23	4	2	0.13	0.213	0.33
	4	C	2000	450	1.33	0.6	0.5	3.75	87	13	0.4	2	0.13	0.254	0.2
Acrisols	1	C	2000	300	1.4	0.6	0.81	0.83	25	19	56	2	0.13	0.148	0
	2	C	2000	700	1.33	0.6	0.35	0.83	36	17	47	2	0.13	0.141	0

Appendix-C: Correlation Coefficient and Consistency of Metrological Stations

Graph –C-1 Double Mass Curve Analysis

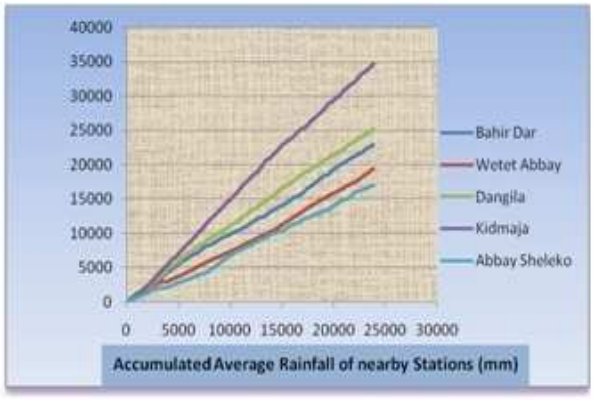

(a) for Gilgel Abbay Catchment

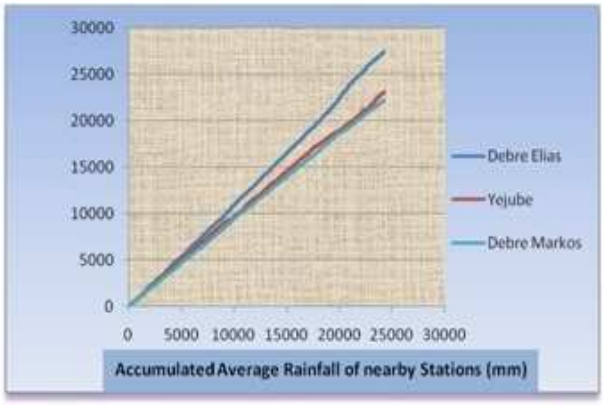

(a) for Chemoga Catchment

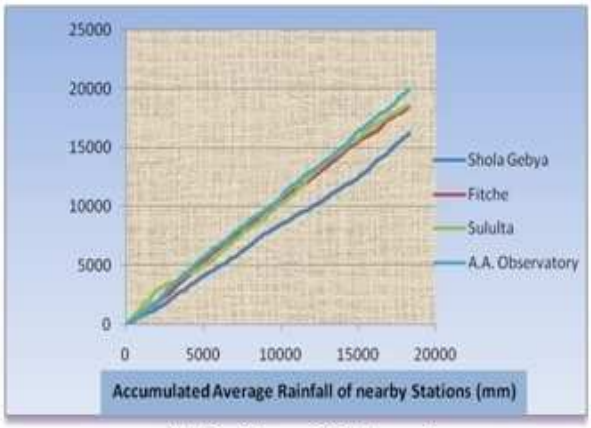

(c) for Muger Catchment

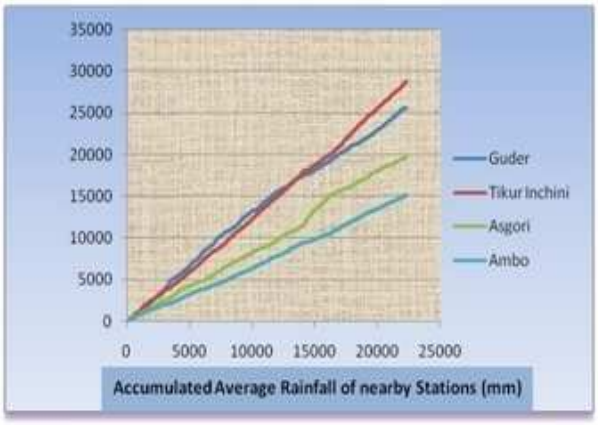

(d) for Guder Catchment

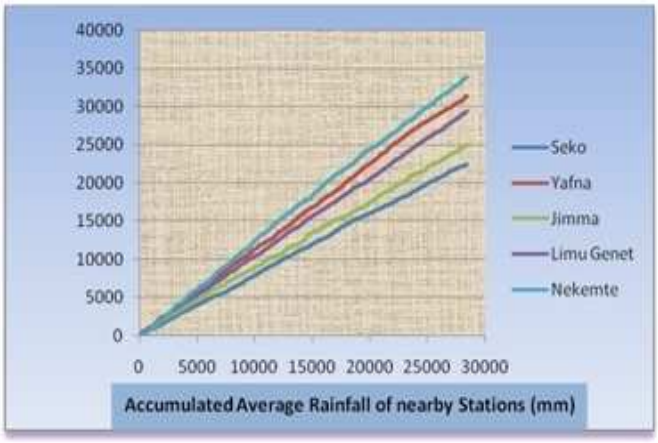

(e) for Guder Catchment

Table –C-2

	Correlation Coefficient between Metrological Stations						
For Gigel Abbay		Bahir Dar	Dangila	Abbay Sheleko		Wetet Abbay	Kidmaja
	Bahir Dar	1.00	0.43	0.34		0.50	0.34
	Dangila			0.35		0.36	0.45
	Abbay Sheleko			1.00		0.75	0.32
	Wetet Abbay					1.00	0.43
	Kidmaja						1.00
For Chemoga		Debre Markos	Debre Elias	Yejube			
	Debre Markos	1.00	0.71	0.68			
	Debre Elias		1.00	0.42			
	yejube			1.00			
For Muger		A.A. Observatory	Shola	Fitche		Sululta	
	A.A. Observatory	1.00	0.43	0.41		0.25	
	Shola		1.00	0.48		0.28	
	Fitche			1.00		0.32	
	Sululta					1.00	
For Guder		Ambo	Guder	Tikur		Asgori	
	Ambo	1.00	0.36	0.52		0.26	
	Guder		1.00	0.30		0.24	
	Tikur			1.00		0.28	
	Asgori					1.00	
For Didessa		Arjo	Nekemte	Seko	Yafna	Jimma	Limu Genet
	Arjo	1.00	0.38	0.20	0.28	0.24	0.30
	Nekemte		1.00	0.25	0.30	0.26	0.35
	Seko			1.00	0.18	0.15	0.19
	Yafna				1.00	0.24	0.34
	Jimma					1.00	0.41
	Limu Genet						1.00

Appendix-D: HBV Model Auto Calibration Best Parameter Values

Table –D-1

	HBV Monthly Auto-Calibration Best Parameters														
	FC_1	LP_1	$BETA_1$	PERC	UZL	K_0	K_1	K_2	MAXBAS	FC_2	LP_2	$BETA_2$	FC_3	LP_3	$BETA_3$
Gilgel Abbay	254.45	0.98	1.60	4.98	71.45	0.19	0.136	0.05	1.95	59.17	0.99	2.72	260.51	0.98	2.99
Chemoga	1102.28	0.46	1.84	0.10	19.48	0.33	0.22	0.033	2.64	250.45	0.86	2.53	291.05	0.61	5.66
Muger	191.71	0.97	3.41	4.19	31.86	0.12	0.29	0.10	3.64	269.14	0.83	5.83	1486.83	0.73	1.06
Guder	368.86	0.62	5.20	0.63	97.99	0.45	0.17	0.06	1.47	409.46	0.66	1.06		0.36	1.67
Didessa	638.79	0.42	5.52	5.50	73.93	0.41	0.13	0.06	1.32	183.78	0.54	5.54	483.91	0.69	2.60
	HBV Daily Auto-Calibration Best Parameters														
	FC_1	LP_1	$BETA_1$	PERC	UZL	K_0	K_1	K_2	MAXBAS	FC_2	LP_2	$BETA_2$	FC_3	LP_3	$BETA_3$
Gilgel Abbay	246.81	0.97	1.53	4.89	69.95	0.18	0.13	0.05	2.89	51.34	0.98	2.69	252.68	0.97	2.96
Chemoga	1459.49	0.55	2.08	0.31	79.84	0.44	0.19	0.07	2.78	793.50	0.36	3.14	72.17	0.60	2.89
Muger	280.00	0.63	5.95	0.86	85.21	0.11	0.22	0.09	2.79	233.54	0.86	1.19	372.93	0.96	4.78
Guder	181.52	0.65	4.44	1.08	20.56	0.09	0.03	0.07	3.49	357.75	0.67	1.31	893.97	0.40	1.15
Didessa	638.79	0.42	5.52	5.50	73.93	0.41	0.13	0.06	1.32	183.78	0.54	5.54	483.91	0.69	2.60

Appendix-E: SWAT Model Auto Calibration Best Parameter Values

Table –E-1

SWAT Monthly Auto-Calibration Best Parameters														
Sensitivity Rank	Gilgel Abbay		Chemoga			Muger			Guder			Didessa		
	Parameter	Adjusted Value	Rank	Parameter	Adjusted Value	Rank	Parameter	Adjusted Value	Rank	Parameter	Adjusted Value	Rank	Parameter	Adjusted Value
1	Cn2	-20.25	1	Cn2	4.14	1	Cn2	23.72	1	Cn2	-18.6	1	Cn2	-24.47
2	Gwqmn	998.8	2	Gwqmn	1000	2	Gwqmn	189.6	2	Sol_Z	18.42	2	Esco	0.91
3	Canmx	9.72	3	Esco	0.03	3	Esco	0.70	3	Esco	0.21	3	Gwqmn	1000
4	Blai	0.10	4	Sol_Z	24.16	4	Blai	1.0	4	Gwqmn	996.6	4	Sol_Awc	-25.0
5	Sol_Z	-16.72	5	Canmx	2.38	5	Canmx	8.60	5	Blai	1.0	5	Sol_Z	15.24
6	Sol_Awc	-19.88	6	Sol_Awc	-24.71	6	Sol_Z	-25.0	6	Canmx	0.71	6	Blai	1.0
7	Esco	0.01	7	Blai	0.39	7	Gw_Revap	0.04	7	Sol_Awc	=25	7	Alpha_Bf	0.01
8	Gw_Revap	0.04	8	Gw_Revap	0.03	8	Epco	0.99	8	Gw_Revap	0.04	8	Gw_Revap	0.04
9	Ch_K2	26.36	9	Slope	-18.04	9	Alpha_Bf	0.79	9	Epco	0.69	9	Canmx	10
10	Epco	0.54				10	Sol_Awc	-25.0	10	Ch_K2	112.4	10	Ch_K2	86.13
11	Alpha_Bf	0.26				11	Ch_K2	37.03	11	Alpha_Bf	0.0	11	Epco	0.64
SWAT Daily Auto-Calibration Best Parameters														
Sensitivity Rank	Gilgel Abbay		Chemoga			Muger			Guder			Didessa		
	Parameter	Adjusted Value	Rank	Parameter	Adjusted Value	Rank	Parameter	Adjusted Value	Rank	Parameter	Adjusted Value	Rank	Parameter	Adjusted Value
1	Cn2	35.0	1	Cn2	4.14	1	Cn2	24.77	1	Cn2	4.14	1	Cn2	-27.97
2	Gwqmn	2858.8	2	Gwqmn	1000	2	Gwqmn	62.32	2	Sol_Z	24.16	2	Esco	0.73
3	Canmx	8.90	3	Esco	0.03	3	Esco	0.99	3	Esco	0.03	3	Gwqmn	717.59
4	Blai	0.56	4	Sol_Z	24.16	4	Blai	0.01	4	Gwqmn	1000	4	Sol_Awc	-25.0
5	Sol_Z	20	5	Canmx	2.38	5	Canmx	0	5	Blai	0.39	5	Sol_Z	0.67
6	Sol_Awc	20.9	6	Sol_Awc	-24.71	6	Sol_Z	-24.9	6	Canmx	2.38	6	Blai	0.59
7	Esco	0.94	7	Blai	0.39	7	Gw_Revap	0.03	7	Sol_Awc	-24.7	7	Alpha_Bf	0
8	Gw_Revap	0.20	8	Gw_Revap	0.03	8	Epco	0.43	8	Gw_Revap	0.03	8	Gw_Revap	0.03
9	Ch_K2	361.07	9	Slope	-18.04	9	Alpha_Bf	0.97	9	Epco	0.94	9	Canmx	3.22
10	Epco	0.89				10	Sol_Awc	-12.2	10	Ch_K2	142.1	10	Ch_K2	74.35

11	Alpha_Bf	0.03			11	Ch_K2	10.0	11	Alpha_Bf	0.01	11	Epco	0.12

Appendix-F: Time Series Data of Observed and Simulated Stream Flow with HBV

The results presented were average daily river flows in a month in m^3/s. Qo and Qs represents Observed and Simulated flow repectively.

HBV Results										
	Gilgel Abbay River		Chemoga River		Muger River		Guder River		Didessa River	
Month- year	Qo (m^3/sec)	Qs (m^3/sec)	Qo (m^3/sec)	Qs (m^3/sec)	Qo (m^3/sec)	Qs (m^3/sec)	Qo (m^3/sec)	Qs (m^3/sec)	Qo (m^3/sec)	Qs (m^3/sec)
Jan-1991	3.69	0.770	0.16	0.126			0.64	0.64	19.97	2.310
Feb-91	2.5	0.193	0.21	0.042			0.62	0.62	12.42	1.155
Mar-91	2.05	0.000	0.3	0.253			0.86	0.86	12.62	1.155
Apr-91	4.4	0.385	0.39	0.295			0.43	0.43	23.5	2.310
May-91	8.86	0.193	1.12	0.295			0.73	0.73	15.7	8.086
Jun-91	55.34	27.733	5.78	1.306			2.06	2.06	57.74	41.588
Jul-91	190.64	270.015	37.5	9.900			14.31	14.31	202.87	165.195
Aug-91	217.3	176.800	50.31	23.003			52.29	52.29	426.67	248.370
Sep-91	162.76	163.126	14.65	16.431			34.36	34.36	236.13	181.368
Oct-91	42.12	78.770	1.3	2.907			3.97	3.97	56.58	62.381
Nov-91	11.05	18.874	0.57	0.758			0.96	0.96	26.27	17.328
Dec-91	6.32	4.237	0.75	1.180			0.73	0.73	14.23	5.776
Jan-92	4.19	0.963	0.28	0.337			0.87	0.87	9.14	2.310
Feb-92	2.94	0.193	0.66	0.295			1.16	1.16	9.55	2.310
Mar-92	2.28	0.000	0.71	0.211			0.81	0.81	5.13	2.310
Apr-92	3.78	0.578	0.5	0.506			0.62	0.62	7.99	4.621
May-92	6.62	3.081	0.39	0.800			2.04	2.04	21.08	33.501
Jun-92	30.55	5.778	0.53	1.601			13.72	13.72	61.98	86.641
Jul-92	121.41	44.874	8.39	4.929			48.47	48.47	137.36	198.696
Aug-92	195.58	110.548	22.29	14.113			56.77	56.77	307.83	337.321
Sep-92	145.13	79.348	23.3	15.799			40.74	40.74	217.78	336.166
Oct-92	89.78	49.111	3.66	10.575			10.03	10.03	300.97	236.818
Nov-92	29.42	22.726	1.86	2.781			2.18	2.18	63.31	103.969
Dec-92	10.91	7.511	0.58	0.674			1.13	1.13	27.4	28.880
Jan-93	5.51	1.926	0.47	0.337			0.81	0.81	15.88	8.086
Feb-93	3.77	0.578	0.45	0.295	0.200	0.000	0.8	0.8	11.52	3.466
Mar-93	3.17	0.385	0.19	0.295	0.170	0.170	0.49	0.49	9.11	2.310
Apr-93	5.02	1.926	1.83	2.233	0.110	0.226	1.28	1.28	21.11	18.483
May-93	8.98	15.985	4.51	3.328	0.360	0.340	2.78	2.78	39.28	39.277
Jun-93	74.92	70.681	9.32	7.625	0.470	0.283	31.21	31.21	120.42	166.350
Jul-93	187.94	131.156	21.09	30.207	1.250	13.187	38.78	38.78	223.86	250.680
Aug-93	179.34	174.296	39.13	28.311	30.440	31.355	49.8	49.8	432.62	317.682
Sep-93	154.84	126.148	28.57	31.218	63.750	19.583	46.24	46.24	243.33	251.835
Oct-93	89.74	68.178	6.21	19.506	42.930	2.490	14.6	14.6	151.95	180.213

Nov-93	22.92	29.852	1.54	1.306	5.320	0.226	5.23	5.23	68.27	76.244
Dec-93	8.19	7.319	0.56	0.253	0.760	0.057	1.39	1.39	23.65	15.018
Jan-94	4.8	1.733	0.24	0.295	0.350	0.000	0.87	0.87	14.58	2.310
Feb-94	3.38	0.385	0.13	0.126	0.230	0.113	0.62	0.62	8.09	1.155
Mar-94	2.44	0.193	0.03	0.295	0.110	0.170	0.82	0.82	5.78	0.000
Apr-94	2.11	0.193	0.11	0.295	0.140	0.679	0.63	0.63	6.05	1.155
May-94	7.17	8.281	0.31	1.138	0.190	0.623	1.2	1.2	22.29	17.328
Jun-94	61.54	51.422	0.5	2.064	0.160	0.283	5.95	5.95	84.95	73.933
Jul-94	147.62	101.304	7.69	11.965	0.910	16.470	38.04	38.04	199.44	201.006
Aug-94	177.61	141.748	19.52	19.506	19.610	39.278	41.56	41.56	455.86	269.164
Sep-94	118.65	104.578	0.8	19.632	39.310	19.017	32.16	32.16	331.03	265.698
Oct-94	23.38	39.289	0.36	0.843	20.500	1.698	3.92	3.92	58.38	79.709
Nov-94	10.46	10.978	0.04	0.590	2.280	0.057	1.32	1.32	26.26	31.191
Dec-94	6.36	3.852	0	0.211	0.530	0.057	0.81	0.81	13.79	6.931
Jan-95	3.57	0.963	0	0.084	0.300	0.170	0.62	0.62	7.6	1.155
Feb-95	2.52	0.193	0.06	0.042	0.160	0.057	0.53	0.53	5.06	0.000
Mar-95	1.88	0.385	0.07	0.084	0.190	0.283	0.48	0.48	5.53	0.000
Apr-95	1.95	1.156	0.32	0.295	0.150	0.736	1.01	1.01	7.5	3.466
May-95	11.07	7.126	0.94	0.716	0.380	1.528	1.45	1.45	14.28	11.552
Jun-95	45.21	44.874	0.44	1.348	0.330	8.207	3.1	3.1	32.02	30.035
Jul-95	92.64	124.415	9.75	6.867	0.360	27.846	20.33	20.33	84	110.900
Aug-95	198.98	163.126	21.22	20.222	14.560	46.749	44.22	44.22	212.42	202.161
Sep-95	131.77	95.333	10.1	14.535	36.130	20.092	29.32	29.32	187.46	232.197
Oct-95	25.43	37.748	1.36	2.907	11.630	3.509	4.18	4.18	58.32	103.969
Nov-95	10.22	13.289	0.35	0.463	1.280	0.170	1.21	1.21	23.12	27.725
Dec-95	5.64	3.467	0.77	1.475	0.390	0.000	0.86	0.86	15.39	6.931
Jan-96	3.58	0.963	0.94	0.421	0.270	0.057	0.92	0.92	7.6	4.621
Feb-96	2.27	0.193	0.43	0.211	0.170	0.113	0.55	0.55	5.05	1.155
Mar-96	4.08	4.237	0.31	0.379	0.200	0.113	2.45	2.45	24.07	2.310
Apr-96	3.91	8.667	2.16	0.927	0.230	0.396	2.16	2.16	11.72	4.621
May-96	19.74	22.341	3.93	2.612	0.290	0.170	6.74	6.74	52.95	36.967
Jun-96	85.19	78.770	5.75	11.881	0.260	0.453	29.46	29.46	143.96	132.849
Jul-96	202.98	132.311	17.38	15.714	0.300	14.432	39.48	39.48	270.03	270.319
Aug-96	223.52	198.370	22.09	25.910	20.390	27.506	45.81	45.81	319.01	299.199
Sep-96	141.7	148.681	11.02	15.462	42.970	9.169	26.49	26.49	230.58	204.472
Oct-96	85.51	67.793	1.85	4.508	10.070	1.755	9.74	9.74	128.59	135.159
Nov-96	68.07	20.993	0.87	1.432	0.910	1.302	2.04	2.04	55.16	34.656
Dec-96	47.88	6.356	0.51	0.843	0.270	0.226	1.08	1.08	32.54	11.552
Jan-97	2.94	1.348	0.3	0.253	0.160	0.113	1.65	1.65	15.46	3.466
Feb-97	1.93	0.385	0.05	0.126	0.110	0.057	0.65	0.65	7.87	1.155
Mar-97	1.75	0.578	0.05	0.295	0.070	0.226	1.68	1.68	5.53	1.155
Apr-97	1.67	0.963	0.18	0.843	0.060	0.170	1.54	1.54	7.5	6.931
May-97	18.39	31.585	0.24	1.180	0.110	0.509	1.32	1.32	14.28	30.035
Jun-97	60.79	72.800	1.46	4.508	0.060	0.283	10.9	10.9	32.02	157.108
Jul-97	160.86	118.059	12.17	14.198	0.190	9.508	36.05	36.05	84	276.095
Aug-97	196.73	154.652	21.16	23.845	12.260	42.052	37.03	37.03	212.42	270.319
Sep-97	125.08	96.296	7.55	16.810	28.640	25.639	18.29	18.29	187.46	172.126
Oct-97	63.56	80.311	3.96	10.827	9.450	6.792	8.77	8.77	58.32	166.350
Nov-97	35.67	51.230	2.9	6.067	0.780	0.623	3.74	3.74	23.12	136.315
Dec-97	10.54	15.600	0.96	0.463	0.390	0.000	2.2	2.2	15.39	34.656
Jan-98	4.48	3.659	0.52	0.211	0.190	0.057	1.35	1.35	15.88	9.242
Feb-98	2.53	0.770	0.2	0.084	0.200	0.000	0.77	0.77	11.52	2.310
Mar-98	1.85	0.385	0.2	0.169	0.100	0.057	1.29	1.29	9.11	2.310
Apr-98	1.28	0.385	0.03	0.126	0.080	0.057	2.06	2.06	21.11	2.310
May-98	10.13	11.170	0.9	0.927	0.070	0.057	0.98	0.98	39.28	10.397
Jun-98	64.3	49.111	1.39	1.222	0.200	0.170	6.98	6.98	120.42	61.226
Jul-98	142.7	146.563	14.7	4.634	0.710	18.847	32.7	32.7	223.86	204.472
Aug-98	184.56	171.022	17.26	15.040	24.710	51.900	45.44	45.44	432.62	311.906
Sep-98	153.73	135.393	13.47	17.357	55.920	18.281	33.39	33.39	243.33	243.749
Oct-98	96.14	86.089	13.49	16.768	25.670	3.849	22.55	22.55	151.95	222.955
Nov-98	18.32	31.200	1.24	1.264	7.960	0.509	3.11	3.11	68.27	105.124

Dec-98	6.54	8.281	0.29	0.211	0.830	0.057	1.06	1.06	23.65	19.639
Jan-99	3.72	1.926	0.21	1.180	0.290	0.000	0.8	0.8	15.88	4.621
Feb-99	2.14	0.578	0.06	0.084	0.180	0.000	0.45	0.45	11.52	1.155
Mar-99	1.43	0.193	0.01	0.042	0.050	0.000	0.47	0.47	9.11	0.000
Apr-99	1.71	0.193	0.01	0.042	0.070	0.170	0.33	0.33	21.11	0.000
May-99	8.91	10.785	0.05	0.253	0.050	0.453	1.47	1.47	39.28	15.018
Jun-99	57.74	59.511	1.08	1.095	0.060	0.226	10.88	10.88	120.42	83.175
Jul-99	163.04	149.644	15.45	8.721	0.290	13.810	33.2	33.2	223.86	161.729
Aug-99	186.86	203.378	29.41	22.287	12.670	40.071	44.46	44.46	432.62	239.128
Sep-99	127.08	151.956	12.49	12.765	57.180	20.262	32.53	32.53	243.33	240.283
Oct-99	122.52	116.904	13.48	13.776	18.350	5.830	23.48	23.48	151.95	304.975
Nov-99	19.66	41.407	1	0.362	3.910	0.736	3.15	3.15	68.27	86.641
Dec-99	7.6	10.593	0.36	0.590	0.560	0.113	1.4	1.4	23.65	13.863
Jan-00	3.42	2.504	0.17	0.126	0.230	0.000	0.97	0.97	7.6	2.310
Feb-00	2.03	0.578	0.05	0.042	0.130	0.057	0.67	0.67	5.05	0.000
Mar-00	1.49	0.193	0.1	0.042	0.060	0.509	0.56	0.56	5.7	0.000
Apr-00	3.1	7.319	0.1	0.716	0.030	0.453	1.43	1.43	7.88	1.155
May-00	6.08	15.985	0.33	0.548	0.070	0.792	2.1	2.1	14.36	16.173
Jun-00	49.04	65.289	1.08	1.348	0.130	1.415	9.58	9.58	34.18	101.658
Jul-00	146.03	152.148	15.45	8.889	0.220	30.110	21.44	21.44	85.43	189.454
Aug-00	203.22	222.444	29.41	15.799	9.780	36.052	41.2	41.2	214.28	249.525
Sep-00	134.16	124.030	23.44	16.178	51.530	14.772	46.16	46.16	184.38	231.042
Oct-00	126.98	120.756	11.46	22.034	14.930	1.415	21.51	21.51	141.19	151.332
Nov-00	36.71	54.696	4	2.612	2.790	0.057	6.03	6.03	93.37	58.916
Dec-00	8.95	14.830	0.67	0.843	0.560	0	2.21	2.21	50.65	12.707
Jan-01	3.83	0.040	0.24	0.169	0.260	0.01	1.2		31.77	2.310
Feb-01	2.33	0.010	0.18	0.084	0.160	0.1	0.83	0.546	24.61	1.155
Mar-01	1.8	0.000	0.22	0.463	0.080	0.08	2.42	3.700	24.66	1.155
Apr-01	1.79	0.020	0.16	0.716	0.180	0.15	1.9	2.487	22.07	5.776
May-01	6	0.010	0.42	1.475	0.130	0.27	3.25	5.822	47.89	21.949
Jun-01	67.17	1.440	2.46	3.834	0.330	5.63	27.99	16.314	154.65	131.694
Jul-01	150.91	14.020	22.04	16.641	3.410	6.19	41.07	38.208	276.4	257.611
Aug-01	205.9	9.180	32.84	22.076	30.450	2.48	37.11	35.358	390.27	255.301
Sep-01	128.7	8.470	6.26	12.597	38.120	0.23	31.11	43.788	387.87	248.370
Oct-01	41.19	4.090	1.66	5.772	13.690	0.01	11.98	13.828	251.66	180.213
Nov-01	13.86	0.980	0.48	0.379	1.000	0	2.48	1.577	82.8	63.536
Dec-01	5.39	0.220	0.28	0.126	0.310	0.02	1.21	0.606	41.71	13.863
Jan-02	3.08	0.050	0.6	0.632	0.180	0.01	1.11	1.759	36.96	5.776
Feb-02	1.79	0.010	0.11	0.126	0.160	0.11	0.76	0.667	23.64	1.155
Mar-02	1.41	0.000	0.49	0.421	0.080	0.09	0.79	1.213	20.63	1.155
Apr-02	1.03	0.030	0.45	0.969	0.110	0.04	6.77	4.306	24.47	2.310
May-02	1.01	0.160	0.07	0.253	0.110	0.12	7.3	5.337	17.27	3.466
Jun-02	38.22	0.300	0.95	1.180	0.070	2.81	6.44	13.343	67.4	34.656
Jul-02	144.92	2.330	14.06	6.951	0.200	8.19	34.79	41.665	170.7	135.159
Aug-02	168.36	5.740	29.41	15.883	21.470	3.09	34.5	43.485	220.65	167.505
Sep-02	99.7	4.120	12.49	15.756	44.040	0.26	22.11	27.656	222.87	185.989
Oct-02	28.95	2.550	13.48	1.769	12.480	0.01	4.08	2.487	78.66	91.261
Nov-02	10.15	1.180	1	0.169	0.400	0.01	1.2	0.303	44.45	25.415
Dec-02	4.18	0.390	0.36	0.969	0.380	0.02	0.98	0.243	31.31	8.086
Jan-03	2.22	0.100			0.200	0.02	0.89	0.849	21.05	2.310
Feb-03	1.5	0.030			0.120	0.05	0.7	0.849	14.98	1.155
Mar-03	1.19	0.020			0.060	0.18	1.32	1.759	20.97	2.310
Apr-03	0.67	0.100			0.080	0.17	1.54	11.281	28.68	3.466
May-03	0.89	0.830			0.150	0.16	0.67	5.762	17.91	2.310
Jun-03	43.49	3.670			0.070	7.52	3.79	14.070	46.38	27.725

Jul-03	178.43	6.810			0.620	9.6	30.19	42.393	185.38	150.177
Aug-03	184.22	9.050			41.400	5.52	41.05	23.228	243.49	277.250
Sep-03	173.78	6.550			48.840	1.07	34.26	19.468	219.63	273.784
Oct-03	32.72	3.540			36.420	0.05	7.81	6.307	78.66	139.780
Nov-03	10.19	1.550			3.430	0.03	1.49	0.849	44.45	30.035
Dec-03	4.03	0.380			0.290	0.02	1.07	0.788	31.31	6.931
Jan-04	2.31	0.090			0.170	0.02	0.86	0.667	19.51	1.155
Feb-04	1.39	0.020			0.100	0.02	0.63	0.910	16.03	0.000
Mar-04	0.93	0.010			0.060	0.16	0.68	1.092	11.3	0.000
Apr-04	2.26	0.010			0.030	0.1	1.42	6.186	11.06	1.155
May-04	1.15	0.430			0.220	0.71	1.09	2.790	24.33	4.621
Jun-04	27.45	2.670			0.090	9.67	4.87	13.888	77.9	49.674
Jul-04	137.39	5.260			0.560	8.12	24.59	36.874	196.51	184.833
Aug-04	165.97	7.360			19.880	3.19	37.08	23.956	238.51	289.957
Sep-04	137.67	5.430			52.700	0.98	35.32	38.694	247.88	251.835
Oct-04	64.01	2.040			18.760	0.08	16.29	16.496	200.91	174.436
Nov-04	11.42	0.570			1.600	0.01	1.48	1.213	54.1	63.536
Dec-04	5.09	0.200			0.310	0.630	0.84	0.788	34.36	16.173
Jan-05	2.62	0.050					0.72	1.031		
Feb-05	1.46	0.010					0.32	0.546		
Mar-05	1.64	0.020					0.72	1.334		
Apr-05	1.04	0.060					1.09	2.911		
May-05	1.71	0.370					2.19	5.701		
Jun-05	33.68	2.330					7.45	11.766		
Jul-05	130.93	6.460			`		30.11	28.747		
Aug-05	118.25	8.470					39.36	44.334		
Sep-05	120.23	4.950					29.01	28.141		
Oct-05	50.29	1.960					10.91	8.673		
Nov-05	15.79	0.690					1.78	2.183		
Dec-05	14.17	0.180					0.7	0.546		

Appendix-G: Time Series Data of Observed and Simulated Stream Flow with SWAT

The results presented were average daily river flows in a month in m^3/s. Qo and Qs represents Observed and Simulated flow repectively.

SWAT Results										
	Gilgel Abbay River		Chemoga River		Muger River		Guder River		Didessa River	
Month- year	Qo (m^3/sec)	Qs (m^3/sec)	Qo (m^3/sec)	Qs (m^3/sec)	Qo (m^3/sec)	Qs (m^3/sec)	Qo (m^3/sec)	Qs (m^3/sec)	Qo (m^3/sec)	Qs (m^3/sec)
Jan-92	4.19	9.688	0.28				0.87	0.870	9.55	3.870
Feb-92	2.94	5.679	0.66	0.330			1.16	1.160	5.13	0.758
Mar-92	2.28	4.176	0.71	0.108			0.81	0.810	7.99	22.180
Apr-92	3.78	15.100	0.5	1.113			0.62	0.620	21.08	42.940
May-92	6.62	17.180	0.39	1.946			2.04	2.040	61.98	80.170
Jun-92	30.55	50.440	0.53	2.643			13.72	13.720	137.36	190.900
Jul-92	121.41	132.500	8.39	6.416			48.47	48.470	307.83	210.100
Aug-92	195.58	149.600	22.29	19.570			56.77	56.770	217.78	301.800
Sep-92	145.13	86.320	23.3	20.360			40.74	40.740	300.97	252.400
Oct-92	89.78	46.150	3.66	16.260			10.03	10.030	63.31	261.400
Nov-92	29.42	16.360	1.86	10.330			2.18	2.180	27.4	122.200
Dec-92	10.91	3.026	0.58	3.944			1.13	1.130	15.88	57.460
Jan-93	5.51	0.068	0.47	0.839			0.81	0.810	11.52	18.480
Feb-93	3.77	0.017	0.45	0.346	0.200	0.723	0.8	0.800	9.11	5.989
Mar-93	3.17	11.610	0.19	0.366	0.170	0.097	0.49	0.490	21.11	3.590
Apr-93	5.02	14.550	1.83	4.192	0.110	16.280	1.28	1.280	39.28	102.700
May-93	8.98	55.390	4.51	7.131	0.360	7.488	2.78	2.780	120.42	98.080
Jun-93	74.92	83.240	9.32	12.440	0.470	2.266	31.21	31.210	223.86	242.400
Jul-93	187.94	145.800	21.09	42.670	1.250	14.520	38.78	38.780	432.62	289.100
Aug-93	179.34	211.200	39.13	27.640	30.440	65.020	49.8	49.800	243.33	371.100
Sep-93	154.84	117.500	28.57	32.760	63.750	47.730	46.24	46.240	151.95	274.900
Oct-93	89.74	37.520	6.21	26.850	42.930	25.430	14.6	14.600	68.27	203.400

Nov-93	22.92	5.462	1.54	11.830	5.320	8.823	5.23	5.230	23.65	127.500
Dec-93	8.19	0.394	0.56	5.393	0.760	2.752	1.39	1.390	14.58	58.260
Jan-94	4.8	0.000	0.24	1.056	0.350	0.763	0.87	0.870	8.09	19.800
Feb-94	3.38	0.154	0.13	0.339	0.230	0.079	0.62	0.620	5.78	4.151
Mar-94	2.44	0.097	0.03	0.280	0.110	0.343	0.82	0.820	6.05	4.897
Apr-94	2.11	1.754	0.11	0.209	0.140	0.254	0.63	0.630	22.29	6.707
May-94	7.17	23.320	0.31	1.677	0.190	0.146	1.2	1.200	84.95	40.780
Jun-94	61.54	56.070	0.5	1.344	0.160	0.171	5.95	5.950	199.44	108.400
Jul-94	147.62	57.540	7.69	10.940	0.910	0.175	16.470	38.040	455.86	194.000
Aug-94	177.61	112.200	19.52	25.800	19.610	0.372	39.278	41.560	331.03	330.300
Sep-94	118.65	59.720	0.8	23.830	39.310	0.260	19.017	32.160	58.38	324.100
Oct-94	23.38	32.010	0.36	12.200	20.500	0.526	1.698	3.920	26.26	125.700
Nov-94	10.46	4.331	0.04	6.158	2.280	0.044	0.057	1.320	13.79	71.370
Dec-94	6.36	0.428	0	2.209	0.530	0.012	0.81	0.810	7.6	22.950
Jan-95	3.57	0.000	0	0.400	0.300	0.008	0.62	0.620	5.06	4.784
Feb-95	2.52	0.000	0.06	0.139	0.160	0.066	0.53	0.530	5.53	1.095
Mar-95	1.88	6.206	0.07	0.103	0.190	0.436	0.48	0.480	7.5	21.670
Apr-95	1.95	5.661	0.32	0.330	0.150	0.145	1.01	1.010	14.28	32.300
May-95	11.07	29.560	0.94	1.191	0.380	0.525	1.45	1.450	32.02	22.060
Jun-95	45.21	58.680	0.44	2.303	0.330	0.337	3.1	3.100	84	53.610
Jul-95	92.64	99.270	9.75	7.560	0.360	0.538	20.33	20.330	212.42	147.900
Aug-95	198.98	129.400	21.22	23.060	14.560	4.777	44.22	44.220	187.46	236.900
Sep-95	131.77	60.410	10.1	20.770	36.130	14.560	29.32	29.320	58.32	194.500
Oct-95	25.43	23.460	1.36	11.930	11.630	8.619	4.18	4.180	23.12	136.300
Nov-95	10.22	4.665	0.35	5.675	1.280	2.480	1.21	1.210	15.39	60.750
Dec-95	5.64	1.038	0.77	3.834	0.390	0.508	0.86	0.860	7.6	26.850
Jan-96	3.58	0.000	0.94	0.701	0.270	0.089	0.92	0.920	5.05	17.200
Feb-96	2.27	0.000	0.43	0.230	0.170	0.263	0.55	0.550	24.07	1.434
Mar-96	4.08	17.390	0.31	0.325	0.200	0.036	2.45	2.450	11.72	28.590
Apr-96	3.91	11.290	2.16	1.084	0.230	0.078	2.16	2.160	52.95	40.450
May-96	19.74	34.880	3.93	8.724	0.290	0.130	6.74	6.740	143.96	99.110
Jun-96	85.19	71.020	5.75	21.250	0.260	0.168	29.46	29.460	270.03	291.300
Jul-96	202.98	148.000	17.38	20.800	0.300	1.552	39.48	39.480	319.01	353.900
Aug-96	223.52	166.100	22.09	35.640	20.390	18.510	45.81	45.810	230.58	257.900
Sep-96	141.7	130.800	11.02	22.150	42.970	29.070	26.49	26.490	128.59	193.400
Oct-96	85.51	35.360	1.85	14.180	10.070	20.310	9.74	9.740	55.16	122.200
Nov-96	68.07	9.739	0.87	7.432	0.910	6.788	2.04	2.040	32.54	48.190
Dec-96	47.88	0.267	0.51	2.702	0.270	2.021	1.08	1.080	15.46	32.170
Jan-97	2.94	0.675	0.3	0.518	0.160	0.481	1.65	1.650	7.87	4.019
Feb-97	1.93	0.002	0.05	0.177	0.110	0.029	0.65	0.650	5.53	0.990
Mar-97	1.75	2.658	0.05	0.155	0.070	0.060	1.68	1.680	7.5	4.008
Apr-97	1.67	7.279	0.18	0.412	0.060	0.161	1.54	1.540	14.28	77.730
May-97	18.39	34.070	0.24	0.687	0.110	1.326	1.32	1.320	32.02	130.700
Jun-97	60.79	79.140	1.46	3.135	0.060	4.655	10.9	10.900	84	189.200
Jul-97	160.86	95.590	12.17	14.440	0.190	11.150	36.05	36.050	212.42	304.700
Aug-97	196.73	131.800	21.16	29.690	12.260	32.630	37.03	37.030	187.46	239.100
Sep-97	125.08	82.760	7.55	25.750	28.640	36.840	18.29	18.290	58.32	174.400
Oct-97	63.56	72.420	3.96	21.350	9.450	20.760	8.77	8.770	23.12	224.600
Nov-97	35.67	25.420	2.9	12.250	0.780	6.705	3.74	3.740	15.39	106.900
Dec-97	10.54	1.574	0.96	5.161	0.390	2.014	2.2	2.200	15.88	46.990
Jan-98	4.48	0.023	0.52	1.524	0.190	0.503	1.35	1.350	11.52	14.470
Feb-98	2.53	0.000	0.2	0.366	0.200	0.311	0.77	0.770	9.11	14.540
Mar-98	1.85	3.381	0.2	0.171	0.100	0.076	1.29	1.290	21.11	11.400

Apr-98	1.28	1.591	0.03	0.055	0.080	0.362	2.06	2.060	39.28	1.240
May-98	10.13	30.010	0.9	0.869	0.070	0.507	0.98	0.980	120.42	33.350
Jun-98	64.3	74.640	1.39	1.928	0.200	0.214	6.98	6.980	223.86	210.700
Jul-98	142.7	119.600	14.7	6.188	0.710	7.284	32.7	32.700	432.62	214.200
Aug-98	184.56	141.700	17.26	16.100	24.710	19.160	45.44	45.440	243.33	273.700
Sep-98	153.73	116.000	13.47	21.420	55.920	39.020	33.39	33.390	151.95	274.200
Oct-98	96.14	72.010	13.49	29.010	25.670	30.570	22.55	22.550	68.27	205.700
Nov-98	18.32	17.680	1.24	14.820	7.960	10.760	3.11	3.110	23.65	106.500
Dec-98	6.54	1.264	0.29	7.483	0.830	3.442	1.06	1.060	15.88	58.380
Jan-99	3.72	1.491	0.21	4.568	0.290	0.966	0.8	0.800	11.52	30.320
Feb-99	2.14	0.000	0.06	0.574	0.180	0.081	0.45	0.450	9.11	7.885
Mar-99	1.43	0.000	0.01	0.195	0.050	0.035	0.47	0.470	21.11	2.830
Apr-99	1.71	5.438	0.01	0.225	0.070	0.035	0.33	0.330	39.28	8.448
May-99	8.91	44.120	0.05	0.274	0.050	0.293	1.47	1.470	120.42	93.900
Jun-99	57.74	90.940	1.08	2.168	0.060	0.149	10.88	10.880	223.86	150.400
Jul-99	163.04	133.500	15.45	9.127	0.290	0.330	33.2	33.200	432.62	197.700
Aug-99	186.86	166.900	29.41	28.010	12.670	6.808	44.46	44.460	243.33	268.900
Sep-99	127.08	127.400	12.49	22.880	57.180	35.640	32.53	32.530	151.95	273.600
Oct-99	122.52	109.600	13.48	24.080	18.350	19.820	23.48	23.480	68.27	251.500
Nov-99	19.66	18.770	1	11.830	3.910	7.037	3.15	3.150	23.65	100.700
Dec-99	7.6	4.262	0.36	5.950	0.560	4.161	1.4	1.400	7.6	43.680
Jan-00	3.42	0.050	0.17	0.113	0.230	1.637	0.97	0.970	5.05	10.630
Feb-00	2.03	0.328	0.05	0.009	0.130	2.188	0.67	0.670	5.7	2.216
Mar-00	1.49	0.149	0.1	0.000	0.060	0.763	0.56	0.560	7.88	0.326
Apr-00	3.1	37.220	0.1	0.272	0.030	0.067	1.43	1.430	14.36	4.471
May-00	6.08	31.150	0.33	0.147	0.070	0.311	2.1	2.100	34.18	33.230
Jun-00	49.04	99.600	1.08	0.462	0.130	5.513	9.58	9.580	85.43	167.300
Jul-00	146.03	136.600	15.45	3.137	0.220	7.966	21.44	21.440	214.28	289.600
Aug-00	203.22	182.400	29.41	4.031	9.780	26.100	41.2	41.200	184.38	318.700
Sep-00	134.16	105.900	23.44	6.010	51.530	40.990	46.16	46.160	141.19	306.800
Oct-00	126.98	109.800	11.46	10.820	14.930	32.110	21.51	21.510	93.37	217.700
Nov-00	36.71	23.520	4	7.917	2.790	14.510	6.03	6.030	50.65	130.100
Dec-00	8.95	1.738	0.67	5.106	0.560	4.974	2.21	2.210	31.77	52.340
Jan-01	3.83	0.820	0.24	1.035	0.260	1.579	1.2	1.604	24.61	3.870
Feb-01	2.33	0.268	0.18	0.014	0.160	0.086	0.83	1.619	24.66	0.758
Mar-01	1.8	1.027	0.22	0.097	0.080	0.022	2.42	5.147	22.07	22.180
Apr-01	1.79	4.272	0.16	0.387	0.180	0.094	1.9	3.119	47.89	42.940
May-01	6	22.570	0.42	0.329	0.130	0.015	3.25	6.255	154.65	80.170
Jun-01	67.17	72.410	2.46	0.802	0.330	0.147	27.99	15.900	276.4	190.900
Jul-01	150.91	90.460	22.04	6.727	3.410	1.182	41.07	44.470	390.27	210.100
Aug-01	205.9	85.490	32.84	16.210	30.450	16.100	37.11	45.700	387.87	301.800
Sep-01	128.7	82.680	6.26	16.070	38.120	40.460	31.11	58.460	251.66	252.400
Oct-01	41.19	32.700	1.66	10.620	13.690	33.460	11.98	33.030	82.8	261.400
Nov-01	13.86	5.286	0.48	4.758	1.000	16.470	2.48	18.850	41.71	122.200
Dec-01	5.39	1.582	0.28	0.192	0.310	5.699	1.21	9.232	36.96	57.460
Jan-02	3.08	1.157	0.6	0.185	0.180	1.682	1.11	2.285	23.64	18.480
Feb-02	1.79	0.212	0.11	0.051	0.160	0.089	0.76	0.756	20.63	5.989
Mar-02	1.41	0.271	0.49	0.134	0.080	0.000	0.79	1.286	24.47	3.590
Apr-02	1.03	3.329	0.45	0.464	0.110	0.004	6.77	6.066	17.27	102.700
May-02	1.01	5.687	0.07	0.062	0.110	0.241	7.3	5.335	67.4	98.080
Jun-02	38.22	49.120	0.95	0.305	0.070	0.481	6.44	15.930	170.7	242.400
Jul-02	144.92	110.400	14.06	2.022	0.200	0.907	34.79	52.780	220.65	289.100
Aug-02	168.36	112.400	29.41	7.843	21.470	10.990	34.5	51.100	222.87	371.100

Sep-02	99.7	48.850	12.49	12.560	44.040	38.250	22.11	42.660	78.66	274.900
Oct-02	28.95	30.130	13.48	11.280	12.480	34.610	4.08	23.720	44.45	203.400
Nov-02	10.15	12.950	1	5.969	0.400	14.130	1.2	11.880	31.31	127.500
Dec-02	4.18	1.501	0.36	0.794	0.380	4.636	0.98	4.211	21.05	58.260
Jan-03	2.22	0.207			0.200	1.363	0.89	1.181	14.98	19.800
Feb-03	1.5	0.286			0.120	0.076	0.7	0.480	20.97	4.151
Mar-03	1.19	1.663			0.060	0.000	1.32	1.090	28.68	4.897
Apr-03	0.67	0.413			0.080	0.708	1.54	12.160	17.91	6.707
May-03	0.89	2.728			0.150	1.306	0.67	5.750	46.38	40.780
Jun-03	43.49	90.120			0.070	0.929	3.79	21.260	185.38	108.400
Jul-03	178.43	102.500			0.620	3.592	30.19	47.330	243.49	194.000
Aug-03	184.22	102.400			41.400	15.720	41.05	36.970	219.63	330.300
Sep-03	173.78	102.700			48.840	24.880	34.26	31.150	78.66	324.100
Oct-03	32.72	38.990			36.420	19.540	7.81	20.650	44.45	125.700
Nov-03	10.19	15.210			3.430	6.318	1.49	9.799	31.31	71.370
Dec-03	4.03	3.000			0.290	1.609	1.07	2.972	19.51	22.950
Jan-04	2.31	1.661			0.170	0.268	0.86	0.849	16.03	4.784
Feb-04	1.39	0.132			0.100	0.140	0.63	0.372	11.3	1.095
Mar-04	0.93	0.131			0.060	0.082	0.68	2.034	11.06	21.670
Apr-04	2.26	10.060			0.030	0.506	1.42	9.257	24.33	32.300
May-04	1.15	9.347			0.220	0.303	1.09	0.860	77.9	22.060
Jun-04	27.45	56.070			0.090	0.087	4.87	16.630	196.51	53.610
Jul-04	137.39	112.200			0.560	0.726	24.59	37.530	238.51	147.900
Aug-04	165.97	105.200			19.880	4.020	37.08	34.280	247.88	236.900
Sep-04	137.67	91.350			52.700	19.050	35.32	51.650	200.91	194.500
Oct-04	64.01	46.950			18.760	18.040	16.29	34.840	54.1	136.300
Nov-04	11.42	15.960			1.600	5.991	1.48	18.640	34.36	60.750
Dec-04	5.09	4.119			0.310	1.615	0.84	9.004	34.5	26.850
Jan-05	2.62	0.256			0.47	0.471	0.72	2.610		
Feb-05	1.46	0.207					0.32	0.629		
Mar-05	1.64	7.856					0.72	1.734		
Apr-05	1.04	1.527					1.09	1.934		
May-05	1.71	14.770					2.19	2.371		
Jun-05	33.68	72.180					7.45	10.960		
Jul-05	130.93	98.030					30.11	35.320		
Aug-05	118.25	112.400					39.36	52.440		
Sep-05	120.23	115.800					29.01	45.330		
Oct-05	50.29	42.180					10.91	30.770		
Nov-05	15.79	17.360					1.78	14.910		
Dec-05	14.17	2.585					0.7	6.567		